5-12-2010

Effect of Anions on the Iron Release Pathways of Human Serum Transferrin

Rashmi Subhash Chander Sharma
University of Missouri-St. Louis, rashmishm@gmail.com

Effect of Anions on the Iron Release Pathways of Human Serum Transferrin

by

Rashmi Subhash Chander Sharma

M.S, Chemistry, University of Missouri-St. Louis, 2007
M.Sc., Inorganic Chemistry, University of Mumbai, 2002
B.Sc., Chemistry, University of Mumbai, 2000

A DISSERTATION

Submitted to the Graduate School of the

UNIVERSITY OF MISSOURI- ST. LOUIS
In partial Fulfillment of the Requirements for the Degree

DOCTOR OF PHILOSOPHY

in

CHEMISTRY

with an emphasis in Biochemistry

May, 2010

Advisory Committee

Dr. Wesley Harris
Chairperson

Dr. Michael Nichols
Dr. Keith Stine
Dr. Chung Wong

Abstract

Effect of Anions on the Iron Release Pathways of Human Serum Transferrin

(May 2010)

Rashmi S. Sharma

Chair of committee: Dr. Wesley R. Harris

Transferrin, the serum iron transport protein in humans, is used to transport 30-40 mg of iron per day through blood. The accessibility of transferrin makes it an attractive target for iron chelating therapeutic agents used in the treatment of iron overload. There is an ongoing search for ligands which can accelerate the rate of iron release, as the currently approved drug DFO has a very slow rate for iron removal. Previous studies have shown that anions can accelerate the rate of iron release.

Studies on the effect of anions on the rates of iron release from C-terminal monoferric transferrin at pH 7.4 have been conducted using the ligands acetohydroxamic acid (AHA) and 1,2-dimethyl-3-hydroxy-pyridinone (L1), which follow saturation kinetics, and the ligands, nitrilotriacetic acid (NTA) and diethylenetriaminepentaacetic acid (DTPA), which follow first order kinetics with respect to the ligand concentration. The effects of sulfonates, phosphonates and phosphonocarboxylates have been studied.

The anions are divided into two types, simple (non-coordinating) and complex (capable of chelating iron). The simple anions accelerate the rate of iron release,

presumably by binding to an allosteric anion binding site on the transferrin. This binding increase the value of k_{max} for the saturation pathway for AHA and L1 and introduces a k_{max} for NTA, which otherwise does not have a saturation component. This changes the kinetic behavior of NTA from a strictly first-order dependence on the ligand concentration to complex kinetics, a combination of saturation and first-order kinetics.

The complex anions, which can also chelate iron, decrease the rate of iron release by the reference ligands. These anions can also generate a small first order component for iron removal by ligands that normally follow saturation kinetics. These studies emphasize that the appearance of the first order component is due to the replacement of synergistic anion by the incoming chelating ligand and is not an allosteric effect of the anionic ligand. Distinct effects of anions on the saturation and first-order components for iron release are reported. For NTA, the major impact of anions is a decrease in the value of k`.

A humble offering at the lotus feet of my guru Mata Amritanandmayi Devi

For my Parents with love

Acknowledgements

I would start with thanking UMSL Chemistry and Biochemistry department for giving me an opportunity to study and for the financial support during my PhD. I express my sincere thanks to my advisor Dr. Wes Harris for his constant guidance throughout these years and for making this opportunity a reality. I also thank him and his wife Marion for opening their home to me and my friends during thanksgiving and several other occasions.

I thank Dr. Michael Nichols, Dr. Keith Stine and Dr. Chung Wong for being my committee members. At this point I would also like thank all the professors in the department who were my instructors for several courses and with whom I got an opportunity to work and interact during all these years. I thank Dr. Dupureur and her group and specially Dr. Charulata Prasannan for the help in protein purification.

I would like to thank my lab members Dr. Sujittra Srisung for initial start up, Julie Stambek during the last one year and Matt, Pete, Sam, Asma, Carlos for filling up the lab in between.

Life at Saint Louis would not have been the same without some good friends that I had and made at UMSL and outside. I want to thank all my friends and colleagues during my years at UMSL, you all were wonderful in your own way, from a casual smile to a hello on the hallway, from a small chat to long talks. I thank my amma satsang group for providing me a home away from home and keep me in constant touch with my spiritual grounds.

I thank my dear parents Subhash and Nirmala, for their unconditional love and for supporting my decision to study in the USA, my brothers Prashant and Prateek for being there during the ups and downs. I would like to thank rest of my family members for being there with me in this process. I cherish all the letters, greeting cards and phone calls received during these years from friends and family.

Finally I want to say thank you to my husband Sushant for being a wonderful friend and life partner and for his patience while I was finishing my studies. Thank you all for being a part of this journey and being part of my life.

Table of contents

List of Figures

List of Tables

List of Abbreviations

ApoTf	Apotransferrin
AHA	Acetohydroxamic acid
Tf	Transferrin
DiTf	Diferric transferrin
DPG	N,N-bis(phosphonomethyl)glycine
CTf	C-terminal monoferric transferrin
NTf	N-terminal monoferric transferrin
NTA	Nitrilotriacetic acid
NTP	Nitrilotrismethylenephosphonic acid
EDTA	Ethylenediaminetetraacetic acid
LICAMS	N,N',N''-tris(5-sulfo-2,3-dihydroxybenzoyl) 1,5,10-triazadecane
PPi	Pyrophosphate
PIDA	N-(phosphonomethyl)iminodiacetic acid
PAGE	Polyacrylamide gel electrophoresis
HEPES	N-2hydroxyethylpiperazine-N'-2-ethane-sulfonic acid
MPA	Methylphosphonic acid
MDP	Methylenediphosphonic acid
EDP	Ethylenediphosphonic acid
SMS	Sodium methane sulfonate
MDS	Methylenedisulfonate
EDS	1,2-ethanedisulfonic acid

PAA	Phosphonoacetic acid
PPA	3-phosphonopropionic acid
PAM	Phosphonoacetamide
DTPA	Diethylenetriaminepentaacetic acid
L1	1,2-dimethyl-3-hydroxy-4-pyridinone
KISAB	Kinetically significant anion binding site
UV	Ultraviolet

Chapter 1

Introduction

This introductory chapter gives an overview of the progress of transferrin research. It explains the requirement of iron transport proteins in humans, and describes the different analogs of transferrin that have been found in other species. Research on the structure of the protein and how structure influences the function of protein is described. A detailed study of the binding of anions to transferrin and its impact on the binding and release of iron is included. The main emphasis of this chapter is on the mechanism of iron release from transferrin by low-molecular-weight chelating agents.

1.1

Chemistry and Biochemistry of Iron

Iron is an element located at position 26 in the middle of the periodic table, in the first row of transition metals. Iron exists in oxidation states ranging from (−II), as in the $Fe(CO)_4^{2-}$ anion, to (+VI), as in the ferrate ion FeO_4^{2-} (*1*). The two most relevant oxidation states in which iron exists biochemically are ferrous, Fe(II) and ferric, Fe(III), followed by Fe(IV) and Fe(V), which have been identified as reactive intermediates in the catalytic cycles of iron-containing enzymes such as monooxygenases (*2;3*).

Iron is an essential element for life, and it plays important roles in biology. The total iron found in the body of an adult human is normally between 3-5 g, and on a daily basis about 0.5-2 mg of iron enters and leaves the body (*3*). As there is no regulated pathway for iron excretion, iron balance in the body is maintained by regulation of iron

absorption from the intestine. The process of iron absorption regulates itself depending on the levels of iron stored in the body (*4*). The iron distribution in the body of a normal human being is demonstrated in Figure 1.1.

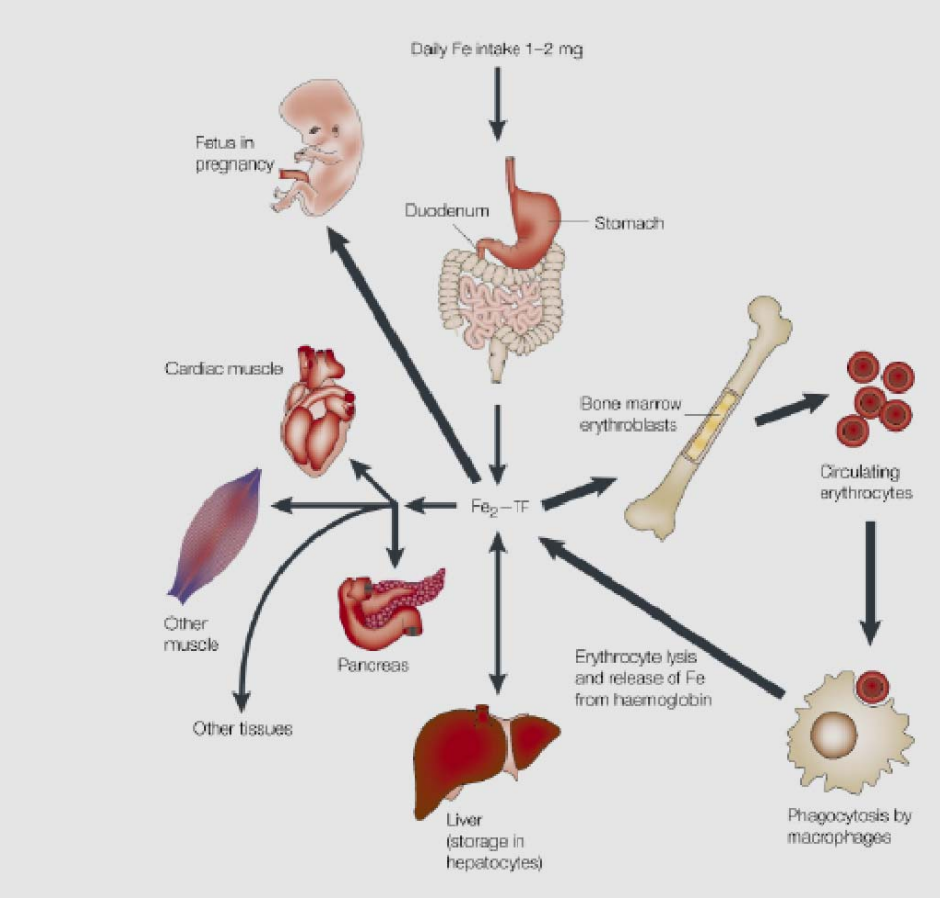

Figure 1.1. Distribution of iron in a body of a normal human being (*4*)

Haemoglobin in the red blood cells contains 65-75% of total body iron. At the end of the life cycle of red blood cells, almost all the iron is removed from haem by the reticuloendothelial macrophages and recycled back to new red blood cells (*4*). Liver cells

store most of the body's excess iron, and small amounts of iron are used by other tissues (*3*). The circulating iron is transported to red blood cell precursors and to other tissues of the body by the plasma protein transferrin (*5*). During iron deficiency, the formation of red blood cells continues at the expense of other tissues. In the case of iron overload, the production of red blood cells continues normally, and other tissues store the excess iron. The liver takes up most excess iron, followed by cardiac, pancreatic and other cells in the body (*4*).

Nature faces an interesting problem while dealing with iron. Iron metabolism requires both the ferrous and ferric states of iron. The presence of free ferrous ion is dangerous, as it can promote free radical formation via Fenton-type reactions as shown in Figure 1.2.

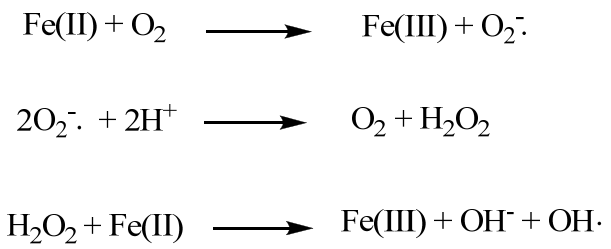

Figure 1.2. Formation of hydroxyl radical via Fenton-type reactions (*6*)

The free superoxide and hydroxyl radicals are highly toxic and can cause oxidative damage to the tissues. To use the ferrous form of iron, nature has devised the oxygen transport protein haemoglobin (*3*), which can stabilize the ferrous oxidation state and prevent the damage. On the other hand, free ferric form is highly insoluble due to its strong tendency to hydrolyze to ferric hydroxide (*1*). For iron transport to occur the ferric

ion must be solubilized and stabilized as Fe(III) by a suitable complexing agent, and this need is fulfilled by the iron transport protein, transferrin (*7*).

1.2

Transferrins

Transferrins are metal binding proteins. This family consists mainly of soluble glycoproteins, as well as the membrane bound protein melanotransferrin (*8*). The soluble glycoproteins include serum transferrin, lactoferrin and ovotransferrin. Serum transferrin is the iron binding protein found in the blood of most vertebrates (*9*). Lactoferrin is found in secretory fluids like milk, tears, saliva etc., where it acts as a bacteriostatic agent by denying the essential nutrient iron to microorganisms (*10;11*). Ovotransferrin, also referred to as conalbumin, is found in avian eggs and also serves a bacteriostatic function (*3;10*). Melanotransferrin is present at very low levels on the surface of normal cells and at high levels in melanoma cells and is also known as melanoma antigen p97 (*12;13*). A number of roles have been proposed for melanotransferrin in various physiological and pathological processes, including iron transport, chondrogenesis, angiogenesis, cell migration, invasion, metastasis, tumourigenesis and the regulation of plasminogen activation, though the precise role of melanotransferrin is unclear (*14*).

Transferrins are considered to have evolved through a gene duplication event (*10*) from the gene of a 40 kDa, single binding site ancestral protein to a double binding site bilobal molecule, as shown in Figure 1.3. Recently more work has focused on a class of single-site periplasmic iron binding proteins known as ferric binding protein (FBP) (*15;16*). The ferric binding proteins are often referred to as bacterial transferrins and are

thought to be distantly related to the true mammalian transferrins, as they share several physical and functional properties with serum transferrin (*17-19*).

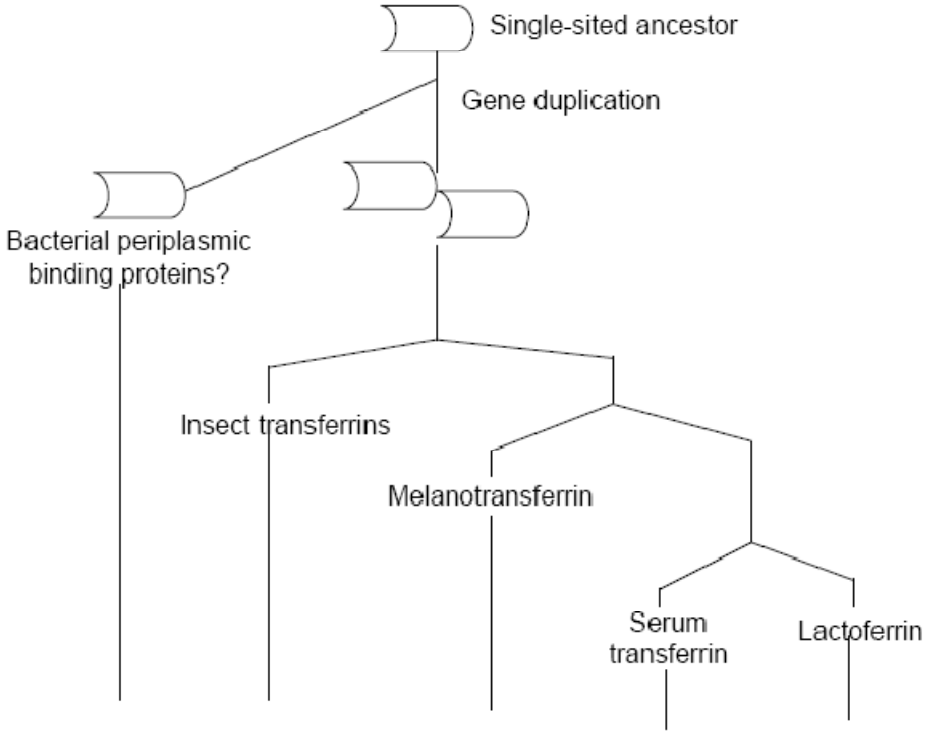

Figure 1.3. Evolutionary development of the transferrin family (*10*)

Before any structural information was available, the transferrins were identified by the unique property that the binding of the iron required the concomitant binding of a bicarbonate anion from the buffer (*20*). In the absence of bicarbonate, no metal binding was observed (*21;22*). For this reason, bicarbonate is referred to as the "synergistic anion".

Crystal structures of various forms of transferrin, such as diferric rabbit serum transferrin (*23*), human diferric lactoferrin (*11*), human apolactoferrin (*24*), apo ovotransferrin (*25*), monoferric human serum transferrin (*26*), human serum apotransferrin (*27*), and the recombinant N-lobe of human serum transferrin (*28*) have been determined. All the transferrins consist of a single polypeptide chain of 600-700 amino acid residues with a molecular mass of around 80 kDa. This polypeptide chain folds into two distinct lobes, designated as the N- and C- lobes. Each lobe is subdivided into two domains (N-I, N-II and C-I, C-II). A single iron binding site is located between the N-I and N-II and C-I and C-II domains, which form an iron binding cleft as shown in Figure 1.4.

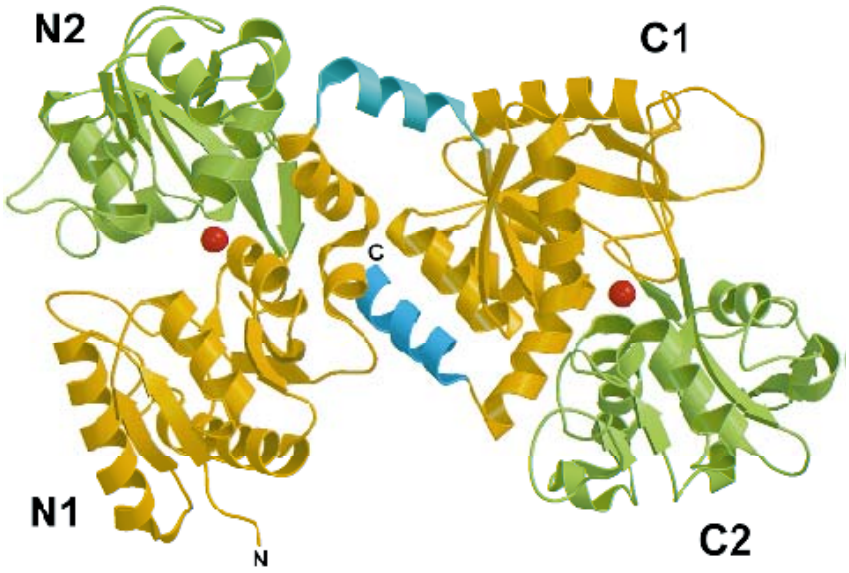

Figure 1.4. The characteristic polypeptide folding pattern of the transferrin family (*29*)

Crystal structures of apo- and holotransferrin have shown that at the base of the iron binding cleft, there is a hinge that contributes to a large scale conformational change in the protein when iron is removed (*27;30*). Figure 1.5, depicts the conformation change in the N-lobe of human transferrin that occurs upon iron binding. A 63˚ rigid rotation of the N-II domain occurs when iron is removed from the closed iron-bound form to the open apo form (*30*). In the hinge region, the two helices in blue act as a fulcrum, where one supports the other to facilitate the movement.

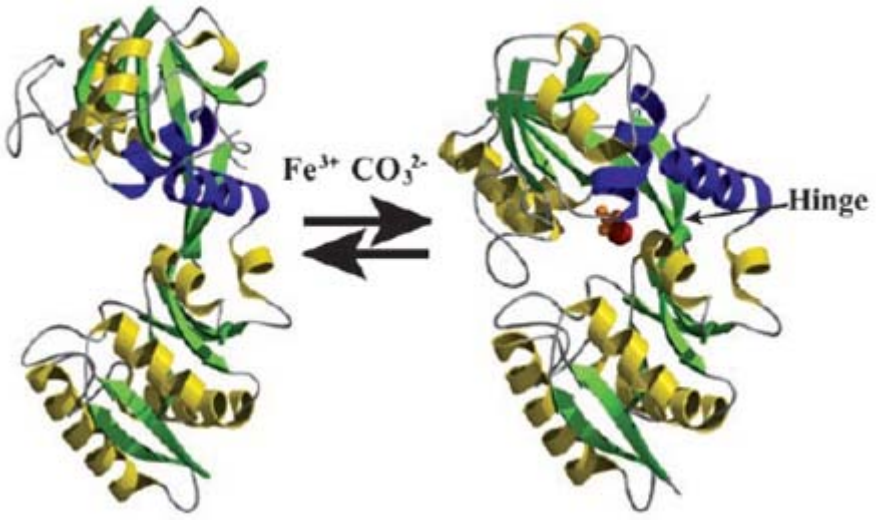

Figure 1.5. Two conformational states of the transferrin N-lobe showing the hinge region (*31*)

1.3.

Metal Binding site

The binding site ligands in most of the transferrins, including serum transferrin, lactoferrin and ovotransferrin, are the same for both the N- and C- lobe. The metal ion is

bound to the phenolic groups of two tyrosines (Tyr 95 and 188 in the N lobe and Tyr 426 and 517 in the C lobe), the imidazole group of one histidine (His 249 in the N lobe and His 585 in the C lobe) and the carboxylate side chain of an aspartic acid (Asp 63 in the N lobe and Asp 392 in the C lobe) (*26;28*). The fifth and sixth coordination sites are filled by the synergistic carbonate anion, which acts as a bidentate ligand to the iron and also hydrogen bonds to residues at the terminus of a nearby α-helix (*26;28*). Figure 1.6, shows the iron binding site in N-terminal monoferric transferrin.

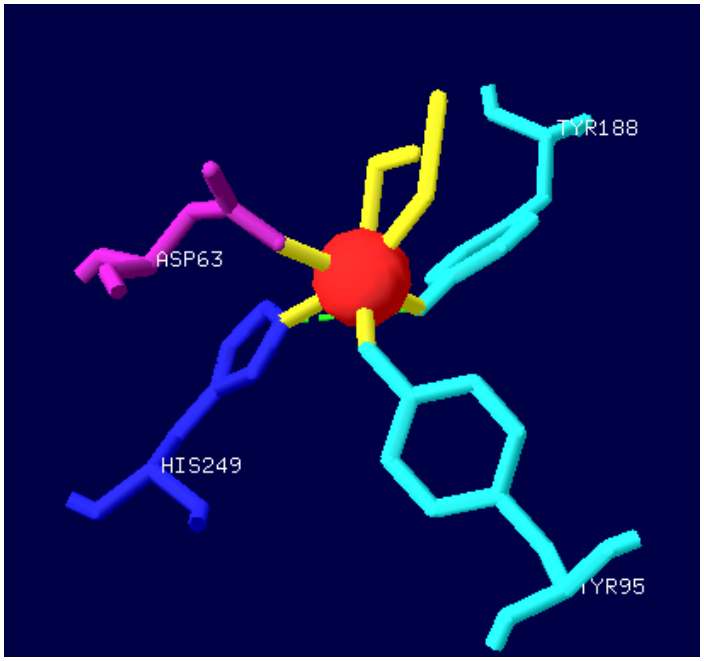

Figure 1.6. A representation of iron binding site in N-terminal human serum transferrin depicting the ligating residues and the synergistic carbonate anion

Apart from binding Fe^{3+}, a large number of di-, tri- and tetravalent metal ions have been reported to bind transferrins and are shown in Table 1.1. Normally serum transferrin tends to be about 30 % saturated with iron, so the remaining 70% is free to bind other metals (*32*). Even though these metals bind to transferrin, the affinity for Fe^{3+} remains the strongest.

Table 1.1.

Metal ions reported to bind transferrins (*33*)

Transition Metal Ions	V^{3+}, Cr^{3+}, $Mn^{2+/3+}$, $Fe^{2+/3+}$, $Co^{2+/3+}$, Ni^{2+}, Cu^{2+}, Zn^{2+}, Cd^{2+}, Hf^{4+}, Sc^{3+}
Lanthanides	$Ce^{3+/4+}$, Pr^{3+}, Nd^{3+}, Sm^{3+}, Eu^{3+}, Gd^{3+}, Tb^{3+}, Ho^{3+}, Er^{3+}, Yb^{3+}, Lu^{3+}
Actinides	Th^{4+}, U^{4+}, UO_2^{2+}, Np^{4+}, Pa^{4+}, Pu^{4+}, Am^{3+}, Cm^{3+}
P-Block Metal Ions	Al^{3+}, Ga^{3+}, In^{3+}, Tl^{3+}, Bi^{3+}

The binding of transferrins to the various metal ions has given rise to multiple applications. These metals can be categorized in groups depending on their importance: Tb^{3+}, Eu^{3+}, and Cu^{2+} are spectroscopically relevant, Mn^{2+} and Cr^{3+} are physiologically relevant, Al^{3+}, Th^{4+}, and Pu^{4+} are toxicologically relevant, and In^{3+} and Ga^{3+} are radiopharmaceutically important (*34-37*).

1.4

Anions in transferrin research

1.4.1.

Synergistic and nonsynergistic anions

Anions studied in the field of transferrin research have been categorized into two classes. The first class includes anions that participate in the binding of the iron to the protein and are described as "synergistic anions". The second class includes anions that are not involved in the binding of iron to the protein and are termed as "nonsynergistic anions". The requirement of a synergistic anion for metal binding is a unique feature of all transferrins. In human serum transferrin carbonate is the synergistic anion required under physiological conditions. The synergistic relationship between the carbonate and iron is due to the interdependence of both on each other for tight binding (*22*). In the absence of the metal, the anion binds weakly to apotransferrin, and in the absence of a synergistic anion, ferric ion hydrolyses rather than bind to apotransferrin.

In the early days of transferrin research, there were attempts to form a binary Fe-Tf complex in the absence of the carbonate synergistic anion. These all failed, and it is now universally accepted that Fe^{3+}, and most other metal ions, will not bind to apoTf in the absence of a synergistic anion (*20-22*). However, carbonate is not the only possible synergistic anion. A study of over 30 anion candidates was done by Schlabach and Bates (*38*). If carbonate is carefully excluded from the solution, then several carboxylic acids, such as oxalate, malonate, glyoxylate, acetoacetate, ketomalonate, nirilotriacetate, and pyruvate can serve as a synergistic anion to form a ternary Fe-anion-Tf complex. It was concluded that all synergistic anions must have a carboxylate group and a proximal

electron donor group. An interlocking sites model for metal and anion binding was proposed in which a carboxylate group of the anion bridges the positively charged groups on the protein and the proximal functional group binds to the metal (*38*). Furthermore, the carboxylate could have one substituent at the carbon α to the carboxylate, but disubstitution at the α-carbon negated the formation of a Fe-anion-Tf ternary complex, presumably due to unfavorable steric effects. These non-physiological ternary complexes are typically quite weak. Oxalate was the only anion that formed a complex with stability comparable to the Fe-carbonate-Tf complex (*38*).

Inorganic anions such as sulfate, sulfite, nitrate, nitrite, borate and phosphate, which have similarities with carbonate with respect to size, structure, charge, hydrogen bonding and ability to function as ligands for the transition metal ion, were also selected for synergistic anion replacement studies (*38*). There was no evidence for the formation of an Fe-anion-Tf ternary complex with any of these anions, and it was concluded that inorganic anions do not substitute for carbonate. Hence all these anions were classified as nonsynergistic anions.

1.4.2.

Binding of anions to apotransferrin

In the 1980s, it was reported that the binding of anions to apoTf could be monitored by using difference UV spectroscopy (*39*). Anion-binding equilibrium constants were measured by direct titrations of apoTf with a series of anions, which produce a negative peak at 245 nm in the UV spectrum. Studies on a series of inorganic anions showed that the binding of bicarbonate to apoTf in the absence of iron is relatively

weak. Divalent anions such as sulfate and HPO_4^{2-} bind more strongly to apoTf, but the resulting binary anion-Tf complex is not capable of binding iron. Among the inorganic anions that have been studied to date, only carbonate gives a binary species capable of binding iron. Dicarboxylates were also evaluated for their binding with apoTf and were found to have binding constants 1 log unit smaller than those for diphosphonates (*40*). On the basis of the binding constants, the binding strength of anions to transferrin has been assigned in the following order: PPi > other phosphonates > phosphate > sulfate > bicarbonate > chloride > perchlorate.

Studies on the mutants K206A, K296A, and R124A of the N-lobe transferrin have indicated that anions bind in the interdomain cleft of apoTf (*41*). Another crystallographic study on apo-ovotransferrin in the presence of ammonium sulfate shows the binding of two sulfate anion within the cleft, indicating the presence of two sulfate binding sites (*25*).

EPR studies of iron transferrin complexes were conducted with 18 different anions, which were divided into three groups: 1) carboxylates with a proximal polar group, 2) dicarboxylates with an additional polar group and 3) dicarboxylates or carboxyamides (*42*). The results produced a modification in the Schlabach and Bates model (*38*) for the mode of anion binding. These studies proposed a model in which the synergistic anions bind as bidentate ligands, with coordination of both carboxylate and proximal groups. This bidentate coordination of the anion to the iron is consistent with carbonate, dicarboxylate anions and other difunctional anions (*42*).

The addition of anions to diferrictransferrin does not produce a difference UV spectrum, presumably because the Fe^{3+} ion is coordinated to the two tyrosine residues

that are responsible for the difference UV spectrum of the anion-apoTf binary complex and blocks anion binding at this site. However, the binding of anions to diferric Tf has been detected by EPR difference spectroscopy (*43*). These studies presented a mathematical model and proposed the paired binding of anions to the protein i.e. four anions bind to diferric Tf, two in each lobe, with positive cooperativity.

The overall association constant for anion binding to diferric transferrin followed the sequence thiocyanate > perchlorate > pyrophosphate > adenosine triphosphate > chloride >> tetrafluoroborate, orthoborate, adenosine monophosphate, fluoride, sulfate and bicarbonate (*43*). This series resembles the lyotropic series, (*44;45*) which is an arrangement of salts, anions or cations in ascending order of their effect on certain physical properties of proteins, with $F^- < SO_4^{2-} < HPO_4^{2-} < CH_3CO_2^- < Cl^- < Br^- < NO_3^- < I^- < CCl_3CO_2^- < ClO_4^- < SCN^-$.

1.5.

Transferrin and transferrin receptor mediated endocytosis

Transferrin delivers iron into cells via receptor mediated endocytosis (*46;47*). Transferrin receptors are present on the outer surface of the cells and are selective for diferric transferrin (*48-50*). As the iron-loaded transferrin binds to the receptor, the transferrin receptor complex is internalized by clathrin coated pits, which form endocytic vesicles, as shown in Figure 1.7. An ATP driven pump lowers the pH of the endosome to 5.5 (*51;52*). This acidic environment facilitates the dissociation of iron from the transferrin, (*47*) which may also involve the reduction of Fe^{3+} to the more weakly bound Fe^{2+} (*53*). The iron is released into the cytoplasm and moved to mitochondria for heme

synthesis or to ferritin for storage. The receptor-bound apotransferrin recycles to the cell surface. The neutral pH at the cell surface promotes the dissociation of the apotransferrin from the receptor and returns it to the bloodstream for further cycles of iron delivery to cells. With a half life of about a week, an average molecule of transferrin may undergo up to 100 cycles of iron delivery (*54*).

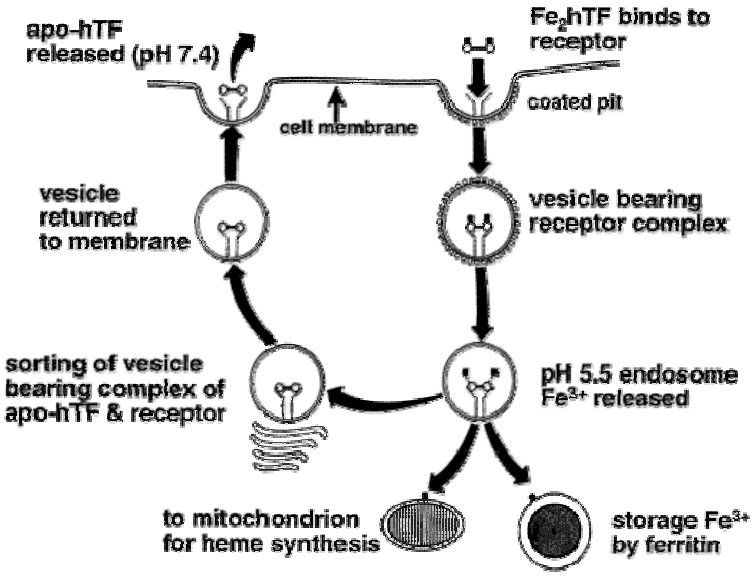

Figure 1.7. Receptor mediated endocytosis of transferrin (*32*)

1.6.

Iron overload

The human body regulates the overall level of iron only by varying the rate of iron absorption, primarily through the duodenum. There is no homeostatically-controlled mechanism for iron excretion (*55*). Acute iron toxicity is usually associated with the accidental ingestion of iron supplements by small children. Primary iron overload is

most often associated with a family of genetic disorders (referred to collectively as hereditary haemochromatosis) that lead to excessive iron uptake from the diet (*3;56*).

Most cases of hereditary haemochromatosis result from mutations in the regulatory protein HFE. The most common mutations in HFE are C282Y and H63D. A patient homozygous for the C282Y mutation will accumulate excessive levels of iron. The second mutation, H63D, is comparatively less prevalent, but when present in the heterozygous state along with the C282Y mutation, will also lead to haemochromatosis. (*57-60*).

The excessive uptake of iron observed in primary haemochromatosis is linked to the dysregulation of hepcidin, a 25 amino acid antimicrobial peptide that plays a central role in the regulation of iron homeostasis (*61*). Hepcidin binds to and regulates ferroportin, a membrane-bound protein that transports iron from intestinal mucosal cells into the blood (*62-64*). Mutations in HFE result in low levels of hepcidin in plasma, which allows increased iron uptake by ferroportin from intestines and leads to increased iron levels in the liver and other tissues (*61*).

The most common procedure for treating primary iron overload is therapeutic phlebotomy (*3;65;66*). The removal of a unit (400-500 ml) of blood from the patient removes about 250 mg of iron, and this treatment continues till the normal serum ferritin (30 μg/l) and transferrin saturation (less than 30%) levels are reached (*67*). Typically the removal of 2-4 units of blood per year will maintain overall iron balance (*3;66*).

There are other genetic disorders such as β-thalassemia that lead to severe anemia. Regular blood transfusions are required to treat the anemia, but this process bypasses the normal intestinal regulation of iron uptake (*3*). Thus the patient becomes severely iron-

overloaded from the iron entering the body via transfusion. This is referred to as secondary iron overload (*68;69*). Secondary iron overload, if untreated, can be fatal. The widely accepted treatment is to couple the transfusions with the use of chelating agents to remove iron, a process known as chelation therapy (*68;70-72*). Iron chelation therapy has been employed for over 50 years, and there has been extensive research in this area, with investigators searching for new synthetic compounds and performing various clinical studies characterizing the long term effects of known and new chelating agents. The following section describes existing and new ligands used in chelation therapy.

1.7.

Ligands for chelation therapy

Desferrioxamine B (DFO, Desferal) is a trihydroxamate microbial iron transport agent produced by *Streptomyces pilosus* (*73*). The structure of DFO is shown in Figure 1.8. This naturally occurring siderophore binds to iron(III) in 1:1 ratio with a stability constant of $10^{30.6}$, but it has a much lower affinity for other biological metal ions such as calcium and zinc (*74*). DFO has been used as an effective chelator since the 1970s and is clinically approved for iron chelation therapy.

In spite of being the most widely used iron chelator for the past 40-50 years, DFO has some disadvantages. DFO is not orally active and is rapidly metabolized in the body (*75*), hence it must be administered subcutaneously or intravenously by slow infusion pumps (*76*). The long infusion time of 8-12 h a day for 5-6 days a week leads to poor patient compliance (*76;77*). In addition this treatment is expensive, which limits its

availability to patients worldwide (*78*). To overcome these disadvantages, there is an extensive area of research focused on the development of orally effective iron chelators.

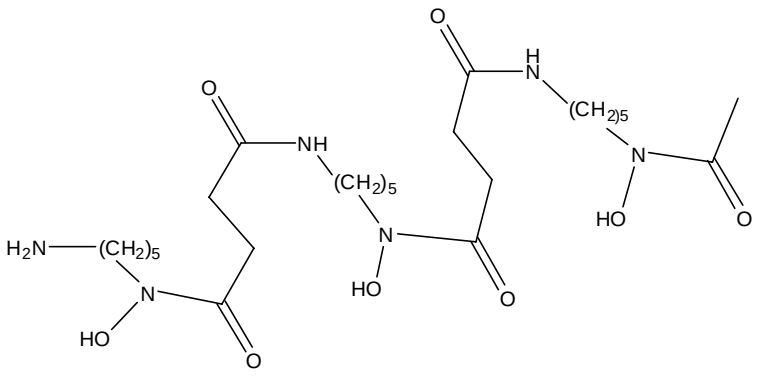

Figure 1.8. Structure of desferrioxamine B (DFO)

An effective chelator for ferric ion must have a high stability constant as well as rapid complexation kinetics (*73;79*). In addition, a chelator should possess in vivo efficacy and low toxicity (*73*). Ligands with structures similar to the siderophores and other strong binding ligands are under investigation for the replacement of DFO. The search for improved, orally effective chelators has led to the rediscovery of old ligands, like N, N'-bis(2-hydroxybenzyl)ethylenediamine-N,N'-diacetic acid (HBED) and 2-pyridylcarboxaldehydeisonicotinoylhydrazone (PCIH) (*78*). HBED has an affinity constant of $10^{39.6}$ for iron(III) and has a low affinity for other metal ions (*77*). HBED and dimethyl-HBED have been reported to be non-toxic in some animal studies and are under further clinical investigations (*80*).

Deferiprone (L1, Ferriprox), shown in Figure 1.9, is a prospective ligand for iron chelation therapy that has been under investigation for many years (*71;81;82*). Unlike

the hexadentate DFO molecule, L1 acts as a bidentate ligand via the 3-hydroxy and 4-keto functional groups and forms a stable FeL_3 complex (*83*).

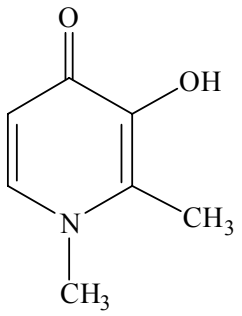

Figure 1.9. Structure of Deferiprone (L1)

The hydroxypyridinone (HOPO) functional group of L1 offers many of the same advantages as the hydroxamate group of DFO. This group binds strongly and selectively to high-valent metal ions like Fe^{3+}, with weaker binding to essential transition metal ions such as Zn^{2+}, and almost no binding affinity for Ca^{2+} (*74*). Moreover, as a neutral low-molecular-weight compound, it is well absorbed from the gut (*84*). Initial clinical studies reported concerns over its long term safety due to several side effects, such as neutropenia, agranulocytosis, zinc deficiency, and gastrointestinal disturbances (*71;76*). A case of progressive hepatic fibrosis was also reported (*81*), and this complication is still controversial. With more studies reported (*82;85*), a safety profile has been established for deferiprone, with certain guidelines to monitor during therapy (*86;87*). The disadvantages of deferiprone therapy are that not all patients reach negative iron levels and the need for a weekly blood count due to the risk of agranulocytosis (*71;87*).

Combined chelation therapy using DFO and L1 has also been reported (*88*), and the preliminary studies suggest that this can be a potential new approach to treat iron overload (*78;85*).

The HOPO group has been incorporated into hexadentate ligands by both Hider and Raymond (*89-92*). The ligands N,N,N-tris[2-(3-hydroxy-2-oxo-1,2-dihydroxypyridin-1-yl)-acetamidoethyl]amine (CP130) (*93*) and TREN-(Me-3,2-hydroxypyridonate), TREN HOPO (*94*) have been prepared as both 3-hydroxy- and 1-hydroxypyridin-2-ones respectively. The hexadentate ligand TREN-(Me-3,2-hydroxypyridonate) has shown promising results in rat studies compared with its bidentate counterparts (*91*), but as yet there is no success in chelation therapy.

In the meanwhile a new orally active iron chelating agent deferasirox (ICL670A) (*95*) has been developed by Novartis and is available for use in the United States (*87*). Deferasirox is 4-[3,5-bis-(hydroxyphenyl)-1,2,4-triazol-1-yl]-benzoic acid, as shown in Figure 1.10 (*96*). It is a tridentate chelator and binds iron(III) in a 2:1 ratio (*76*). It has been approved for the treatment of chronic iron overload in patients from the age of 2 years and older (*87*). Deferasirox can be easily administered orally once a day and has shown equivalency with desferrioxamine at high dosages (*76;87;97*). Due to the limited long term data, several questions may arise in terms of its effectiveness and safety. Further studies will determine the overall success of deferasirox. In the meanwhile more promising chelators are being synthesized. One such chelator, deferitrin, belongs to the ferrithiocin class of chelators and is undergoing preliminary trials (*87;98;99*).

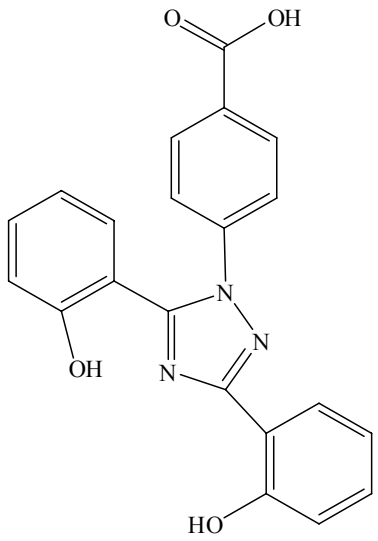

Figure 1.10. Structure of Deferasirox

Historically, chelation therapy has targeted the large amounts of iron stored intracellularly as a complex with the iron storage protein ferritin (*100;101*). Ferritin consists of 24 subunits which pack together to form a hollow sphere (*3*). The iron is stored in the interior of this sphere, and is physically inaccessible to most chelating agents. As a result, removing iron from ferritin is extraordinarily difficult (*100*). The most effective approach is a two-step process. The ferritin is incubated with a mixture of the chelating agent and a small reducing agent. The reducing agent is small enough to enter the protein shell and reduce the ferric ion to soluble ferrous ion, which then diffuses out of the protein and is captured by the chelating agent (*102;103*).

The iron in transferrin is a much more accessible target, as it is present in the serum, circulating freely in the body. In addition, by maintaining a low level of iron-

saturation for serum transferrin, one can avoid the oxidative damage from non-transferrin-bound-iron that is usually seen when iron overload leads to saturation of the transferrin binding capacity (*104*). The direct loss of iron to a chelator seems to be the most likely mechanism of iron release, but this process tends to be quite slow (*7*). Hence the need to study the kinetics of iron removal from transferrin.

1.8

Kinetic mechanisms for iron release

Iron release from transferrin is studied by monitoring changes in the spectral properties of the protein. The kinetic assays are most commonly done on a Uv-vis spectrophotometer or a fluorimeter. The paramagnetic ferric ion in holotransferrin quenches the intrinsic fluorescence of the protein, so that iron release results in an increase in fluorescence intensity (*105*). Whereas the absorbance in the ultraviolet and visible spectra increases due to the charge transfer band of the Fe(III) bound to the two tyrosine ligands, so on iron release there is a decrease in absorbance (*105*). For kinetic studies, the rate of iron release can be determined by monitoring the increase in fluorescence intensity or the decrease in absorbance with time.

Iron release kinetics have been studied using a wide range of ligand types, including catechols (*49;73;106-112*), hydroxamates (*107;113;114*), hydroxypyridinones (*111;114;115*), phosphonates (*116-127*), and aminocarboxylates (*128;129*). Early studies examined iron release from diferric transferrin (*73;79;113;116;118;119;121;126;130;131*). After methods were developed to prepare both forms of monoferric transferrin (C- and N-lobe) (*120;121*), most studies have used

one of the monoferric forms to avoid the complexity of the simultaneous release of iron at different rates from two sites. The degree of cooperativity between iron release from the two sites has been examined by monitoring iron release from one site while the kinetically inert Co^{3+} ion occupies the other site (*120;132*). Cooperativity has also been addressed by comparing iron release from N-lobe monoferric transferrin with iron release from the recombinant N-lobe half-transferrin molecule (*120;132;133*). Most studies report rather limited cooperativity between the two sites (*128;129;132;133*).

Over the years several different mechanisms for iron removal from transferrin have been proposed (*73;113;121;125;128;129;134*). These mechanisms are based on the kinetic order of the iron removal reaction with respect to the ligand concentration. The exact mechanism of iron release is not yet determined. In general there is a consensus that iron removal kinetics from transferrin fall into three categories: saturation kinetics, first order kinetics and complex kinetics (a combination of first order and saturation kinetics) as shown in Figure 1.11. The following sections describe the development of various mechanisms for iron release, with an emphasis on certain factors such as the binding of allosteric anions, which influences the iron release kinetics.

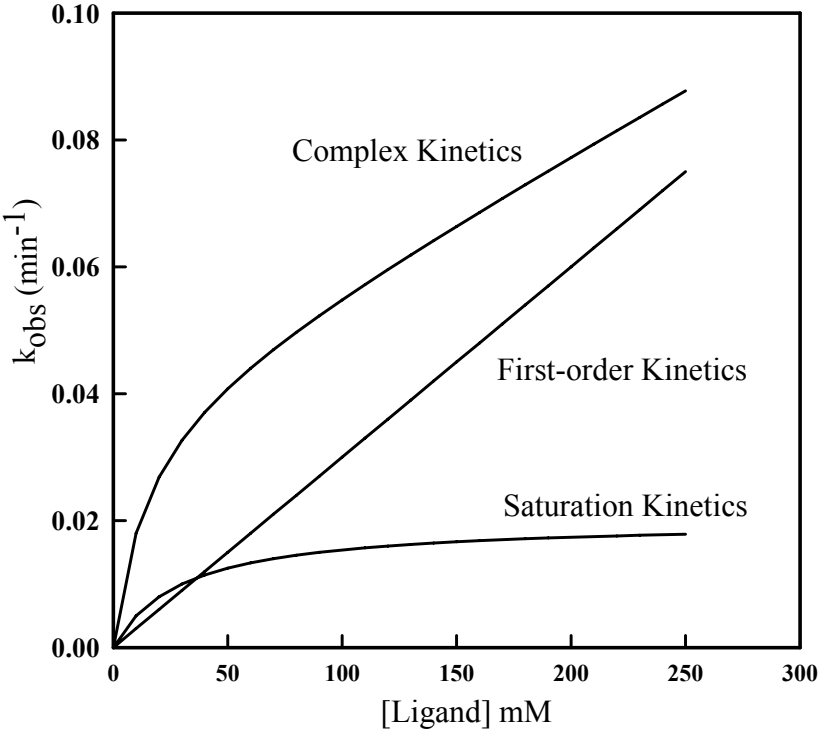

Figure 1.11. Simulated plots of k_{obs} versus ligand concentration that illustrate saturation, first order and complex kinetics

1.9.

Early iron release studies

The initial studies on iron removal from diferric transferrin were performed in the 1970s by using chelators like nitrilotriacetic acid (NTA), citrate and ethylenediaminetetraacetate (EDTA) (*126;135*). Egyed studied iron removal using physiological ligands such as adenosinetriphosphate (ATP), which might be involved in intracellular iron release (*127*). Around the same time two groups reported the percentage of iron removal from transferrin by various chelating agents. Pollack et al.

(*131*) performed iron removal from transferrin by using mixtures of the strong chelator desferrioxamine (DFO) with various weak chelators and anions that facilitate the transfer of iron from transferrin to DFO. Morgan investigated the ability of various cellular metabolites to release iron from transferrin on the basis of the rate at which they could transfer iron between rabbit transferrin and human apotransferrin. Pyrophosphate removed the maximum amount of iron, followed by ketomalonate, NTA, ATP and citrate (*126*). Some of these anions are also effective chelators (anionic ligands), and iron removal of these anionic ligands was also evaluated in the absence of DFO (*126*). Different trends were seen in the results.

Ligands also affect the rate of exchange of the synergistic carbonate anion. Aisen et al. (*20*) proposed that the ligands served as a temporary substitute for the carbonate, as shown in Figure 1.12.

$$FeTfH^{*}CO_3 + A^- \longrightarrow FeTfA + H^{*}CO_3^-$$

$$FeTfA + HCO_3^- \longrightarrow FeTf\ HCO_3^- + A^-$$

* ^{14}C

Figure 1.12. Carbonate exchange mechanism (*20*)

The effect of adenosine nucleotides and pyrophosphate (PPi) on the exchange of transferrin bound carbonate was investigated by Egyed (*127*). The exchange of carbonate in the ternary complex of transferrin was accelerated by adenosine triphosphate (ATP), adenosine diphosphate (ADP) and PPi, while adenosine monophosphate (AMP), cyclic AMP and phosphate had no effect. ATP has been proposed to accelerate carbonate

exchange but does not remove any iron, and PPi was proposed to replace the anion as well as remove iron from the ternary complex. These studies also proposed two mechanisms explaining how ATP, as opposed to PPi, is found within the endosome and might play a direct role in intracellular iron release.

Morgan investigated the effect of several phosphate compounds and iron chelators as mediators of iron release and also studied the effect of hydrogen ion concentration on iron release (*135*). The rate of iron release was accelerated in the presence of several mediators and also with an increase in the hydrogen iron concentration. Morgan's work with mediators at high concentration indicated the presence of saturation kinetics. A two-step reaction mechanism was proposed. The first step involved labilization of the iron by the interaction of hydrogen ion with the transferrin-iron-anion complex. The second step involved the release of iron from the transferrin by the mediator, forming a complex to facilitate the transfer of iron to the passive iron acceptor ligand, DFO (*135*).

1.10.

Saturation kinetics and its development

In the late 1970s Raymond and co-workers (*73*) began studies on iron release by synthetic catechols (*3,4-LICAMS and MECAM*), which were based on the structure of the siderophore enterobactin, a naturally occurring iron chelator. A hyperbolic dependence of the rate on the chelator concentration was observed. Carrano and Raymond (*73*) proposed a pre-equilibrium mechanism, which predicts the formation of a ternary intermediate consisting of Fe^{3+}, transferrin (Tf) and the competing ligand [L]. In the rate-limiting step, this ternary intermediate dissociates to release the iron from transferrin.

This mechanism was consistent with the observation of saturation kinetics, but there was no direct evidence of the formation of the proposed ternary intermediate complex.

Figure 1.13. Pre equilibrium mechanism for iron release from transferrin

Cowart et al. (*113*) investigated the release of iron by AHA and also observed saturation kinetics. However, they also studied the donation of iron from the $Fe(AHA)_3$ complex to apoTf. These studies on iron donation allowed them to characterize the spectrum of an Fe-AHA-Tf intermediate. This intermediate was not formed to a detectable level during iron removal, which eliminated Raymond's pre-equilibrium mechanism. They proposed a new mechanism as shown in Figure 1.14.

According to Cowart et al. (*113*), the observed saturation kinetics reflect the presence of a rate-limiting conformational change in ferric transferrin from a closed to an open form as shown in step 1 of Figure 1.14. Once the protein is in the open form, the incoming ligand binds to the iron and forms a quaternary complex L-Fe-CO_3-Tf, which then falls apart to release iron from the transferrin. In the closed conformation, the iron is well shielded from the incoming ligand. Thus the ligand can remove iron only when the protein is in the open conformation. At high concentrations of the ligand, i.e. under saturating conditions, the rate constant for iron release corresponds to the forward rate constant (k_1) for the conformational change from the "closed" native form to the "open" more reactive conformation of transferrin. The Bates mechanism is further supported by

the crystal structures of the 'closed' ferric transferrin and the 'open' apotransferrin form of the protein (*26;28;30;136*).

$$\text{Fe-CO}_3\text{-Tf} \underset{k_{-1}}{\overset{k_1}{\rightleftharpoons}} \text{Fe-CO}_3\text{-Tf*}$$

$$\text{Fe-CO}_3\text{-Tf*} + \text{L} \underset{k_{-2}}{\overset{k_2}{\rightleftharpoons}} \text{L-Fe-CO}_3\text{-Tf*}$$

$$\text{L-Fe-CO}_3\text{-Tf*} \underset{k_{-3}}{\overset{k_3}{\rightleftharpoons}} \text{FeL} + \text{Tf} + \text{CO}_3^{2-}$$

*Open conformation

Figure 1.14. Bates conformational change mechanism (*113*)

Ligands like acetohydroxamic acid (AHA) (*113;114*), 3,4-LICAMS (*109*), enterobactin (*73*), and 1,2-dimethyl-3-hydroxyl-4-pyridinone (L1) (*114*) show saturation kinetics with respect to the free ligand concentration. On the basis of this mechanism, the ligand dependence of the observed rate constant for iron removal is given by the equation (1.1),

$$k_{obs} = \frac{k_{max}[L]}{k_d + [L]} \qquad (1.1)$$

where, k_{max} is the rate constant under saturating conditions and k_d is a kinetic parameter corresponding to the ligand concentration at half saturation. If k_{max} simply represents the rate constant for the conformational change of the transferrin, then the rate should be

independent of the nature of the ligand. Studies have shown that many ligands have similar values for k_{max}, but there are significant deviations (*114;120;128;129;132;137*).

1.11

Effect of anions on iron release

Various salts of nonsynergistic and non-chelating anions (e.g. Cl^- and ClO_4^-) have been shown to affect the rates of iron release from transferrin (*114;138;139*). These anion effects have been studied extensively, but with rather confusing results. Some anions increase the rate of iron release, some decrease the rate of iron release, and some have no effect. The effect also varies between the C- and N-lobes of the protein. For example, perchlorate accelerates the rate of iron removal from the C-lobe, but retards iron removal from the N-lobe (*138*).

The anion effect can also depend on the chelating agent that is being used to remove the iron. At pH 7.4 chloride increased the rate of iron release from C-terminal monoferric transferrin by EDTA, but retarded iron release from N-terminal monoferric transferrin (*138;140*). In other studies at the same pH, chloride accelerated the iron release by citrate (*134*), AHA (*114*) and L1 (*114*) from both C-terminal Tf and N-terminal Tf. When used in the presence of PPi, Cl^- increased the rate of iron release from C-terminal monoferric Tf but had no effect on the rate of iron release from N-terminal monoferric Tf at pH 7.4 (*117;123*).

The anion studies suggested that binding of an anion to the protein can either increase or decrease k_{max}, depending on the specific combination of anion and ligand (*134;138*). It was proposed (*134*) that there is an allosteric **Ki**netically **S**ignificant **A**nion

Binding (KISAB) site, which is likely to play an important role in iron release kinetics. Raymond and coworkers (*107*) studied the rate of iron release by LICAMS as a function of the chloride concentration and concluded that the KISAB site must be occupied by an anion for any iron release to occur. Site directed mutagenesis (*75;141*) and computational studies (*142*) have attempted to locate the KISAB site, but the exact location is still unclear.

In the closed structure of the transferrin N-lobe, Lys-206 and Lys-296, form a hydrogen bond which appears to help link the two N-lobe domains in the closed form of the protein. The presence of the hydrogen bond indicates that the two lysines share a single proton (*143*). It has been suggested that the addition of a second proton to this pair to form two charged lysine side chains would favor the open protein conformation, and thus could play a critical role as a trigger for iron release (*75*). Site directed mutagenesis on the recombinant N-lobe half-transferrin molecule (hTf/2N) has confirmed that mutation of either of the lysines to alanine, glutamate or glutamine dramatically slows down the rate of iron release (*75;141*).

1.12.

First order and complex kinetics

The original Bates mechanism (*113*) was consistent with iron release by ligands such as AHA and LICAMS, but subsequent studies have identified a variety of ligands that do not follow simple saturation kinetics with respect to the free ligand concentration. The aminocarboxylate ligands, nitrilotriacetic acid (NTA) (*129*) and

diethylenetriaminepentaacetic acid (DTPA) (*128*) show simple first order kinetics with respect to the ligand concentration.

Ligands like PPi (*117;119-122;125*) and aminophosphonic acids (*117;119;121;128;129*) follow complex kinetics, which is a combination of saturation and first order kinetics. At low concentrations these ligands follow saturation kinetics, but at higher concentrations of the ligand, the rate constant shows a linear increase rather than reaching a plateau. These complex kinetics can be described by equation (1.2).

$$k_{obs} = \frac{k_{max}[L]}{k_d + [L]} + k'[L] \qquad (1.2)$$

1.13

Proposed mechanisms to explain complex kinetics

Three mechanisms have been proposed to explain complex kinetics. The physical significance of the rate parameters in equation (1.2) depends on the mechanism.

1.13.1

Bertini's mechanism

Bertini and co-workers (*125*) observed complex kinetics for iron release by PP_i. They attributed the saturation component to the Bates conformational change mechanism and proposed that the linear increase in the rate constant at high ligand concentration is due to the binding of the anionic PP_i ligand to an allosteric binding site (the KISAB site) on the protein, as shown in Figure 1.15.

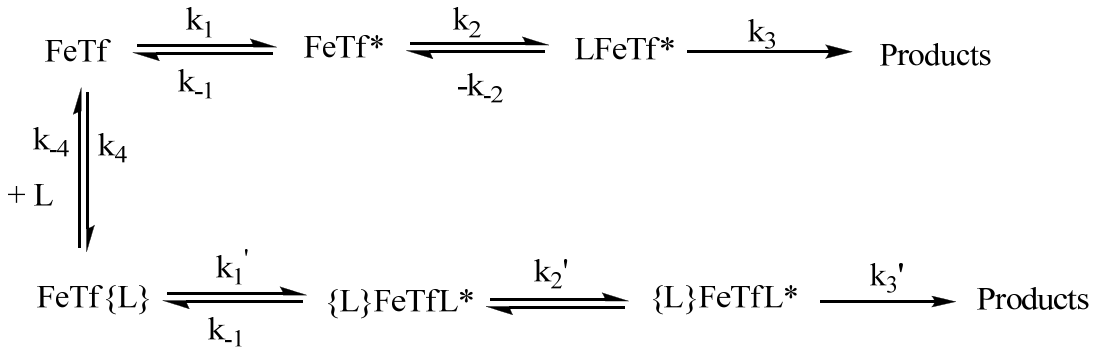

Figure 1.15. Bertini's mechanism for iron release by PP_i (*125*)

The { } brackets are used to indicate the binding of the anionic ligand to an allosteric site on the protein. In this mechanism, there are two saturation pathways one with the KISAB empty and one with the KISAB site occupied by the anionic ligand. In order to explain the linear increase at higher ligand concentration, it is necessary to assume that ligand binding to the KISAB site is far from saturation.

1.13.2

Egan's mechanism

According to Egan's model (*123;134*) there is no saturation component at all. Instead, he proposes that iron release takes place by two first order pathways, one fast and one slow, which are linked by an anion binding equilibrium. The representation of the Egan's model is shown in Figure 1.16, where the { } brackets represent the KISAB site.

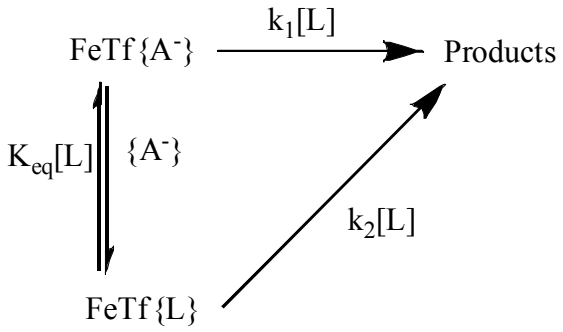

Figure 1.16. Egan's mechanism for iron release

At low ligand concentration, the KISAB site is occupied by the anion from the buffer or from the added salts, while at high ligand concentrations, the ligand competes with the anion to occupy the KISAB site. Under these conditions, k_{obs} is defined by the equation,

$$k_{obs} = \frac{(k_1[L] + k_2 K_{eq}'[L]^2)}{(1 + K_{eq}'[L])} \quad (1.3)$$

$$K_{eq} = \frac{[\{L\}FeTf][A]}{[\{A\}FeTf][L]} \quad (1.4)$$

$$K'_{eq} = \frac{K_{eq}}{[A]} \quad (1.5)$$

Egan accounts for the downward curvature in the plot of k_{obs} versus ligand concentration as a consequence of the fact that $k_2 < k_1$. In order to account for simple saturation kinetics, one would have to assume that k_2 is essentially zero.

1.13.3

Harris' mechanism for iron release

Harris and co-workers accepted the Bates mechanism for the saturation component (*116;119;132*). Since neutral ligands tended to follow saturation kinetics, while anionic ligands often followed complex kinetics, they proposed that the first order component represents a separate reaction pathway for iron release that involves the slow replacement of the synergistic carbonate anion by the incoming ligand, followed by the rapid dissociation of ternary Fe-L-Tf complex (*116;132*), as shown in Figure 1.17.

$$\text{Fe-}CO_3^{2-}\text{-Tf} + L \xrightarrow{\text{slow}} \text{Fe-L-Tf} + CO_3^{2-}$$

$$\text{Fe-L-Tf} \xrightarrow{\text{fast}} \text{apo-Tf} + \text{Fe-L}$$

Figure 1.17. Proposed mechanism for first-order component of iron removal

If a ligand can function as a suitable replacement for the synergistic carbonate anion, then it can follow this pathway for iron release. Ligands like NTA (*129*) show simple first order kinetics and appear to utilize this pathway exclusively, while ligands like pyrophosphate (PP_i) (*119;129*), and *N*,*N*-bis(phosphonomethyl)glycine (DPG) (*119;129*) show complex kinetics, which indicates that they use both the conformational change and carbonate substitution pathways to release iron from transferrin.

Iron release by phosphonoacetic acid (PAA) has been studied extensively in our lab (*137;144*). The rate of iron release was shown to slow down with the elongation of the ligand and with disubstitution at the central methylene group of PAA. The half lives

of iron removal by PAA, monobenzyl and dibenzyl derivatives of PAA were measured, and it was found that the half life of iron release increased from 20 min for PAA to 30 min for the monobenzyl PAA to more than 600 min for dibenzyl PAA (*137*). This pattern is consistent with the early studies that established structural criteria for compounds that are able to substitute for the bicarbonate synergistic anion (*38*). For example, glycolate and lactate can both substitute for carbonate. But the addition of a second methyl substituent to form methyllactate destroys the ability to substitute for carbonate.

Other evidence in support of this model comes from a study which involved iron release by pyrophosphate (PP_i) and tripolyphosphate (TPP) (*137*). Iron release by PP_i follows complex kinetics, whereas iron release by TPP follows simple saturation kinetics. It was proposed that the first order component is not seen with the longer TPP because the additional phosphate group prevents this compound from replacing the synergistic carbonate anion (*137*). PP_i and PAA can form six membered chelate rings and are expected to serve as synergistic anions (*137;144*). The presence of a first order component for PP_i and PAA further supports the hypothesis that the ability to function as a synergistic anion is a key requirement for a ligand to remove iron via the first order pathway.

Most of the groups agree that a conformational change of the protein is required for the incoming ligand to access the iron binding site of the transferrin using the saturation pathway. The first-order pathway that some ligands can use still needs to be characterized more clearly. It is likely that iron removal kinetics follows a combination of more than one mechanism.

1.14

Variation in k_{max}

According to the Bates conformational change mechanism, as discussed in section 1.10, $k_{max,}$ the maximum rate constant, is the forward rate constant for the conformational change from the close to the open form of ferric transferrin as shown in Figure 1.5. This conformational change occurs prior to any interaction with the ligand, and thus the value of k_{max} for all ligands should be the same. However this is not the case. The k_{max} values for iron removal from both the C-terminal and N-terminal sites vary by about an order of magnitude for the ligands that have been studied to date (*128;144*). This assessment excludes the results for iron release by NTA and DTPA, which show k_{max} values of zero (*128;129*).

Can this variation in k_{max} be linked to the anionic effects ? As discussed in earlier sections, anions are known to alter the rate of iron release by binding to the allosteric KISAB site. Raymond and co-workers have proposed the absolute requirement of some sort of anion binding for the conformational change to occur followed by iron release (*107;110*). Zak et al. (*145*) have proposed that anionic ligands are in competition with inorganic anions such as chloride to occupy KISAB site. The anion effects are inconsistent, as some anions increase the rate of iron release and some decrease the rate of iron release. Thus anion effects might either increase or decrease the k_{max} value.

Our group speculates that the variation in k_{max} might reflect the binding of anionic ligands to the allosteric KISAB site (*137;144*). In this model, an anionic ligand might self-regulate the rate of iron release by binding to the KISAB site in addition to chelating the iron. We are also interested in the extent to which anion binding alters the rate of iron

removal through the proposed first order pathway. To address these issue, we have chosen a set of reference ligands, consisting of AHA and L1, which show simple saturation kinetics (*113;114*), and NTA and DTPA, which show simple first order kinetics (*119;128;129*). We have evaluated the impact on iron release by these reference ligands from the addition of simple, non-chelating anions as well as the addition of chelating anions.

References

1. Harris, W. R. (2002) in *Molecular and cellular iron transport* (Templeton, D. M., Ed.) pp 1-40, *Marcel Dekker Inc.*, New york.

2. Lippard, S. J. and Berg, J. M. (1994) *Principles of bioinorganic chemistry* University Science Books.

3. Crichton, R. R. (2009) *Iron Metabolism-From molecular mechanisms to clinical consequences* Wiley.

4. Andrews, N. C. (2000) *Nat Rev Genet 1*, 208-217.

5. Andrews, N. C. and Schmidt, P. J. (2007) *Ann. Rev. of Physiol. 69*, 69-85.

6. Lindley, P. F. (1996) *Reports on Progress in Physics 59*, 867-933.

7. Aisen, P. (1998) in *Metal Ions in Biological Systems Iron transport and storage in Microorganisms, Plants and Animals* (Sigel, A. and Sigel, H., Eds.) pp 585-631, Marcel Dekker, New York.

8. Baker, E. N. and Lindley, P. F. (1992) *J. Inorg. Biochem. 47*, 147-160.

9. Chasteen, N. D. (1977) *Coordination Chemistry Reviews 22*, 1-36.

10. Baker, E. N. (1994) *Adv. Inorg. Chem. 41*, 389-463.

11. Anderson, B. F., Baker, H. M., Dodson, E. J., Norris, G. E., Rumball, S. V., Waters, J. M., and Baker, E. N. (1987) *Proc. Natl. Acad. Sci. U. S. A 84*, 1769-1773.

12. Farnaud, S., Amini, M., Rapisarda, C., Cammack, R., Bui, T., Drake, A., Evans, R. W., Rahmanto, Y. S., and Richardson, D. R. (2008) *The International Journal of Biochemistry & Cell Biology 40*, 2739-2745.

13. Woodbury, R. G., Brown, J. P., Yeh, M. Y., Hellstrom, I., and Hellstrom, K. E. (1980) *Proc. Natl. Acad. Sci. U. S. A 77*, 2183-2187.

14. Dunn, L. L., Sekyere, E. O., Suryo Rahmanto, Y., and Richardson, D. R. (2006) *Carcinogenesis 27*, 2157-2169.

15. Nowalk, A. J., Burroughs Tencza, S., and Mietzner, T. A. (1994) *Biochemistry 33*, 12769-12775.

16. Bruns, C. M., Nowalk, A. J., Arvai, A. S., Mc Tigue, M. A., Vaughan, K. G., Mietzner, T. A., and McRee, D. E. (1997) *Nature Structural Biology 4*, 919-924.

17. Mietzner, T. A. and Morse, S. A. (1994) *Ann. Rev. Nutr. 14*, 471-493.

18. Taboy, C. H., Vaughan, K. G., Mietzner, T. A., Aisen, P., and Crumbliss, A. L. (2001) *J. Biol. Chem. 276*, 2719-2724.

19. Dhungana, S., Taboy, C. H., Anderson, D. S., Vaughan, K. G., Aisen, P., Mietzner, T. A., and Crumbliss, A. L. (2003) *Proc. Natl. Acad. Sci. U. S. A 100*, 3659-3664.

20. Aisen, P., Leibman, A., Pinkowitz, R. A., and Pollack, S. (1973) *Biochemistry 12*, 3679-3683.

21. Price, E. M. and Gibson, J. F. (1972) *Biochem. Biophys. Res. Commun. 46*, 646-651.

22. Bates, G. W. and Schlabach, M. R. (1973) *FEBS Letters 33*, 289-292.

23. Bailey, S., Evans, R. W., Garratt, R. C., Gorinsky, B., Hasnain, S., Horsburgh, C., Jhoti, H., Lindley, P. F., and Mydin, A. (1988) *Biochemistry 27*, 5804-5812.

24. Anderson, B. F., Baker, H. M., Morris, G. E., Rumball, S. V., and Baker, E. N. (1990) *Nature 344*, 784-787.

25. Mizutani, K., Yamashita, H., Mikami, B., and Hirose, M. (2000) *Biochemistry 39*, 3258-3265.

26. Zuccola, H. J. (1992) *The crystal structure of monoferric human serum transferrin (Ph.D. thesis)* Georgia Institute of Technology, Atlanta, GA.

27. Wally, J., Halbrooks, P. J., Vonrhein, C., Rould, M. A., Everse, S. J., Mason, A. B., and Buchanan, S. K. (2006) *J. Biol. Chem. 281*, 24934-24944.

28. MacGillivray, R. T. A., Moore, S. A., Chen, J., Anderson, B. F., Baker, H., Luo, Y., Bewley, M., Smith, C. A., Murphy, M. E. P., Wang, Y., Mason, A. B., Woodworth, R. C., Brayer, G. D., and Baker, E. N. (1998) *Biochemistry 37*, 7919-7928.

29. Baker, E. N., Baker, H. M., and Kidd, R. D. (2002) *Biochemistry and cell biology 80*, 27-34.

30. Jeffrey, P. D., Bewley, M. C., MacGillivray, R. T. A., Mason, A. B., Woodworth, R. C., and Baker, E. N. (1998) *Biochemistry 37*, 13978-13986.

31. Baker, H. M., Anderson, B. F., and Baker, E. N. (2003) *Proc. Natl. Acad. Sci. U. S. A 100*, 3579-3583.

32. Sun, H., Li, H., and Sadler, P. J. (1999) *Chem. Rev. 99*, 2817-2842.

33. Harris, W. R. (1998) in *Less Common Metals in Proteins and Nucleic Acid Probes* pp 121-162, Springer Berlin / Heidelberg.

34. Donovan, J. W. and Ross, K. D. (1975) *J. Biol. Chem. 250*, 6022-6025.

35. Harris, W. R., Carrano, C. J., Pecoraro, V. L., and Raymond, K. N. (1981) *J. Am. Chem. Soc. 103*, 2231-2237.

36. Harris, W. R. and Pecoraro, V. L. (1983) *Biochemistry 22*, 292-299.

37. Aisen, P., Aasa, R., and Redfield, A. (1969) *J. Biol. Chem. 244*, 4628-4633.

38. Schlabach, M. R. and Bates, G. W. (1975) *J. Biol. Chem. 250*, 2182-2188.

39. Harris, W. R. (1985) *Biochemistry 24*, 7412-7418.

40. Harris, W. R. and Nesset-Tollefson, D. (1991) *Biochemistry 30*, 6930-6936.

41. Harris, W. R., Cafferty, A. M., Trankler, K., Maxwell, A., and MacGillivray, R. T. (1999) *Biochim. Biophys. Acta 1430*, 269-280.

42. Dubach, J., Gaffeny, B. J., More, G. R., and Eaton, S. S. (1991) *Biophys J. 59*, 1091-1100.

43. Folajtar, D. A. and Chasteen, D. N. (1982) *J. Am. Chem. Soc. 104*, 5775-5780.

44. Zhang, Y., Furyk, S., Bergbreiter, D. E., and Cremer, P. S. (2005) *J. Am. Chem. Soc. 127*, 14505-14510.

45. Zhang, Y. and Cremer, P. S. (2006) *Curr. Opin. Chem. Biol. 10*, 658-663.

46. Iacopetta, B. J. and Morgan, E. H. (1983) *J. Biol. Chem. 258*, 9108-9115.

47. Hradilek, A. and Neuwirt, J. (1987) *Journal of Cellular Physiology 133*, 192-196.

48. Williams, S. C. and Woodworth, R. C. (1973) *J. Biol. Chem. 248*, 5848-5853.

49. Konopka, K., Bindereif, A., and Neilands, J. B. (1982) *Biochemistry 21*, 6503-6508.

50. Hemadi, M., Kahn, P. H., Miquel, G., and El Hage Chahine, J.-M. (2004) *Biochemistry 43*, 1736-1745.

51. Sipe, D. M. and Murphy, R. F. (1987) *Proc. Natl. Acad. Sci. U. S. A 84*, 7119-7123.

52. Kohno, H. and Tokunaga, R. (1985) *J. Biochem. 97*, 1181-1188.

53. Trinder, D. and Morgan, E. (2002) in *Molecular and Cellular Iron Transport* (Templeton, D. M., Ed.) pp 427-449, Dekker Marcel, New York.

54. Jandl, J. H. and Katz, A. H. (1963) *J. Clin. Invest. 42*, 314-326.

55. Batts, K. P. (2007) *Mod Pathol 20*, S31-S39.

56. Pippard, M. J. (1994) (Brock, J. H., Halliday, J. W., Pippard, M. J., and Powell, L. W., Eds.) pp 271-309, W. B. Saunders, London.

57. Longo, F., Zecchina, G., Sbaiz, L., Fischer, R., Piga, A., and Camaschella, C. (1999) *Haematologica 84*, 799-803.

58. Merryweather-Clarke, A. T., Pointon, J. J., Shearman, J. D., and Robson, K. J. (1997) *J. Med. Gen. 34*, 275-278.

59. McLaren, C. E., Li, K. T., Gordeuk, V. R., Hasselblad, V., and McLaren, G. D. (2001) *Blood 98*, 2345-2351.

60. Gottschalk, R., Seidl, C., Schilling, S., Braner, A., Seifried, E., Hoelzer, D., and Kaltwasser, J. P. (2010) *European Journal of Immunogenetics 27*, 129-134.

61. Lee, P. L. and Beutler, E. (2009) *Annual Review of Pathology: Mechanisms of Disease 4*, 489-515.

62. Papanikolaou, G., Tzilianos, M., Christakis, J. I., Bogdanos, D., Tsimirika, K., MacFarlane, J., Goldberg, Y. P., Sakellaropoulos, N., Ganz, T., and Nemeth, E. (2005) *Blood 105*, 4103-4105.

63. Ganz, T. (2004) *Current Opinion in Hematology 11*.

64. Nicolas, G., Bennoun, M., Devaux, I., Beaumont, C., Grandchamp, B., Kahn, A., and Vaulont, S. (2001) *Proc. Natl. Acad. Sci. U. S. A 98*, 8780-8785.

65. Angelucci, E., Muretto, P., Lucarelli, G., Ripalti, M., Baronciani, D., Erer, B., Galimberti, M., Giardini, C., Gaziev, D., Polchi, P., and the Italian Cooperative Group for Phlebotomy Treatment of Transplanted Thalassemia Patients (1997) *Blood 90*, 994-998.

66. Adams, P. C. (2002) in *Molecular and Cellular Iron Transport* (Templeton, D. M., Ed.) pp 699-724, Dekker Marcel, New York.

67. Pietrangelo, A. (2006) *Ann. Rev. Nutr. 26*, 251-270.

68. Kushner, J. P., Porter, J. P., and Olivieri, N. F. (2001) *Hematology 2001*, 47-61.

69. Weatherall, D. J. (1981) in *Development of iron chelators for clinical use* (Martell, A. E., Anderson, W. F., and Badman, D. G., Eds.) pp 3-12, Elsevier, New York.

70. Giardini, C., Galimbbrti, M., Lucarelli, G., Polchi, P., Angelucci, E., Baronciani, D., Gaziev, D., Erer, B., La Nasa, G., Barbanti, I., and Muretto, P. (1995) *British Journal of Haematology 89*, 868-873.

71. Olivieri, N. F., Brittenham, G. M., Matsui, D., Berkovitch, M., Blendis, L. M., Cameron, R. G., McClelland, R. A., Liu, P. P., Templeton, D. M., and Koren, G. (1995) *N Engl J Med 332*, 918-922.

72. Olivieri, N. F. and Brittenham, G. M. (1997) *Blood 89*, 739-761.

73. Carrano, C. J. and Raymond, K. N. (1979) *J. Am. Chem. Soc. 101*, 5401-5404.

74. Liu, Z. D. and Hider, R. C. (2002) *Coordination Chemistry Reviews 232*, 151-171.

75. He, Q. Y., Mason, A. B., Tam, B. M., MacGillivray, R. T. A., and Woodworth, R. C. (1999) *Biochemistry 38*, 9704-9711.

76. Neufeld, E. J. (2006) *Blood 107*, 3436-3441.

77. Hershko, C. (1998) *British Journal of Haematology 101*, 399-406.

78. Wong, C. and Richardson, D. R. (2003) *The International Journal of Biochemistry & Cell Biology 35*, 1144-1149.

79. Rodgers, S. J. and Raymond, K. N. (1983) *J Med Chem 26*, 439-442.

80. Bergeron, R. J., Wiegand, J., and Brittenham, G. M. (2002) *Blood 99*, 3019-3026.

81. Olivieri, N. F., Brittenham, G. M., McLaren, C. E., Templeton, D. M., Cameron, R. G., McClelland, R. A., Burt, A. D., and Fleming, K. A. (1998) *N Engl J Med 339*, 417-423.

82. Hoffbrand, A. V., AL-Refaie, F., Davis, B., Siritanakatkul, N., Jackson, B. F. A., Cochrane, J., Prescott, E., and Wonke, B. (1998) *Blood 91*, 295-300.

83. Dobbin, P. S., Hider, R. C., Hall, A. D., Taylor, P. D., Sarpong, P., Porter, J. B., Xiao, G., and van der Helm, D. (1993) *J Med Chem 36*, 2448-2458.

84. Liu, D. Y., Liu, Z. D., and Hider, R. C. (2002) *Best Practice & Research Clinical Haematology 15*, 369-384.

85. Hoffbrand, A. V., Cohen, A., and Hershko, C. (2003) *Blood 102*, 17-24.

86. Cohen, A., Galanello, R., Piga, A., De Sanctis, V., and Tricta, F. (2003) *Blood 102*, 1583-1587.

87. Cohen, A. (2006) *Hematology 2006*, 42-47.

88. Wonke, B., Wright, C., and Hoffbrand, A. V. (1998) *British Journal of Haematology 103*, 361-364.

89. Streater, M., Taylor, P. D., Hider, R. C., and Porter, J. (1990) *J Med Chem 33*, 1749-1755.

90. White, D. L., Durbin, P. W., Jeung, N., and Raymond, K. N. (1988) *J Med Chem 31*, 11-18.

91. Yokel, R. A., Fredenburg, A. M., Durbin, P. W., Xu, J., Rayens, M. K., and Raymond, K. N. (2000) *Journal of Pharmaceutical Sciences 89*, 545-555.

92. Xu, J., O'Sulliva, B., and Raymond, K. N. (2002) *Inorg. Chem. 41*, 6731-6742.

93. Xiao, G., van der Helm, D., Hider, R. C., and Dobbin, P. S. (1995) *Inorg. Chem. 34*, 1268-1270.

94. Bergeron, R. J., Wiegand, J., McManis, J. S., and Bharti, N. (2006) *J Med Chem 49*, 7032-7043.

95. Cappellini, M. D. (2005) *Best Practice & Research Clinical Haematology 18*, 289-298.

96. Hershko, C., Konijn, A. M., Nick, H. P., Breuer, W., Cabantchik, Z. I., and Link, G. (2001) *Blood 97*, 1115-1122.

97. Choudhry, V. P. and Naithani, R. (2007) *Indian Journal of Pediatrics 74*, 759-764.

98. Donovan, J. M., Yardumian, A., Gunawardena, K. A., Plone, M. A., and Wonke, B. (2004) *Blood 104*, 504.

99. Donovan, J. M., Plone, M. A., Dagher, R., Bree, M., and Marquis, J. (2005) *Annals of the New York Academy of Sciences 1054*, 492-494.

100. Tufano, T. P., Pecoraro, V. L., and Raymond, K. N. (1981) *Biochim. Biophys. Acta 668*, 420-428.

101. Chasteen, N. D. (1998) in *Metal Ions in Biological Systems* (Sigel, A. and Sigel, H., Eds.) pp 479-514, Marcel Dekker Inc., New York.

102. Boyer, R. F. and McCleary, J. (1987) *Free Radical Biology and Medicine 3*, 389-395.

103. Montiero, H. P., Vile, G. F., and Winterbourn, C. C. (1989) *Free Radical Biology and Medicine 6*, 587-591.

104. Hershko, C., Link, G., and Cabantchik, Z. I. (1998) *Annals of the New York Academy of Sciences 850*, 191-201.

105. Lehrer, S. S. (1969) *J. Biol. Chem. 244*, 3613-3617.

106. Weitl, F. L., Harris, W. R., and Raymond, K. N. (1979) *J Med Chem 22*, 1281-1283.

107. Kretchmar Nguyen, S. A., Craig, A., and Raymond, K. N. (1993) *J. Am. Chem. Soc. 115*, 6758-6764.

108. Harris, W. R., Raymond, K. N., and Weitl, F. L. (1981) *J. Am. Chem. Soc. 103*, 2667-2675.

109. Kretchmar, S. A. and Raymond, K. N. (1986) *J. Am. Chem. Soc. 108*, 6212-6218.

110. Kretchmar, S. A. and Raymond, K. N. (1988) *Inorg. Chem. 27*, 1436-1441.

111. Turcot, I., Stintzi, A., Xu, J., and Raymond, K. N. (2000) *J. Biol. Inorg. Chem. 5*, 634-641.

112. Kretchmar, S. A. and Raymond, K. N. (1989) *BioMetals 2*, 65-68.

113. Cowart, R. E., Kojima, N., and Bates, G. W. (1982) *J. Biol. Chem. 257*, 7560-7565.

114. Li, Y. and Harris, W. R. (1998) *Biochim. Biophys. Acta 1387*, 89-102.

115. Scarrow, R. C., White, D. L., and Raymond, K. N. (1985) *J. Am. Chem. Soc. 107*, 6540-6546.

116. Harris, W. R. (1984) *J. Inorg. Biochem. 21*, 263-276.

117. Harris, W. R. and Bali, P. K. (1988) *Inorg. Chem. 27*, 2687-2691.

118. Cowart, R. E., Swope, S., Loh, T. T., Chasteen, N. D., and Bates, G. W. (1986) *J. Biol. Chem. 261*, 4607-4614.

119. Harris, W. R., Rezvani, A. B., and Bali, P. K. (1987) *Inorg. Chem. 26*, 2711-2716.

120. Bali, P. K. and Harris, W. R. (1989) *J. Am. Chem. Soc. 111*, 4457-4461.

121. Bali, P. K. and Harris, W. R. (1990) *Arch. Biochem. Biophys. 281*, 251-256.

122. Marques, H. M., Egan, T. J., and Pattrick, G. (1990) *South African Journal of Science 86*, 21-24.

123. Egan, T. J., Ross, D. C., Purves, L. R., and Adams, P. A. (1992) *Inorg. Chem. 31*, 1994-1998.

124. Bertini, I., Hirose, J., Kozlowski, H., Luchinat, C., Messori, L., and Scozzafava, A. (1988) *Inorg. Chem. 27*, 1081-1086.

125. Bertini, I., Hirose, J., Luchinat, C., Messori, L., Piccioli, M., and Scozzafava, A. (1988) *Inorg. Chem. 27*, 2405-2409.

126. Morgan, E. H. (1979) *Biochim. Biophys. Acta 580*, 312-326.

127. Egyed, A. (1975) *Biochim. Biophys. Acta 411*, 349-356.

128. Harris, W. R., Bali, P. K., and Crowley, M. M. (1992) *Inorg. Chem. 31*, 2700-2705.

129. Bali, P. K., Harris, W. R., and Nesset-Tollefson, D. (1991) *Inorg. Chem. 30*, 502-508.

130. Bates, G. W., Billups, C., and Saltman, P. (1967) *J. Biol. Chem. 242*, 2816-2821.

131. Pollack, S., Vanderhoff, G., and Lasky, F. (1977) *Biochim. Biophys. Acta 497*, 481-487.

132. Harris, W. R. and Bao, G. (1997) *Polyhedron 16*, 1069-1079.

133. Li, Y., Harris, W. R., Maxwell, A., MacGillivray, R. T., and Brown, T. (1998) *Biochemistry 37*, 14157-14166.

134. Marques, H. M., Watson, D. L., and Egan, T. J. (1991) *Inorg. Chem. 30*, 3758-3762.

135. Morgan, E. H. (1977) *Biochim. Biophys. Acta 499*, 169-177.

136. Mizutani, K., Yamashita, H., Kurokawa, H., Mikami, B., and Hirose, M. (1999) *J. Biol. Chem. 274*, 10190-10194.

137. Brook, C. E., Harris, W. R., Spilling, C. D., Peng, W., Harburn, J. J., and Srisung, S. (2005) *Inorg. Chem. 44*, 5183-5191.

138. Baldwin, D. A. and De Sousa, D. M. R. (1981) *Biochem. Biophys. Res. Commun. 99*, 1101-1107.

139. He, Q. Y., Mason, A. B., Nguyen, V., MacGillivray, R. T., and Woodworth, R. C. (2000) *Biochem. J. 350*, 909-915.

140. Williams, J., Chasteen, N. D., and Moreton, K. (1982) *Biochem. J. 201*, 527-532.

141. Nurizzo, D., Baker, H. M., He, Q. Y., MacGillivray, R. T. A., Mason, A. B., Woodworth, R. C., and Baker, E. N. (2001) *Biochemistry 40*, 1616-1623.

142. Amin, E. A., Harris, W. R., and Welsh, W. J. (2004) *Biopolymers 73*, 205-215.

143. Dewan, J. C., Mikami, B., Hirose, M., and Sacchettini, J. C. (1993) *Biochemistry 32*, 11963-11968.

144. Harris, W. R., Brook, C. E., Spilling, C. D., Elleppan, S., Peng, W., Xin, M., and Wyk, J. V. (2004) *J. Inorg. Biochem. 98*, 1824-1836.

145. Zak, O., Aisen, P., Crawley, J. B., Joannou, C. L., Patel, K. J., Rafiq, M., and Evans, R. W. (1995) *Biochemistry 34*, 14428-14434.

Chapter 2

Materials and Methods

This chapter provides detailed information about the methods and materials required during the course of the studies on the kinetics of iron release. The preparation of proteins, along with the techniques used to quantify the proteins, such as spectrophotometry and electrophoresis, are included. The solutions of ligands and buffers used during the kinetic studies of iron release are listed. This chapter also discusses the spectroscopic methods, such as Uv-vis spectroscopy and fluorescence spectroscopy that were used to follow iron removal from transferrin.

All solutions were prepared by using Millipore MilliQ water. This system purifies the building deionized water further to remove any organic and inorganic contaminants to give a resistance of 18 mΩ cm^{-1}. The experiments done during this study involve transferrin, a high-affinity Fe(III)-binding protein, and other chelators. Hence it was important to maintain metal free conditions. All glassware and containers used during the course of the study were soaked in acid overnight and then washed thoroughly with Millipore water.

2.1

Preparation of solutions

2.1.1

Preparation of HEPES buffer

N-2-Hydroxyethylpiperazine-N'-2-ethanesulfonic acid (HEPES) was the buffer used in all studies. A 0.1 M solution was prepared by dissolving 23.83 g of HEPES in Millipore water and adjusting the pH to 7.4 by the addition of concentrated sodium hydroxide solution. The pH was confirmed after a final dilution to one liter. The pH was monitored with a Fischer accumet 25 pH meter equipped with a combination electrode that was calibrated with pH 7.0 and pH 4.0 buffers. The pH of the buffer solution was monitored on a daily basis before starting the kinetic experiments.

2.1.2

Preparation of HEPES and sodium perchlorate buffer

A buffer solution of 0.1 M was prepared by dissolving 12.24 g of sodium perchlorate ($NaClO_4$) and 23.83 g of HEPES in Millipore water. The final dilution was made to one liter and the pH was adjusted to 7.40.

2.1.3

Preparation of iron solutions

Ferric ion stock solutions were prepared by dissolving solid ferric chloride in standardized 0.1 M nitric acid. The final concentration of the ferric ion was determined by complexometric titrations with EDTA (*1*). The stock solution is stable due to the low pH, which prevents hydrolysis of the ferric ion.

Ferric nitrilotriacetic acid ($Fe(NTA)_2^{3-}$) was prepared by adding 2 equivalents of NTA to a known quantity of ferric ion and diluting to volume. The final pH of these

solutions was approximately 3. All solutions of the $Fe(NTA)_2$ were freshly prepared to avoid the slow hydrolysis of the ferric ion.

2.1.4

Preparation of ligand solutions

The ligands used in this study were commercially available as high-purity compounds. Acetohydroxamic acid (AHA), phosphonoacetic acid (PAA), sodium methanesulfonate (SMS), 3-phosphonopropionic acid (3-PPA), N-(phosphonomethyl)iminodiacetic acid (PIDA), methylenediphosphonic acid (MDP), nitrilotriacetic acid (NTA), diethylenetriaminepentaacetic acid (DTPA) and 2,3-dihydroxypyridine (2,3-DHP) were purchased from Sigma Aldrich. Methylphosphonic acid (MPA) and the dipotassium salt of methane disulfonic acid (MDS) were purchased from Fluka. The disodium salt of 1,2-ethanedisulfonic acid (EDS) was purchased from Eastman Kodak company. 1,2-Ethylene diphosphonic acid (EDP) was purchased from Lancaster. 1,2-Dimethyl-3-hydroxy-4-pyridone (L1) was purchased from Acros Organics. 5-Chloro-2,3-dihyroxypyridine was purchased from Alfa Aesar. Phosphonoacetaamide (PAM) and 1-methyl-3-hydroxy-2-pyridone (3HMPY) were prepared at UMSL by Dr. Spilling's group. The ligand stock solutions were prepared in 0.1 M HEPES buffer and adjusted to pH 7.4.

2.2

Preparation, purification, confirmation and quantitation of proteins

The iron free (apo) and diferric (holo) forms of human serum transferrin were purchased from Sigma Aldrich. The commercially available apo and holo transferrin

were further purified to remove low-molecular-weight (LMW) components. All the absorbance measurements were recorded by CARY 100 Bio Uv-vis spectrophotometer.

2.2.1

Purification of Apotransferrin

Apotransferrin was purified by following literature procedures (*2*). Approximately 200 mg of solid apotransferrin was dissolved in 8 ml of 0.1 M HEPES/ perchlorate buffer at pH 7.4. The apotransferrin solution was then transferred to a 10 ml Amicon ultrafiltration cell fitted with an XM-50 filter membrane, which has a molecular weight cut off filter of 50 kDa. As the name suggests, this membrane retains the protein but allows small chelates and inorganics to be removed. The stirrer was then set to a relatively slow speed, and a pressure of about 60 psi N_2 was applied to the Amicon cell to force buffer through the filter and reduce the volume to 1 ml. The cell was refilled with 0.1 M HEPES 6-8 times to ensure complete removal of perchlorate. The final concentrated protein was transferred to a small vial through a syringe filter to remove debris that accumulates in the solution during ultrafiltration.

The UV-vis spectrum of the apotransferrin was recorded between 240-600 nm on a Cary 100 spectrophotometer. A baseline for 0.1 M HEPES was recorded and stored. The protein concentration was determined by diluting 50 µl of protein in 1000 µl of 0.1 M HEPES buffer. A protein spectrum was recorded as shown in Figure 2.1. A single protein peak at 278 nm was observed. The molar extinction coefficient at 278 nm of 93,000 $M^{-1}cm^{-1}$ (*3*) was used to determine the apotransferrin concentration for the dilute solution, and appropriate dilution factors were used to calculate the exact concentration for the concentrated apotransferrin stock solution. The sample was confirmed to be iron

free by the lack of a Fe-protein charge-transfer peak at 465 nm and also by using urea-PAGE electrophoresis as described in the following section.

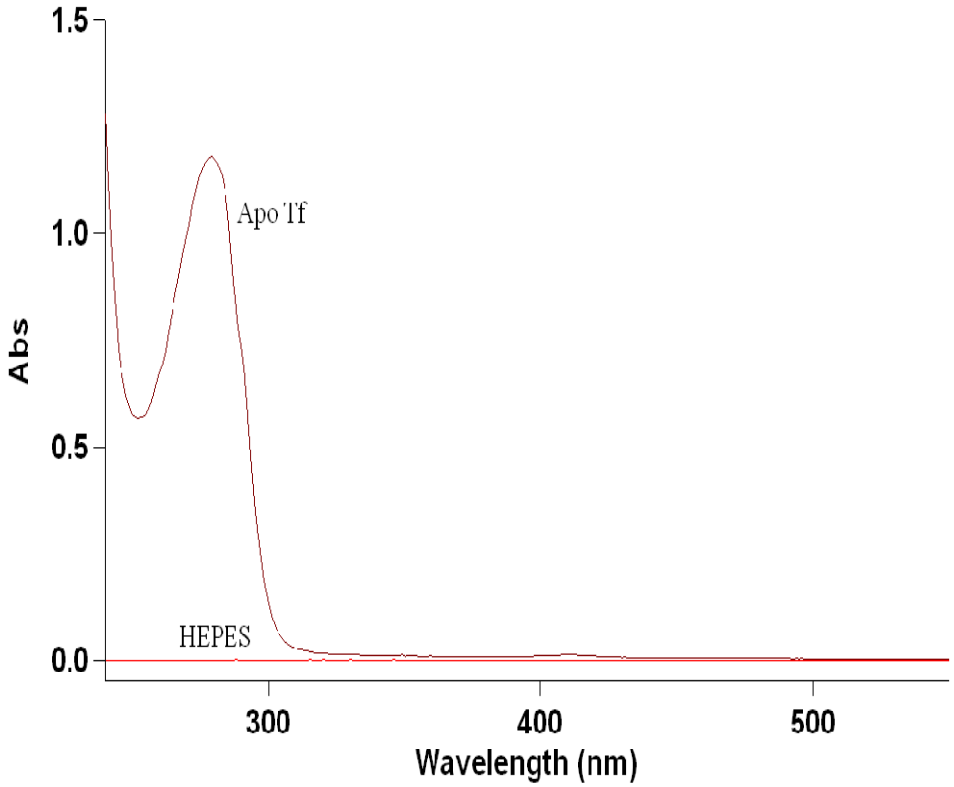

Figure 2.1. UV-vis spectrum of apotransferrin in 0.1 M HEPES buffer at pH 7.4. The baseline trace for 0.1 M HEPES is shown in red. The trace in brown color is for the 50 fold dilution of the stock apotransferrin.

2.2.2

Preparation of Diferric (Holo) transferrin

Approximately 200 mg of solid diferric transferrin was dissolved in 8 ml of 0.1 M HEPES/perchlorate buffer at pH 7.4. The protein solution was transferred in a 10 ml Amicon ultrafiltration cell fitted with a XM-50 filter membrane. The protein was washed

with 0.1 M HEPES buffer 6-8 times to remove the perchlorate and any other low-molecular-weight contaminants. The UV-vis spectrum of diferric transferrin is shown in Figure 2.2, with the protein peak in the UV range and the Fe^{3+}-tyrosine charge transfer peak in the visible range.

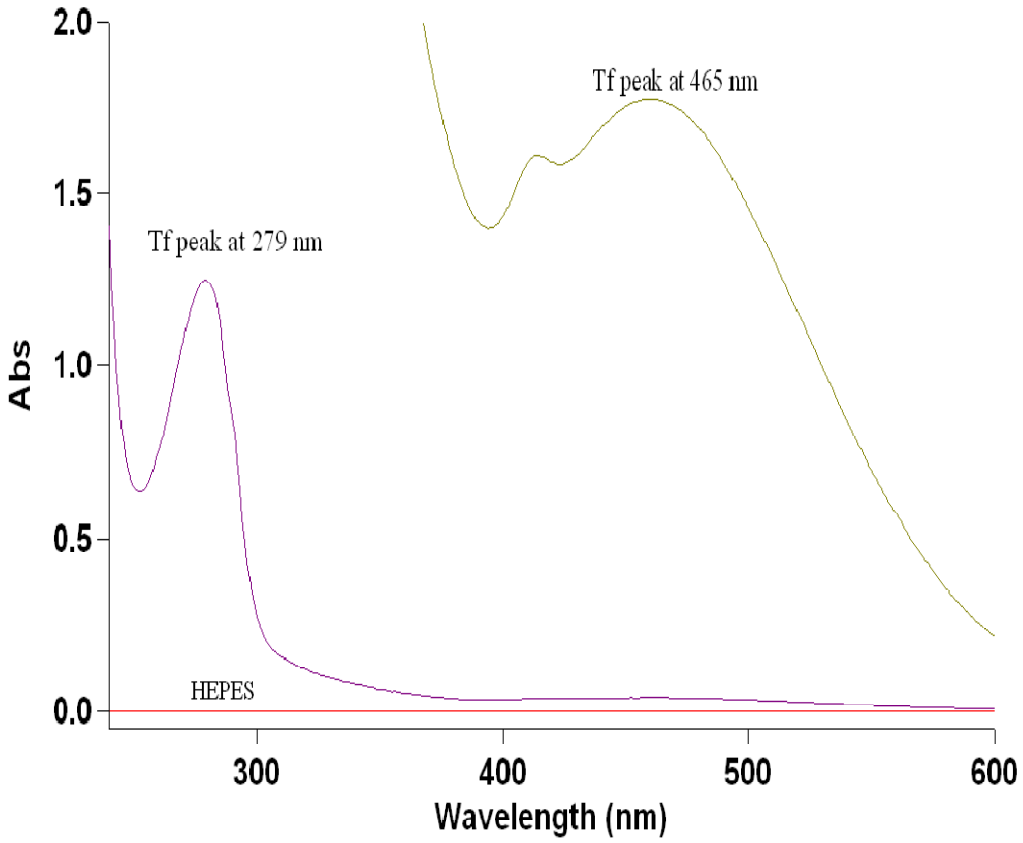

Figure 2.2. The UV-vis spectrum of diferric transferrin in 0.1 M HEPES buffer at pH 7.4. The baseline trace for 0.1 M HEPES is shown in red. The trace in purple is for the 50 fold dilution of the stock diferric transferrin. The trace in green is for the undiluted stock solution of diferric transferrin.

The protein concentration of the purified diferric transferrin was calculated from the UV-vis spectrum using a molar extinction coefficient of 113,000 $M^{-1}cm^{-1}$ at 278 nm (*3*). The iron concentration was determined by using a molar extinction coefficient of 5,000 $M^{-1}cm^{-1}$ at 465 nm (*3*). The iron:protein ratio was estimated from the ratio of the concentrations of iron and protein. Solutions with a ratio of 2.0 ± 0.05 were used in subsequent studies. The purity of the diferric transferrin was also confirmed by urea-PAGE.

2.2.3

Preparation of C- terminal monoferric transferrin

C-terminal monoferric transferrin was prepared from apotransferrin by the addition of one equivalent of $Fe(NTA)_2$ following procedures in the literature (*3;4*). It is well-established that NTA delivers Fe^{3+} selectively to the C-terminal binding site (*3-5*). A weighed amount of solid sodium bicarbonate corresponding to 5 mM was added to an aliquot of apotransferrin. The pH of the protein was adjusted to pH 6.0 and an $Fe(NTA)_2$ solution was added drop wise with constant stirring. The solution was allowed to equilibrate for about 20 min.

The iron loaded protein was then washed extensively with 0.1 M HEPES buffer in an Amicon ultrafiltration cell fitted with an XM50 filter membrane to remove any traces of the NTA that was used for the delivery of the ferric ion to the protein. The absorbances at 278 nm and 465 nm were measured, and the concentration of the protein and the ferric ion were determined using the extinction coefficients of 103,000 $M^{-1}cm^{-1}$ and 2950 M^{-1} cm^{-1}, respectively (*3*). The percentage of transferrin binding sites occupied by iron was calculated from the iron and protein concentrations. The selective binding at

the C-terminal site was confirmed by using urea-PAGE electrophoresis discussed in detail in section 2.3.

2.2.4

Preparation of N- terminal monoferric transferrin

N-terminal monoferric transferrin was prepared from diferric transferrin by following a modified version of a literature procedure (*3;4*). It is known from the literature that perchlorate accelerates iron removal by EDTA from the C-terminal site and retards release of iron from the N-terminal site (*4*). One ml of diferric transferrin was added to 3 ml of 2.67 M sodium perchlorate and 0.134 M ethylenediaminetetraacetic acid (EDTA). The removal of iron by EDTA was monitored by following the change in absorbance at 465 nm until the absorbance was 50% of the initial absorbance value. The above solution was then transferred to an Amicon ultrafiltration cell and washed 6 times with 0.1 M HEPES buffer to remove the $NaClO_4$, Fe-EDTA and free EDTA. The concentration of the protein was determined from the absorbance at 465 nm using an extinction coefficient of 2150 M^{-1} cm^{-1} and at 278 nm with an extinction coefficient of 103,000 $M^{-1}cm^{-1}$ (*3*). The selective loading of iron into the N-terminal binding site was confirmed using urea-PAGE electrophoresis.

2.3

Urea-PAGE gel electrophoresis

Commercial tris-boric acid-urea (TBE) denaturing gels for the Protean 3 mini-gel electrophoresis cell were purchased from Bio-Rad laboratories. The composition of the gels is 5% polyacrylamide-methylene-bis-acrylamide, 1.0-2.5% tris(hydroxylmethyl)-

aminomethane (tris), with 35-40% urea. The gel was removed from the packaging, and the comb was removed carefully from the wells without causing any damage to the wells. The wells were then washed with Millipore water to ensure that they were free from any urea. Protein samples were analyzed using a slight modification of the procedure published by Makey and Seal (*6*).

2.3.1

Solutions prepared for urea-PAGE electrophoresis

The TBE running buffer containing 89 mM tris base, 89 mM boric acid and 2 mM EDTA was prepared in Millipore water and adjusted to pH 8.3. The TBE sample loading buffer containing 45 mM tris base, 45 mM boric acid, 1 mM EDTA, 3.5 M urea, 0.005% bromophenol blue and sucrose was prepared and stored at 4 ˚C. A 0.27% solution of Coomassie blue R 250 in 500 ml methanol, 100 ml glacial acetic acid and 500 ml Millipore water was used as a staining solution. The destaining solution was prepared by mixing 100 ml of methanol and 150 ml of glacial acetic acid, and diluting to a final volume of 2 L with Millipore water.

Samples were loaded with a 2-20 µl Eppendorf pipetter with a gel loading pipette tip attached to ensure the accurate loading on the gel. The tip was disposed of after every loading to prevent contamination of the protein samples. Each well on the gel was loaded with 5 µg of protein contained in a 10 µl sample volume. The sucrose in the sample loading buffer holds the sample in the well until the electrophoresis is started. A 1:1 ratio of loading buffer to transferrin sample was used. The stock transferrin samples were stored in the refrigerator at 4 ˚C.

Gels were run for 4.5 hours at a constant voltage of 100 V using a Biorad Model 500/200 power supply. The initial current was about 20 mA. On completion of the run, the precast gel was removed from the mini protean electrophoresis cell, and the gel was carefully removed from the plastic plates. The gel was stained by soaking in the staining solution for half an hour, followed by destaining. The destaining solution was exchanged till the background color was removed and the bands were clearly visible on the gel. Once the gel was visibly destained, it was scanned on the Dell A920 scanner and the pictures were saved. A typical Urea-PAGE gel is shown in Figure 2.3.

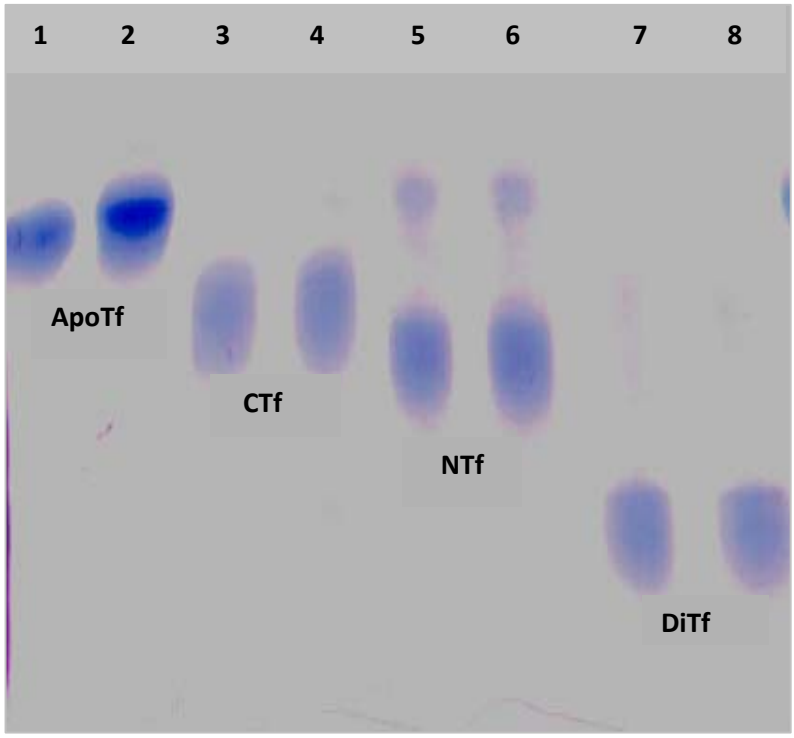

Figure 2.3. 5% TBE-Urea PAGE, with the characteristic bands for the four forms of transferrin denoted as ApoTf for apotransferrin, CTf for C-terminal monoferric transferrin, NTf for N-terminal monoferric transferrin and DiTf for diferric transferrin.

2.4

Instrumentation

The main emphasis of our research is the kinetics of iron release from transferrin protein by low-molecular-weight chelating agents. These reactions can be monitored by following the changes in the Uv-visible or fluorescence spectrum of the protein (*7*). These changes are measured on the instruments listed below.

2.4.1

Uv-vis Spectrophotometer

Uv-vis absorbance spectra were measured on a dual beam Varian Cary 100 spectrophotometer equipped with a temperature control accessory and a multicell holder transport accessory. The Cary Win UV software was used to operate the instrument. All experiments were carried out at 25 °C, pH 7.4 in 0.1 M HEPES. A protein concentration of about 30 μM was used in the experiments.

2.4.2

Fluorescence spectrophotometer

Fluorescence spectra were recorded using a Jobin Yvon Horiba FluroMax-3 spectrofluorometer. This instrument is equipped with a four-cuvette rotating sample holder. The cell holder was attached to an external water bath to control the temperature. The FluoroMax-3 was operated using the DataMax spectroscopy software provided by the manufacturer. A protein concentration of approximately 1.0 μM was used in the experiments. The emission intensity was recorded using an excitation wavelength of 280 nm and an emission wavelength of 338 nm with a band pass of 3 nm for both excitation

and emission slits. Wavelength calibrations for both the excitation and emission monochrometers were performed regularly using xenon lamp and water Raman scans as described by the manufacturer.

2.5

Kinetic assays for the effect of anions on iron removal from transferrin by the saturation and first order pathways

2.5.1

Ligands that follow saturation kinetics

The ligands acetohydroxamic acid and deferiprone follow saturation kinetics for iron release by transferrin (*8*). Iron release from C-terminal monoferric transferrin by 200 mM AHA was monitored for 4.5 hours. Similarly, iron release from C-terminal monoferric transferrin by 20 mM deferiprone (L1) was monitored for 10 hours.

2.5.2

Ligands that follow first order kinetics

The ligands nitrilotriacetic acid and diethylenetriaminepentaacetic acid follow first order kinetics for iron release from transferrin (*9;10*). Iron release from C-terminal monoferric transferrin by 100 mM NTA was monitored for 4.5 hours. Similarly, iron release from C-terminal monoferric transferrin by 200 mM DTPA was monitored for 10 hours.

2.5.3

Effect of simple anions

The anions methanesulfonate, methylenedisulfonate, ethylenedisulfonate, methylphosphonate, 3-phosphonopropionate, and phosphonoacetaamide are not effective

chelating agents, and were classified as simple anions to indicate that they were incapable of removing iron from C-terminal transferrin. Iron release reactions with ligands that follow saturation (AHA and L1) and or first order pathway (NTA and DTPA) were monitored in the presence of increasing concentrations of these anions. To better compare results with and without anions, reactions were run side-by-side in two cuvettes. It was presumed that any change in the overall rate of iron release in the presence of these non-chelating molecules was a reflection of their binding at the KISAB on transferrin in such a way as to alter the rate of iron release by the reference ligand (i.e. AHA, L1 or NTA).

2.5.4

Effects of iron chelating anions

Some anions like phosphonoacetate and methylenediphosphonate are known to function as iron chelating agents (*11*). The effect of these iron chelating anions were monitored on the ligands that follow saturation or first order pathway for iron removal from transferrin. For these systems, in order to account for any day to day fluctuations in rate constants, three reactions were run simultaneously: one with the reference ligand that follows saturation or first order pathway alone, one with the chelating anion alone and one with a mixture of the reference ligand and the chelating anion.

In the cuvette with the mixture of reference ligand and chelating anion, the overall rate of iron release would reflect the combined rates of the two chelating agents. To partition this overall rate between the two compounds, it was assumed that the reference ligands had no allosteric effect on the chelating anions. Whenever the rate of the mixture was different from the sum of the rates of the individual components, it was assumed that

the deviation was due to an allosteric effect of the chelating anion on the rate of iron release by the reference ligand.

2.6

Data analysis

2.6.1

Kinetic assays for iron removal from ferric transferrin.

C-terminal monoferric transferrin was used to determine the rate constant for iron removal. The ligand was always in large excess to provide pseudo first order kinetics with respect to iron removal. The value of k_{obs} is calculated for each ligand concentration from a least squares fit of fluorescence intensity or absorbance versus time.

At high concentrations of ligand, the iron removal reactions go to completion, and the kinetic data are fit to equation (2.1).

$$I_t = \left(I_o - I_\infty\right)e^{-k_{obs}\,t} + \quad I_\infty \qquad (2.1)$$

where, I_0, I_∞ and I_t are the intensities at time zero, at infinite time and at any intermediate time t, and k_{obs} is the first order rate constant. Depending on the type of methods used the intensity (I) obtained from the fluorimeter can be replaced by absorbance (A) as measured using the UV-vis spectrophotometer.

The release of iron from transferrin is a reversible process. At low ligand concentrations, the reaction does not go to completion. Instead, it reaches equilibrium as shown in equation 2.2.

$$\text{Fe-Tf} + \text{L} \underset{k_r}{\overset{k_f}{\rightleftharpoons}} \text{Fe-L} + \text{Apo-Tf} \qquad (2.2)$$

Even when the reactions do not go to completion, there is still a significant excess of ligand over transferrin, so this equilibrium is pseudo first order in the forward direction. However, the products, FeL and apoTf, are produced in equimolar concentrations, so the reaction is second order in the reverse direction. The treatment of such systems is described by Moore and Pearson (*12*). For these systems, the final intensity (I_e), is the intensity at equilibrium. The final intensity that would have been observed if the reaction had gone to completion (I_∞) was obtained from a parallel reaction run using a ligand concentration high enough to force the iron removal reaction to go to completion. For reactions going to equilibrium, the intensity change at any intermediate time (ΔI_t) is $I_t - I_0$ where I_0 is the intensity at time zero. The value of ΔI_t as the function of time is given by the equation 2.3.

$$\Delta I_t = \frac{\Delta I_0 \Delta I_e \left(e^{k_f \alpha t} - 1\right)}{\Delta I_0 - \Delta I_e + \Delta I_0 e^{k_f \alpha t}} \qquad (2.3)$$

where, $\Delta I_0 = I_\infty - I_0$, $\Delta I_e = I_e - I_0$, $\alpha = \frac{\left(2\Delta I_0 - \Delta I_e\right)}{\left(\Delta I_e\right)}$ and k_f is the rate constant for iron release in equation (2.2). Rate constants were calculated by using equation (2.1) or equation (2.3) and are referred to as k_{obs}.

2.6.2

Effect of simple anions on the saturation and first order pathways for iron release from transferrin

The simple (i.e. non-chelating) anions used in this study are listed in section 2.5.1. Pseudo-first-order rate constants were measured for paired samples of the reference ligand, one with and one without the added anion The change in the apparent rate of iron release by the reference ligand is expressed as shown in equation (2.4),

$$\%\Delta k = \frac{k'_{obs} - k_{obs}}{k_{obs}} \; x100 \qquad (2.4)$$

where k_{obs} is the rate constant for iron release by the reference ligand alone, and k'_{obs} is the rate constant for the same concentration of the reference ligand in the presence of the added anion. The reference ligands and their concentrations were AHA (200 mM), L1 (20 mM), NTA (100 mM) and DTPA (200 mM).

2.6.3

Effect of chelating anions on the saturation and first order pathways for iron release from transferrin

Pseudo-first-order rate constants were measured simultaneously in three cuvettes, one for the reference ligand (L), one for the chelating anion (A) and one for the mixture of ligand and anionic ligand (L+A). The apparent rate constant for iron release reflected the combination of iron release by the ligand (L) and the chelating anion (A) as shown in equation (2.5). If there are no allosteric effects, the observed rate constant for the mixture should be the sum of the rate constants of the two components. When the observed rate constant of the mixture is other than the simple sum of the rates for the two

components, it is assumed that the chelating anion has acted allosterically to alter the rate of iron release by the reference ligand. This altered rate of iron release by the reference ligand is referred to as k_{app}, and is calculated as shown in equation (2.5)

$$k_{app}(L) = k_{obs}(L + A) - k_{obs}(A) \qquad (2.5)$$

The effect of the chelating anion on the reference ligand was expressed as shown in equation (2.6)

$$\%\Delta k_{obs} = \frac{k_{app}(L) - k_{obs}(L)}{k_{obs}(L)} \times 100 \qquad (2.6)$$

The program SigmaPlot from SYSTAT was used extensively to analyze the data. The analyses involved some library functions from Sigmaplot as well as some user-defined functions coded and stored in the program. SigmaPlot was also used to prepare all the graphs contained in this dissertation.

References

1. Welch, F. J. (1958) *Analytical Uses of Ethylenediaminetetraacetic acid* Van Nostrand, Princeton, NJ.

2. Harris, W. R., Wang, Z., Brook, C., Yang, B., and Islam, A. (2003) *Inorg. Chem. 42*, 5880-5889.

3. Bali, P. K. and Harris, W. R. (1990) *Arch. Biochem. Biophys. 281*, 251-256.

4. Baldwin, D. A. and De Sousa, D. M. R. (1981) *Biochemical and Biophysical Research Communications 99*, 1101-1107.

5. Aisen, P., Leibman, a., and Zweier, J. (1978) *J. Biol. Chem. 25*, 1930-1937.

6. Makey, D. G. and Seal, U. S. (1976) *Biochimica et Biophysica Acta (BBA) - Protein Structure 453*, 250-256.

7. Li, Y. and Harris, W. R. (1998) *Biochim. Biophys. Acta 1387*, 89-102.

8. Bali, P. K., Harris, W. R., and Nesset-Tollefson, D. (1991) *Inorg. Chem. 30*, 502-508.

9. Harris, W. R., Bali, P. K., and Crowley, M. M. (1992) *Inorg. Chem. 31*, 2700-2705.

10. Harris, W. R., Brook, C. E., Spilling, C. D., Elleppan, S., Peng, W., Xin, M., and Wyk, J. V. (2004) *J. Inorg. Biochem. 98*, 1824-1836.

11. Moore, J. W. and Pearson, R. G. (1981) *Kinetics and Mechanisms* Wiley, New York.

Chapter 3

Kinetics of Iron Removal from C-terminal Monoferric Human Serum Transferrin by Bifunctional Ligands

3.1

Introduction

The concept of bifunctional ligands arises from previous studies involving mediated iron release (*1;2*), in which a smaller, weaker ligand mediates the transfer of iron from transferrin to a larger, more powerful iron sequestering agent. Ligands like desferrioxamine B (DFO) have a strong iron binding affinity (*3*), but the rate of iron release from transferrin is very slow (*4*). In the course of studies involving the synthesis of potential orally active ligands that can replace DFO, a class of iron(III)-selective chelators, the hydroxypyridinones, have been studied (*5;6*). These are six membered rings with adjacent keto and hydroxyl functional groups. 3-Hydroxy-4-pyridinones (Figure 3.1a) and 3-hydroxy-2-pyridinones (Figure 3.1b) have both been used to remove iron from iron overloaded animals (*7-10*). The 3-hydroxy-4-pyridinones have been more extensively investigated in humans (*11-13*).

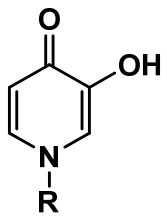

a) 3-hydroxy-4-pyridinones

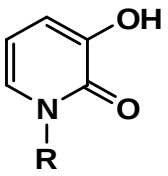

b) 3-hydroxy-2-pyridinones

Figure 3.1 Structures of hydroxypyridinones

Compared with the hydroxypyridinones, ligands like phosphonoacetic acid (PAA) are weaker binding agents, but they can remove iron from transferrin more rapidly. Any potential candidate for iron chelation therapy must have a higher binding affinity than simple ligands like PAA. The presence of the central methylene group in PAA makes it possible to add a new functionality to this ligand. Also, previous studies on monosubstituted PAA derivatives indicate that a metal-binding functional group can be added to PAA (*14;15*). Thus a potential bifunctional ligand that is expected to increase the metal-binding affinity without drastically decreasing the rate of iron release can be synthesized. We are interested in evaluating iron release kinetics by bifunctional ligands. These ligands contain one functional group that accelerates iron release and a second functional group that increases the iron-binding affinity.

One such bifunctional ligand, 3,2-hopoPAA was synthesized for our studies by Dr. C. Spilling's group at UMSL. The structure for 3,2-hopoPAA is shown in Figure 3.2 and has a phosphonoacetic acid at one end conjugated to 3-hydroxy-2-pyridinone by four methylene groups.

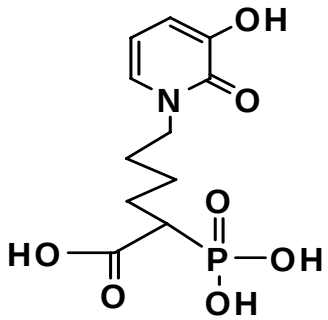

3,2-hopo-PAA

Figure 3.2 Structure of 3-hydroxy-2-pyridinone-PAA

The rationale is that PAA would facilitate the rapid release of iron. The four -CH_2 groups can fold to bring the PAA and 3-hydroxy-2-pyridinone together to act as a tetradentate ligand, so 3,2-hopo-PAA is expected to bind iron much more strongly than PAA alone.

The main focus of this research project is to measure the rate of iron release by 3,2-hopo-PAA and compare this to the rates obtained by PAA and 3-hydroxy-2-pyridinone individually. We measured the rates of iron release at low ligand concentrations of phosphonoacetic acid (PAA) and its methyl and ethyl derivatives to study the impact of alkyl substituents on iron release by PAA and on the concentration of ligand required to reach saturation. This was important in relation to clinically useful drug concentrations. We attempted to measure the rates of iron release from 2,3-dihyroxy pyridine (2,3 DHP) and N-methyl-3-hyroxypyridin-2-one (3HMPY) to get an estimation for the rates before we switched to 3,2-hopo-PAA. The experiments with 2,3 DHP and 3HMPY were difficult to carry out due to the problem of slow air oxidation of the ligand. These kinetics studies using 2,3 DHP and 3HMPY are reported in this chapter.

3.2

Results

Iron release kinetics from C-terminal monoferric transferrin at low concentrations of phosphonocarboxylates

Phosphonocarboxylates appear to be able to substitute for the synergistic carbonate anion (*15*) and show a significant rate of iron removal from transferrin. Iron

removal kinetics by phosphonoacetic acid (PAA) have been studied previously by using Uv-vis spectroscopy (*2;15*). Iron release from N-terminal monoferric transferrin by PAA shows a linear dependence of the rate constant k_{obs} on the ligand concentration over the concentration range of 20-200 mM PAA. The linearity of the plot and the nonzero intercept are consistent with equation (3.1) for complex kinetics, assuming that [L] >> k_d over the available range of ligand concentrations. Under these conditions, equation (3.1)

$$k_{obs} = \frac{k_{\max}[L]}{k_d + [L]} + k'[L] \qquad (3.1)$$

reduces to equation (3.2), a simple linear equation with slope of k' and a y-intercept of k_{max}.

$$k_{obs} = k_{\max} + k'[L] \qquad (3.2)$$

Under these conditions k_d, which is the concentration of ligand required to reach half saturation, could not be determined. It was assumed that the plot of k_{obs} versus PAA concentration would curve towards zero at low ligand concentrations (*2;15*). For any ligand to be a potential drug, it is important to study its behavior at low concentrations. Hence, we are interested in studying iron release at low concentrations of PAA to define the k_d value.

3.2.1

Kinetic studies of iron removal from C-terminal monoferric transferrin by PAA, methyl-PAA and ethyl-PAA.

Iron release kinetics from C-terminal monoferric transferrin by PAA were monitored by using fluorescence spectroscopy, where we could follow kinetics at low concentrations of PAA. As expected, the plots curve towards zero at low concentrations of PAA, as shown in Figure 3.4. The data in Figure 3.4 were fitted to equation (3.1) for complex kinetics, and the rate parameters obtained are listed in Table 3.1. The presence of the central methyl group in PAA provides a position for substitution, and various PAA derivatives are available commercially. Kinetics of iron removal from N-terminal monoferric transferrin by methyl and ethyl derivatives of PAA have been studied by our group previously using Uv-vis spectroscopy (*2;15*). The methyl and ethyl groups are noncoordinating substituents and can be used for elongation of the ligand.

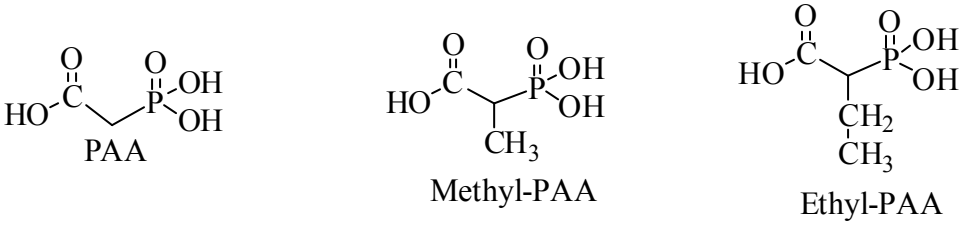

Figure 3.3. Structures of phosphonoacetic acid, methyl-PAA and ethyl-PAA

We monitored iron release from C-terminal monoferric transferrin using methyl- and ethyl-PAA at low concentrations using fluorescence spectroscopy. The observed rates were plotted against the concentrations of the ligands in Figure 3.4. The rates for iron release decrease in the order PAA > methyl-PAA > ethyl-PAA. It was previously

reported that elongation of the ligands slows the rate of iron release from N-terminal monoferric transferrin (*2*), and the same trend on elongation of PAA is observed for iron release from C-terminal monoferric transferrin. The methyl-PAA and ethyl-PAA also follow the combination of saturation and first order pathway as observed for PAA. The rate parameters for these ligands are listed in Table 3.1.

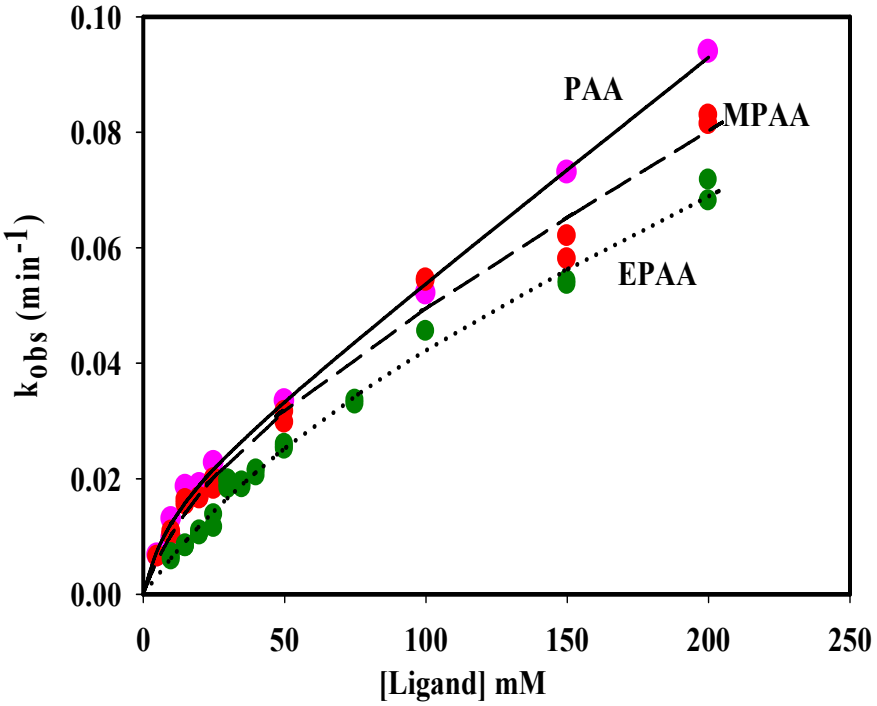

Figure 3.4. Rate constant for iron release from C-terminal monoferric transferrin by phosphonoacetic acid (PAA), methyl phosphonoacetic acid (MPAA) and ethyl phosphonoacetic acid (EPAA) in 0.1 M Hepes at pH 7.4 and 25 °C

Table 3.1

Rate parameters for iron release from C-terminal monoferric transferrin

	k_{max} (min^{-1}) x 10^3	k_d (mM)	k' (M^{-1} min^{-1})
PAA	17 ± 4	10 ± 5	0.38 ± 0.02
MPAA	26 ± 9	25 ± 14	0.28 ± 0.04
EPAA	40 ± 18	82 ± 37	0.20 ± 0.05

In this study we report the rate parameters for C-terminal monoferric transferrin with respect to the methyl and ethyl derivatives of PAA for the first time, as the earlier studies were focused on N-terminal transferrin. Also, we report the k_d values for PAA for the C-terminal monoferric transferrin, which could not be determined by using uv-vis spectroscopy.

3.2.2

Iron removal from C-terminal monoferric transferrin by 2, 3-dihydroxypyridine (2,3 DHP).

After completing the iron removal studies by PAA and its derivatives, we selected 2,3-dihyroxypyridine (2,3 DHP) for the second phase of our kinetic studies as it was commercially available. Before we get on to the results that we obtained, we would discuss some of the issues that we faced during the course of our research. The commercial sample of 2,3 DHP is a brown colored solid and gives a light brown colored solution in 0.1 M Hepes at pH 7.4. We treated the ligand solution with activated

charcoal, but did not observe any drastic change in the color of the solution. The solutions of 2,3 DHP also appeared to be unstable, presumably due to slow air oxidation. Over time, the light brown colored solution would change to dark brown, making it even more difficult to obtain accurate visible spectra of the iron-DHP complex and of mixtures of ferric-transferrin and DHP. We prepared 2,3 DHP solutions by bubbling with argon for 5-10 min, filtering the oxygen-free solutions, and adjusting the pH to 7.4. Thus freshly prepared solutions of the ligand were clear and yellowish brown in color. The visible spectrum for the Fe(2,3-DHP)$_3$ complex was obtained by using the 2,3 DHP solution as a reference. As shown in Figure 3.5, the iron complex has two peaks at 410 nm and 500 nm, which represent ligand-to-metal charge transfer bands.

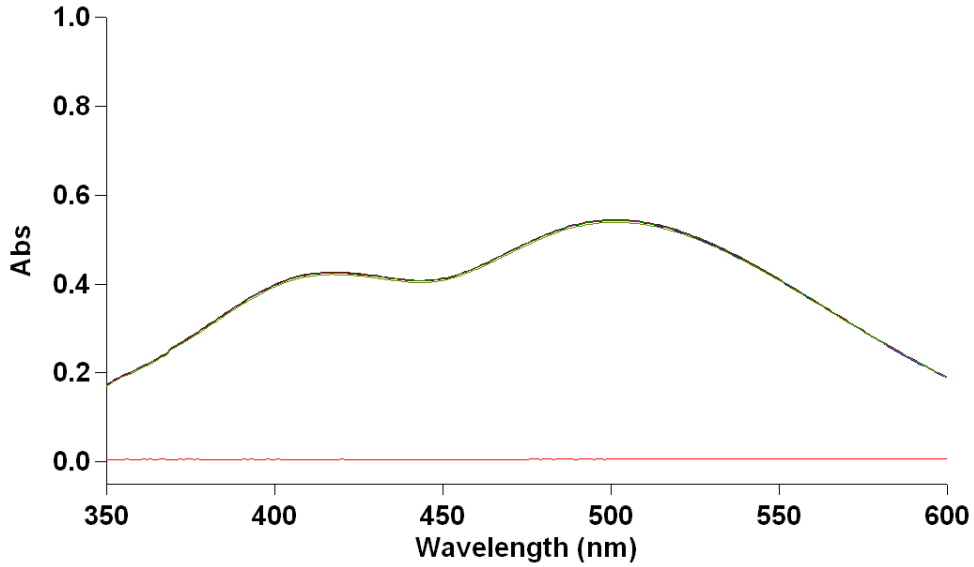

Figure 3.5. The visible spectrum of the Fe(2,3 DHP)$_3$ complex in 0.1 M Hepes pH 7.4 at 25 °C. The trace in green is the iron complex and the trace in red is for the blank (2,3 DHP).

After determining the wavelengths at which the Fe tris 2,3 DHP complex is formed, we began kinetic studies with C-terminal monoferric transferrin and 2,3 DHP. The ligand was added to samples of C-terminal monoferric transferrin, and spectra from 350-600 nm were recorded. Representative scans for the reaction of 30 μM CTf and 50 mM 2,3 DHP over the course of 4 to 5 hours are shown in Figures 3.6 and 3.7.

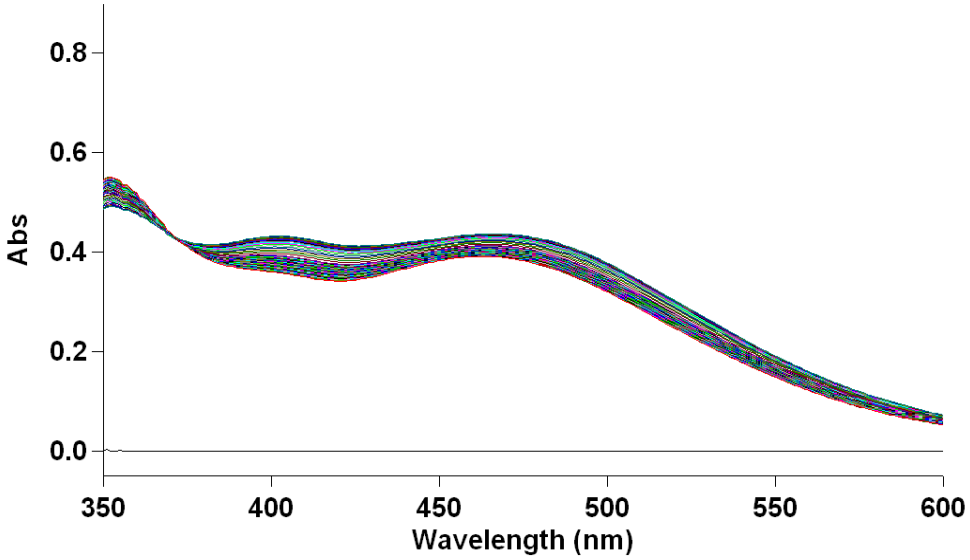

Figure 3.6. Spectra collected during the reaction of monoferric transferrin with 50 mM 2,3- dihydroxypyridine (2,3 DHP) for 4 hours at 25 °C in 0.1 M Hepes. The isosbestic point at 370 nm was maintained during the course of the reaction.

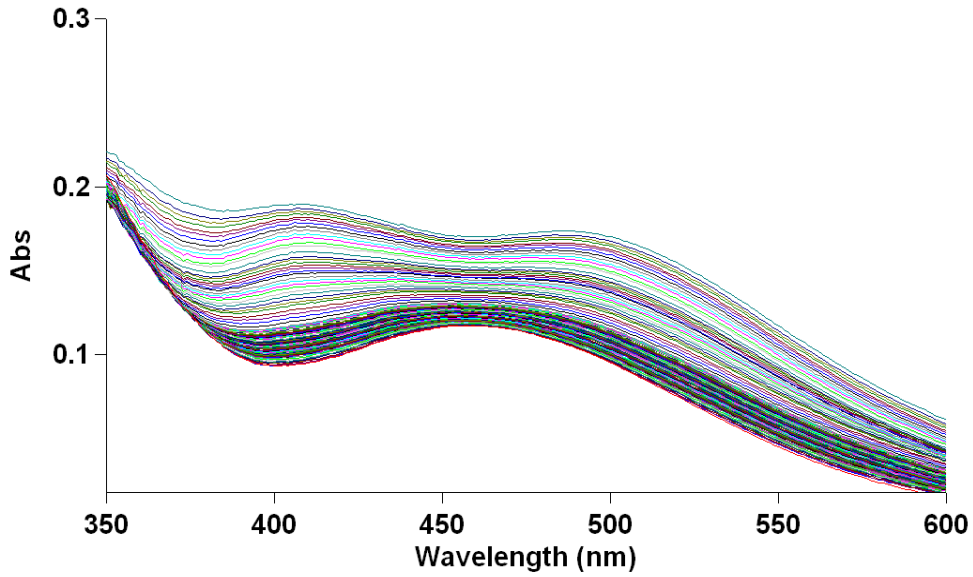

Figure 3.7. Spectra collected during the reaction of monoferric transferrin with 50 mM 2,3-dihyroxy pyridine (2,3 DHP) for 5 hours at 25 °C in 0.1 M Hepes. The isosbestic point at 370 nm was maintained till 50 min.

Figures 3.6 and 3.7 show the spectra obtained for the same reaction on two different days. In Figure 3.6, the isosbestic point was maintained throughout the reaction, whereas in Figure 3.7, we observed an isosbestic point around 370 nm that was maintained for about an hour, but was lost with the progression of time. The loss of the isosbestic point was indicative of some form of ligand oxidation. Due to this sort of variability observed for the same and different ligand concentrations, it was difficult to reproduce our data. For our studies to continue, we needed stable ligand solutions.

We also attempted to prepare the hydrochloride salt of 2,3 DHP in an effort to obtain a colorless sample of the ligand. We tried several experiments under different

conditions but could never obtain a colorless salt of 2,3 DHP. Simultaneously, we searched for commercial sources of derivatives of 2,3 DHP that might be more air-stable and obtained 5-chloro-2,3-dihyroxypyridine from Alfa Aesar. This ligand was also light brown to buff in color and had a very low solubility in 0.1 M Hepes buffer. The issue with colored ligand solutions was not resolved.

3.2.3

Iron removal from C-terminal monoferric transferrin by N-methyl-3-hydroxypyridin-2-one (3HMPY)

We decided to switch to the ligand N-methyl-3-hyroxypyridin-2-one (3HMPY). This ligand was off white in color and was soluble in 0.1 M Hepes at pH 7.4. To determine the spectrum of the $Fe(3HMPY)_3$ complex, we added 0 to 1 equivalents of Fe(III) to 3HMPY solutions. We observed two peaks, a smaller peak at 410 nm and at larger peak at 500 nm. During experiments on the removal of iron from transferrin, we monitored the kinetics at these two wavelengths because they present the maximum change in the absorbance. Rate constants were calculated using data from each wavelength.

We carried out kinetic studies on the removal of iron from C-terminal monoferric transferrin by 150, 125, 100 and 50 mM concentrations of 3HMPY. The experiments were difficult to carry out at 50 mM 3HMPY concentrations. The ligand solutions were very unstable, and it was difficult to distinguish between the degassed and not degassed samples. For the higher concentrations of 3HMPY, we performed scanning kinetics over the range of 350-600 nm and obtained an isosbestic point around 370 nm. Representative

scans for iron removal by 100 mM 3HMPY and 125 mM 3HMPY are shown in the Figure 3.8 and Figure 3.9, respectively.

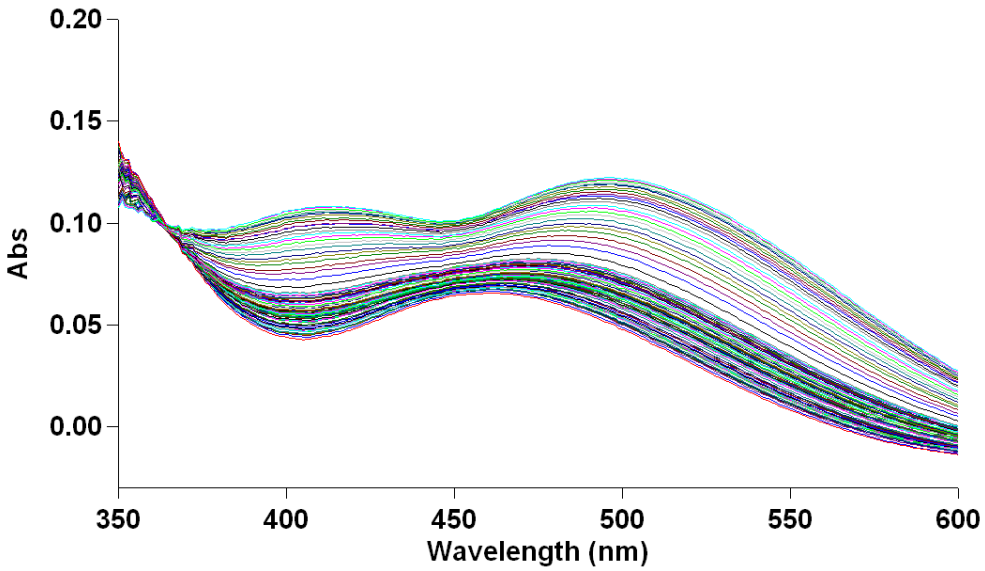

Figure 3.8. Spectra collected during the reaction of monoferric transferrin with 100 mM 3HMPY for 5 hours at 25 °C in 0.1 M Hepes. There is an isosbestic point at 370 nm, which was maintained during the course of the reaction.

The isosbestic point for the reaction of monoferric transferrin and 100 mM 3HMPY as shown in Figure 3.8 was maintained for the entire duration of the reaction. However, the stability of the isosbestic point was inconsistent. For example, when the reaction of monoferric transferrin with 125 mM 3HMPY was monitored, the isosbestic point was lost after about 4 hours, and a new peak at 375 nm appeared, as shown in Figure 3.9. The loss of the isosbestic point indicates the formation of some other species.

The absorbance changes measured up to the loss of the isosbestic point were fit to equation (2.1) from Chapter 2, and the resulting rate constants are listed in Table 3.2.

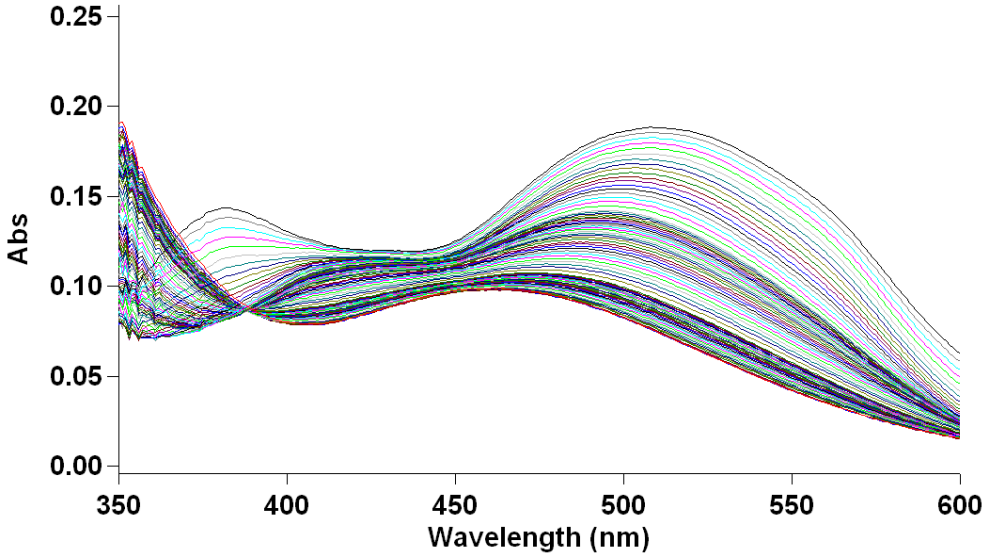

Figure 3.9. Spectra collected during the reaction of monoferric transferrin with 125 mM 3HMPY for 9 hours at 25 °C in 0.1 M Hepes. The isosbestic point is lost after about 4 hours and the emergence of a new peak at 375 nm was observed.

Table 3.2

The observed rates for iron removal from 30 μM C-terminal monoferric transferrin by 3HMPY in 0.1 M Hepes, pH 7.4 at 25 °C.

3HMPY (mM)	k_{obs} (min^{-1})	
	410 nm[a]	500 nm[a]
100	0.0077	0.0087
125	0.0080	0.0089
150	0.0110	0.0119

[a]Wavelength at which absorbance changes were monitored.

The observed rates for the higher concentration of 3HMPY indicate that the rate of iron release is close to reaching saturation with respect to the ligand concentration. The rates also indicate that the removal of iron by 3HMPY is very slow. These rates are comparable to the rate of L1 at 100 mM (0.007 min^{-1}) (*16*).

3.3

Discussion

Rate constants for iron release from C-terminal monoferric transferrin over a wide ligand concentration range were measured for PAA and its methyl- and ethyl-derivatives. The plots in Figure 3.4 show that the short alkyl substituents cause a modest decrease in the overall rate of iron release. This suggests that steric factors are unlikely to drastically reduce the rate of iron release by bifunctional PAA ligands such as 3,2-hopo-PAA.

The data in Figure 3.4 were then used to determine the rate parameters listed in Table 3.1. The rate parameters indicate that the overall rates of iron release remain relatively constant due to offsetting effects on the parameters for the saturation and first-order components. Alkyl substituents increase the k_{max} value for the saturation component, but reduce the rate constant k' of the first-order component.

A higher k_{max} should be an advantage for in vivo iron chelation since the ligand concentrations in vivo must be low. Unfortunately, this potential advantage is negated by the increase in k_d values for the alkyl substituents, which reduces the degree of saturation at low ligand concentrations. One can speculate that the alkyl substituents increase k_d by weakening the binding of the ligand in the mixed-ligand intermediate of the Bates mechanism (*17*). The k_{max} value represents the forward rate constant of the protein conformational change. In the simple Bates mechanism, this value should be independent of the ligand. The variations in k_{max} shown in Table 3.1 are likely to be due to the binding of the ligands to an allosteric anion binding site. This type of allosteric effect is discussed in detail in Chapters 4 and 5.

The second part of this study on iron removal by 2,3 DHP and 3HMPY obviously has serious limitations. Both ligands give a high background absorbance spectrum, but the much more serious problem is that the ligand spectrum changes over the long time frames needed to measure the relatively slow iron release from transferrin by these ligands. We were unable to develop an experimental procedure that could avoid or compensate for these slow changes in the ligand spectrum, and thus we did not attempt a detailed kinetics analysis.

In spite of the experimental problems, the rate constants in Table 3.2 provide useful information on iron release by 3,2-hopo ligands. There is only a small increase in the rate constant over the concentration range of 100-150 mM ligand, which indicates that the reaction follows saturation kinetics, and is running close to saturation over this concentration range. Since saturation requires a ligand concentration of about 5 x k_d, we can make a rough estimate of k_d of around 25 mM. This appears to be slightly higher than the k_d values of 0.8 mM for L1 and 6 mM for 1-hydroxypyridin-2-one (*16*). Nevertheless, the k_d for 3HMPY is clearly much lower than the value of 180 mM previously reported for acetohydroxamic acid (*16*).

The rate constants for HMPY listed in Table 3.2 are rather low, ~0.01 min^{-1}. One would certainly prefer higher rate constants, but these values are quite similar to the k_{max} value of 0.007 min^{-1} reported for L1 (*16*). Since L1 has shown reasonable biological activity (*5;7*), one would conclude that the rates of iron removal by 3HMPY are large enough to make this group viable as an in-vivo chelator.

In summary, the observations that 3HMPY has a rate of iron release comparable to L1 and that substitution at the methylene group of PAA does not significantly reduce the rates of iron release by PAA derivatives are both favorable indicators that the proposed bifunctional ligand shown in Figure 3.2. Unfortunately, experimental problems associated with changes in the ligand spectrum, possibly due to slow ligand oxidation, have thus far prevented any assessment of the rates of iron release by 3,2-hopo-PAA. There is a very limited supply of this compound, and we are unwilling to use it until we are confident that we have an effective experimental protocol.

References

1. Morgan, E. H. (1977) *Biochim. Biophys. Acta 499*, 169-177.

2. Harris, W. R., Brook, C. E., Spilling, C. D., Elleppan, S., Peng, W., Xin, M., and Wyk, J. V. (2004) *J. Inorg. Biochem. 98*, 1824-1836.

3. Weitl, F. L., Harris, W. R., and Raymond, K. N. (1979) *J Med Chem 22*, 1281-1283.

4. Rodgers, S. J. and Raymond, K. N. (1983) *J Med Chem 26*, 439-442.

5. Dobbin, P. S., Hider, R. C., Hall, A. D., Taylor, P. D., Sarpong, P., Porter, J. B., Xiao, G., and van der Helm, D. (1993) *J Med Chem 36*, 2448-2458.

6. Liu, Z. D. and Hider, R. C. (2002) *Coordination Chemistry Reviews 232*, 151-171.

7. Streater, M., Taylor, P. D., Hider, R. C., and Porter, J. (1990) *J Med Chem 33*, 1749-1755.

8. Liu, D. Y., Liu, Z. D., and Hider, R. C. (2002) *Best Practice & Research Clinical Haematology 15*, 369-384.

9. Xu, J., O'Sulliva, B., and Raymond, K. N. (2002) *Inorg. Chem. 41*, 6731-6742.

10. Yokel, R. A., Fredenburg, A. M., Durbin, P. W., Xu, J., Rayens, M. K., and Raymond, K. N. (2000) *Journal of Pharmaceutical Sciences 89*, 545-555.

11. Hoffbrand, A. V., Cohen, A., and Hershko, C. (2003) *Blood 102*, 17-24.

12. Olivieri, N. F., Brittenham, G. M., McLaren, C. E., Templeton, D. M., Cameron, R. G., McClelland, R. A., Burt, A. D., and Fleming, K. A. (1998) *N Engl J Med 339*, 417-423.

13. Olivieri, N. F., Brittenham, G. M., Matsui, D., Berkovitch, M., Blendis, L. M., Cameron, R. G., McClelland, R. A., Liu, P. P., Templeton, D. M., and Koren, G. (1995) *N Engl J Med 332*, 918-922.

14. Gottschalk, R., Seidl, C., Schilling, S., Braner, A., Seifried, E., Hoelzer, D., and Kaltwasser, J. P. (2010) *European Journal of Immunogenetics 27*, 129-134.

15. Brook, C. E., Harris, W. R., Spilling, C. D., Peng, W., Harburn, J. J., and Srisung, S. (2005) *Inorg. Chem. 44*, 5183-5191.

16. Li, Y. and Harris, W. R. (1998) *Biochim. Biophys. Acta 1387*, 89-102.

17. Cowart, R. E., Kojima, N., and Bates, G. W. (1982) *J. Biol. Chem. 257*, 7560-7565.

Chapter 4

Effect of Sulfonate Anions on the Kinetic Pathways for Iron Removal from Transferrin

4.1

Introduction

This chapter is an attempt to have a better understanding of the effects of allosteric anions on the saturation and first order pathways of iron release. We have focused on a series of sulfonates with one or two anionic functional groups to study their effect on the first order and saturation pathways of iron release. The results obtained are presented in this Chapter.

4.1.1

Kinetic Pathways for Iron removal from Transferrin

The dependence of the rate of iron release on the ligand concentration shows a complex variation among different chelating agents. Iron removal by many ligands, such as acetohydroxamic acid (AHA) and deferiprone (*1;2*), follows simple saturation kinetics with respect to the ligand concentration, as described by equation (4.1).

$$k_{obs} = \frac{k_{\max}[L]}{k_d + [L]} \qquad (4.1)$$

This kinetic behavior is usually explained by the Bates mechanism (*1*), which is shown below as originally proposed for iron release by the bidentate chelating agent acetohydroxamic acid (AHA).

$$\text{Fe-CO}_3\text{-Tf} \underset{k_{-1}}{\overset{k_1}{\rightleftharpoons}} \text{Fe-CO}_3\text{-Tf}^* \qquad (4.2)$$

$$\text{Fe-CO}_3\text{-Tf}^* + \text{AHA} \underset{k_{-2}}{\overset{k_2}{\rightleftharpoons}} \text{AHA-Fe-CO}_3\text{-Tf}^* \qquad (4.3)$$

$$\text{AHA-Fe-CO}_3\text{-Tf}^* + 2\ \text{AHA} \xrightarrow{k_3} \text{Fe(AHA)}_3 + \text{apoTf} + \text{CO}_3^{2-} \qquad (4.4)$$

The first step in the mechanism is a conformational change from the normal "closed" form of the holoprotein into an "open" conformation designated by the asterisk. In the second step, the incoming ligand attacks the now exposed ferric ion, which is removed from the protein in the third step. The intermediate complex was detected spectroscopically during the donation of iron from $Fe(AHA)_3$ to apoTf, but was not detected during iron release. This led to the hypothesis that it is the slow conformational change in equation (4.3) that is rate limiting for iron release in the presence of high concentrations of the ligand. Based on this mechanism, the k_{max} parameter in equation (4.1) corresponds to k_1 in equation (4.2), the forward rate constant for the conformational change between the "closed" and "open" forms of the protein.

Many more recent studies have shown that not all systems conform to the Bates mechanism. Several ligands, particularly pyrophosphate (*3-7*) and phosphonic acids (*3;6;8*) appear to follow saturation kinetics at low concentrations, but at higher ligand concentrations, the rate of iron release does not level off. Instead, it continues to increase

linearly with the ligand concentration. The kinetic data for this class of ligands has been described by equation (4.5).

$$k_{obs} = \frac{k_{\max}[L]}{k_d + [L]} + k'[L] \qquad (4.5)$$

There have been various hypotheses to explain the first-order term in equation (4.5) (*4;7;9;10*). This laboratory has proposed that k' is the rate constant for a reaction pathway that involves the removal of iron from the closed conformation of the holoprotein (*6;8;11*).

Perhaps the most intriguing variation in the pattern of ligand-dependence for iron removal from transferrin is shown by two simple aminocarboxylic acids, nitrilotriacetic acid (NTA) (*11*) and diethylenetriaminepentaacetic acid (DTPA) (*8*). Iron release by both these ligands follows simple first order kinetics with respect to the ligand concentration. It has been proposed that for these ligands, k_{max} is very small, such that equation (4.5) reduces to simple first-order dependence. However, if k_{max} is associated with a protein conformational change, there is no obvious explanation for why these ligands are apparently unable to remove iron more rapidly from the open conformation.

Iron release by any particular ligand is also affected by the presence of non-synergistic anions. This is not simply due to changes in ionic strength, nor can these anion effects be correlated with the lyotropic series. The strongest effect is typically seen with perchlorate, which accelerates iron release from the C-terminal site, but significantly retards iron release from the N-terminal site (*12*). Because the anion effects are so selective and variable, Egan and co-workers have proposed that there is an allosteric

anion binding site in each lobe, referred to as the kinetically significant anion binding (KISAB) site (*13*). Within the context of the Bates conformational change mechanism, one might expect that anion-binding at the KISAB site alters the rate of the conformational change between open and closed forms of the protein. However, neither the location and nor the structure of the purported allosteric anion binding site has been identified, and these anion effects on iron release rates are poorly understood (*14-16*).

We have initiated a study to obtain a better understanding of the effects of allosteric anions on the saturation and first order pathways for iron release. A series of sulfonates with one or two anionic functional groups were evaluated for their ability to alter the rate of iron removal from transferrin by acetohydroxamic acid (AHA), 1,2-dimethyl-3-hydroxy-4-pyridinone (deferiprone), nitrilotriacetic acid (NTA), and diethylenetriaminepentaacetic acid (DTPA). These ligands were chosen because AHA and deferiprone remove iron via simple saturation kinetics (*1;2*), while NTA and DTPA remove iron via simple first-order kinetics (*8;11*). Sulfonic acids were chosen because they are strictly non-chelating molecules that cannot remove any iron from transferrin, and thus introduce no complications in the analysis of the kinetic data. Iron removal from C-terminal monoferric transferrin has been studied to avoid the complications of analyzing simultaneous iron release from both of the binding sites in diferric transferrin.

4.2

Results

4.2.1

Effect of simple anions on iron release by AHA

The rates of iron release from transferrin by 200 mM AHA in the presence of a series of anions have been measured. These include the simple inorganic anions chloride and perchlorate, as well as the organic anions methylphosphonate (MPA), methylsulfonate (SMS), and acetate. The results are shown in Table 4.1. The acceleration of iron release by chloride and perchlorate agrees with several previous studies (*2;12;17;18*). The organic anions used in this study also accelerate iron release, but to a lesser degree compared with chloride and perchlorate.

Table 4.1

Effect of simple anions on the rate of iron removal by 200 mM AHA[a]

	k_{obs} (min^{-1}) x 10^3
200 mM [AHA]	16.2 ± 0.4
[AHA] + 100 mM Cl^-	31.8 ± 1.5
[AHA] + 100 mM ClO_4^-	69.0 ± 0.4
[AHA] + 100 mM MPA	25.4 ± 0.2
[AHA] + 100 mM SMS	22.9 ± 0.2
[AHA] + 100 mM Acetate	20.4 ± 0.3

[a]0.1 M HEPES, pH 7.4, 25 ºC

4.2.2

Effect of sulfonates on iron removal by the saturation pathway

Rates of iron release by AHA were measured in the presence of increasing concentrations of methanesulfonate (SMS), methanedisulfonate (MDS) and

ethanedisulfonate (EDS). Sulfonic acids are extremely weak coordinating groups, and separate experiments verified that these anions do not remove any significant amount of iron from transferrin over the concentration range used in this study. Thus any change in the observed rate constant for iron release in the presence of the sulfonate has been attributed to the allosteric effect of the anions binding to the KISAB site on the protein and altering the rate constant for iron removal by AHA.

Iron removal from C-terminal monoferric transferrin by 200 mM AHA went to completion in all the sulfonate samples, and values of k_{obs} were calculated as described in Chapter 2 by use of equation 2.1. To minimize the effect of any day-to-day variations in the rate constants on the assessment of the anion effects, pseudo-first-order rate constants were measured for paired samples, one with and one without, the added sulfonate anion.

In the absence of added anion, the average rate constant for iron release by 200 mM AHA is 0.016 min^{-1}. All three sulfonate anions increased this rate constant. This acceleration is expressed as shown in equation (4.6),

$$\%\Delta k = \frac{k'_{obs} - k_{obs}}{k_{obs}} x100 \qquad (4.6)$$

where k_{obs} is the rate constant for iron release by 200 mM AHA alone, and k'_{obs} is the rate constant for the same concentration of AHA in the presence of the added anion. Values of %Δk as a function of the anion concentration for the series of sulfonate anions are shown in Figure 4.1.

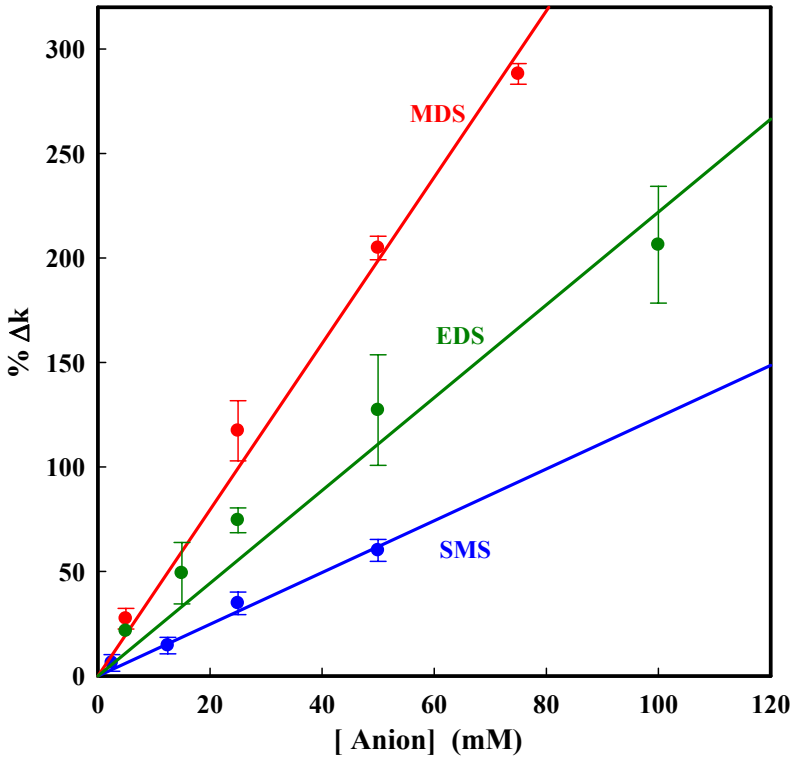

Figure 4.1. Plots of %Δk (equation 4.6) for the removal of iron from C-terminal monoferric transferrin by 200 mM AHA in the presence of sodium methane sulfonate (SMS), methanedisulfonate (MDS), and ethanedisulfonate (EDS) at 25 ^{o}C in 0.1 M Hepes, pH 7.4. The concentration shown for SMS is the actual molarity divided by two to give the equivalent concentration of a disulfonic acid.

A similar set of kinetic experiments with sulfonates were conducted using 20 mM deferiprone to remove the iron. Iron release went to completion in all cases, and rate constants with (k_{obs}') and without (k_{obs}) anions were calculated as described in Chapter 2 by using the version of equation (2.1) with absorbance rather than fluorescence intensity.

The average rate constant for iron release in the absence of anions was 0.005 min^{-1}. The effect of sulfonates on the rate of iron release by deferiprone is shown in Figure 4.2.

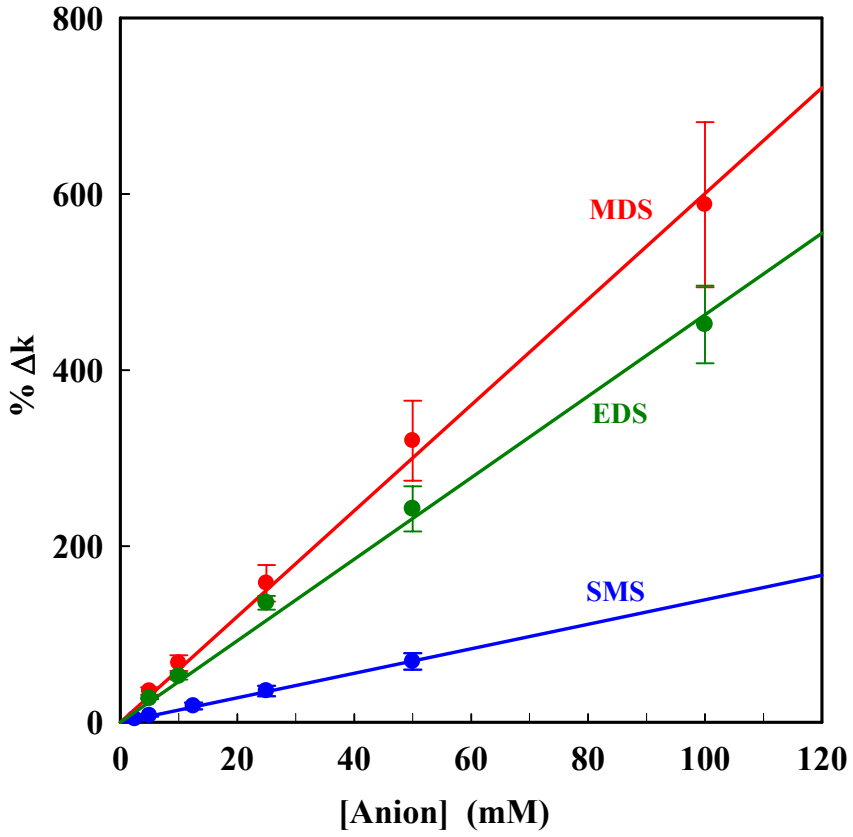

Figure 4.2. Plots of %Δk (equation 4.6) for the removal of iron from the C- terminal monoferric transferrin by 20 mM deferiprone in the presence of sodium methanesulfonate (SMS), methanedisulfonate (MDS), and ethanedisulfonate (EDS) at 25 °C in 0.1 M Hepes, pH 7.4. The concentration shown for SMS is the actual molarity divided by two to give the equivalent concentration of a disulfonic acid.

As seen in Figures 4.1 and 4.2, the %Δk values for these two neutral ligands show a linear dependence on the concentration of the sulfonates. For both ligands, disulfonates have a significantly greater impact than SMS. For the two disulfonates, the length of the alkyl linker between the two anionic functional groups has an effect on the kinetics. Faster rates are observed with MDS, in which the sulfonates are separated by a single methylene group.

Iron release by 200 mM AHA was also measured in the presence of 100 mM perchlorate. This concentration of perchlorate increased the rate constant from 0.0162 min^{-1} to 0.069 min^{-1}, which corresponds to a %Δk of 330. Thus for iron release by AHA, it appears that the effect of MDS is essentially the same as the effect of perchlorate.

It is possible that each of the sulfonic acid groups of the disulfonate anions interacts independently with the protein, and that the greater effect on iron release compared with SMS just reflects the fact that the effective molarity of sulfonic acid groups is doubled for MDS and EDS. We have corrected for this mismatch in stoichiometry by plotting the SMS data using the actual molarity of SMS divided by two. Thus when one compares the kinetic effects at any given concentration in Figures 4.1 and 4.2, each of the three solutions contains the same total concentration of sulfonate groups. Even with this correction, it is quite clear that the disulfonates have a greater impact on iron release kinetics. In addition, MDS produces a larger effect than does EDS. Thus our hypothesis is (a) these anions are binding to a specific allosteric site on the protein, (b) this binding involves both sulfonated groups of the anion, and (c) the structure of the allosteric site results in a preference for the shorter MDS dianion.

Previous studies on iron removal by AHA and deferiprone have shown that the ligand dependence of k_{obs} reflects simple saturation kinetics as described by equation (4.1) (*1;2*). The presence of a sulfonate in the solution could accelerate the observed rate of iron release at a given concentration of AHA by increasing the value of k_{max}, by decreasing the value of k_d, or by producing a first-order term for iron release as shown in equation (4.5). To differentiate among these possibilities, values of k_{obs} were measured for iron removal by varying concentrations of AHA in the presence of a constant concentration of 50 mM MDS. The results are shown in Figure 4.3. Below 75 mM AHA, the iron removal reaction no longer goes to completion, and the value of k_{obs} was calculated as described in Chapter 2 using equation (2.3) to fit the intensity versus time data.

The ligand-dependence of k_{obs} in the absence and in the presence of 50 mM MDS has been modeled using both equation (4.1) (simple saturation kinetics using two adjustable parameters) and equation (4.5) (saturation-linear kinetics using three adjustable parameters). The results from the least squares fits are listed in Table 4.2. For iron release when MDS is present, the functions in equations (4.1) and (4.5) give essentially identical fits to the experimental data. This can be seen visually from the overlap of the plots of these two functions. The addition of the third adjustable parameter in equation (4.5) produces a statistically insignificant improvement in the sum of squares of the residuals from the fit, as assessed by an R-factor ratio test (*2*). In addition, the value of k' calculated by use of equation (4.5) has an error of almost 100%.

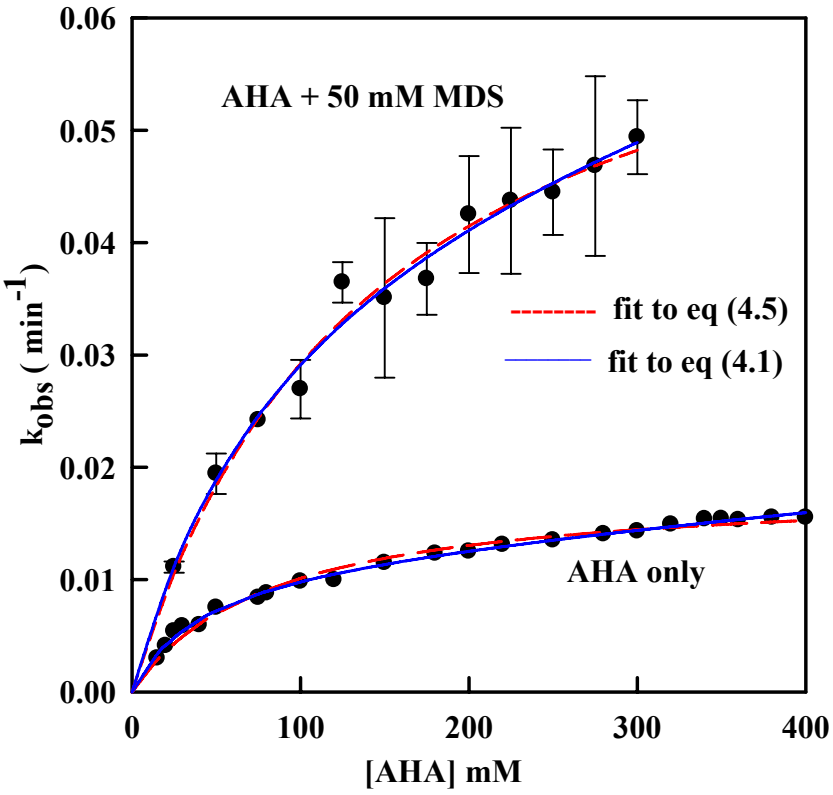

Figure 4.3. Plots of k_{obs} for the removal of iron from C-terminal monoferric transferrin by varying concentrations of AHA alone and in the presence of 50 mM MDS at 25 ^{o}C, in 0.1 M Hepes, pH 7.4.

Figure 4.3 also shows that there is a very strong overlap in the fits of the data in the absence of MDS to equation (4.1) and (4.5). Iron release by AHA has been previously reported to follow simple saturation kinetics (*1;2*). Thus it was surprising that the addition of the third adjustable parameter resulted in a small, but statistically significant, improvement in the fit obtained using equation (4.5). The reason for this is not clear. Given the previous literature reports of simple saturation kinetics and the

strong similarity in the fits to equation (4.1) and (4.5), we feel it is most appropriate to accept the fit to simple saturation kinetics as described by equation (4.1). Thus we conclude that iron release by AHA follows simple saturation kinetics as described by equation (4.1) both alone and in the presence of MDS.

Based on a comparison of the fits to equation (4.1), the results in Table 4.2 show that the presence of 50 mM MDS produces a four-fold increase in the k_{max} for iron release by AHA from 0.018 min^{-1} to 0.072 min^{-1}. The MDS also causes an increase in k_d from 81.8 mM to 145 mM. Because of this change in k_d, a given concentration of AHA corresponds to different degrees of saturation with and without MDS. The plot in Figure 4.3 for iron release in the absence of MDS extends to 400 mM AHA, which corresponds to 83% of saturation. The data for iron release in the presence of MDS extend to 300 mM, but due to the larger value of k_d, this represents only 67% of saturation. Thus the increase in the rate of iron release in the presence of MDS that is shown in Figure 4.3 is due entirely to a large increase in the k_{max} for iron release.

Table 4.2

Rate constants for iron removal from C-terminal monoferric transferrin by AHA[a]

	k_{max} (min^{-1}) x 10^3	k_d (mM)	k' (M^{-1} min^{-1})	. σ_y
AHA alone[b]	18.4 + 0.4	81.8 $\pm$ 5.8	--	0.00052
AHA alone[c]	12.1 $\pm$ 0.1	42.2 $\pm$ 4.7	0.012 $\pm$ 0.002	0.00031
AHA + 50 mM MDS[b]	71.6 $\pm$ 0.4	145 ± 18	--	0.0017
AHA + 50 mM MDS[c]	50 $\pm$ 20	97 $\pm$ 47	0.037 $\pm$ 0.036	0.0017

[a] 25 ^{o}C, 0.1 M Hepes, pH 7.4

[b]Data fit using two adjustable parameters to equation (4.1)

[c]Data fit using three adjustable parameters to equation (4.5)

4.2.3

Effect of sulfonates on iron removal by the first order pathway

The rates of iron release from transferrin are first-order with respect to the ligand concentration for both NTA and DTPA. Rates of iron release by NTA and DTPA were measured in the presence of increasing concentrations of methanesulfonate (SMS), methanedisulfonate (MDS) and ethanedisulfonate (EDS). Iron removal from C-terminal monoferric transferrin by 100 mM NTA goes to completion, and rate constants with (k_{obs}') and without (k_{obs}) anions were calculated from data on paired samples using equation (4.6). The acceleration in the presence of sulfonates is expressed as an increase

in %Δk as defined in equation (4.9). The results for the effect of sulfonates on iron release by 100 mM NTA are shown in Figure 4.4.

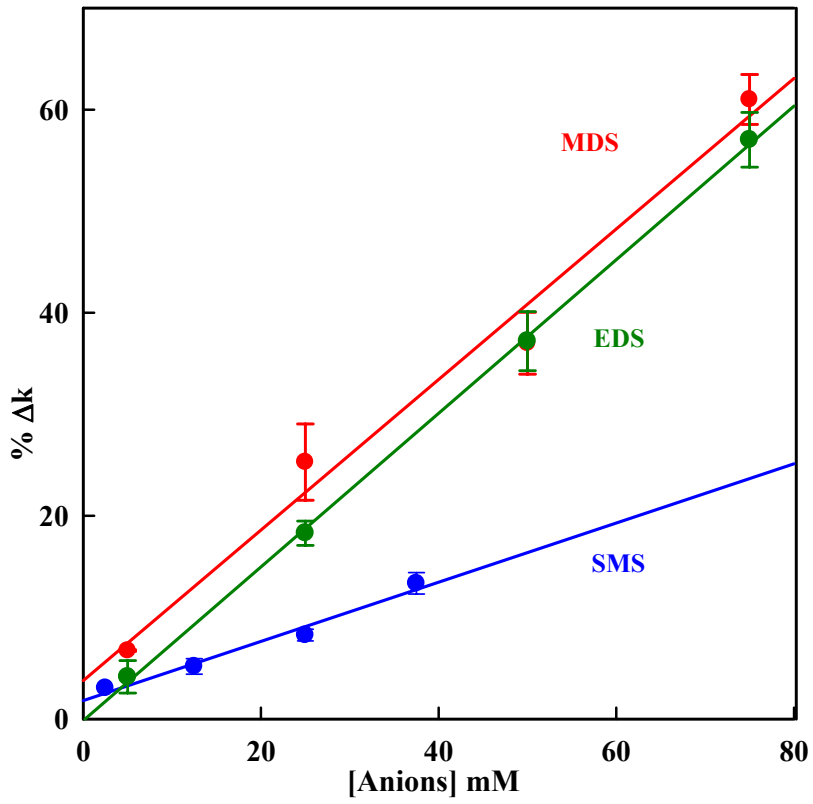

Figure 4.4. Plots of %Δk (equation 4.6) for the removal of iron from C- terminal monoferric transferrin by 100 mM nitrilotriacetic acid (NTA) in the presence of sodium methanesulfonate (SMS), methanedisulfonate (MDS), and ethanedisulfonate (EDS) at 25 °C in 0.1 M Hepes, pH 7.4. The concentrations shown for SMS are the actual molarities divided by two to give the equivalent concentrations of a disulfonic acid.

The effect of sulfonates on iron removal by 200 mM DTPA was also studied, and the results are shown in Figure 4.5.

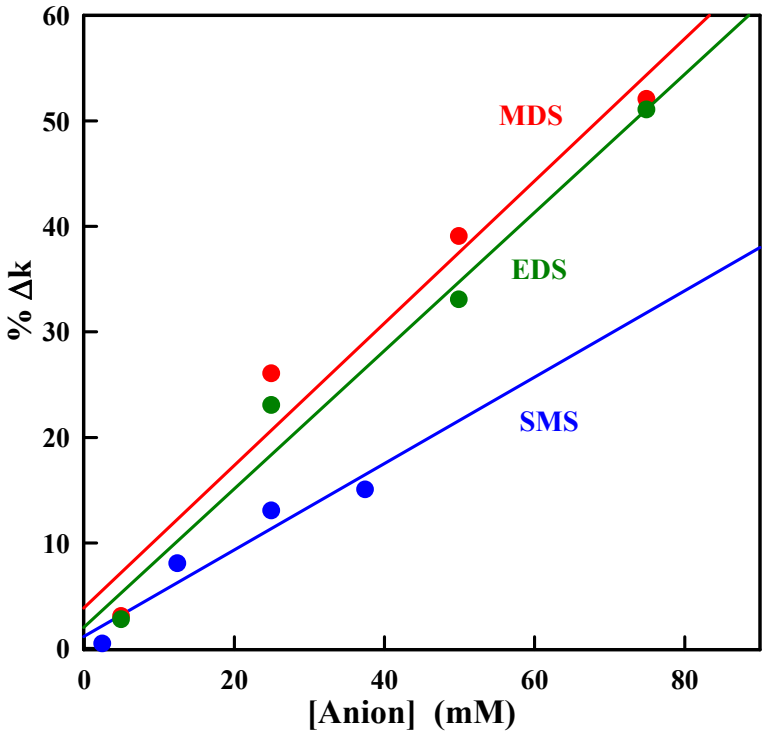

Figure 4.5. Plots of %Δk (equation 6) for the removal of iron from C- terminal monoferric transferrin by 200 mM diethylenetriaminepentaacetic acid (DTPA) in the presence of sodium methanesulfonate (SMS), methanedisulfonate (MDS), and ethanedisulfonate (EDS) at 25 °C in 0.1 M Hepes, pH 7.4. The concentrations shown for SMS are the actual molarities divided by two to give the equivalent concentrations of a disulfonic acid.

The effect of sulfonates on iron release by NTA and DTPA follows the same pattern as described above for AHA and deferiprone. There is a smaller effect for the

monosulfonate, and a larger effect for both the disulfonates. There is no significant difference in the effects of the two disulfonates. However, the magnitude of the effect on iron release by NTA and DTPA is quantitatively smaller. The rates of iron release by AHA and deferiprone were increased by ~400% by MDS, as compared to an increase of about 60% for iron release by NTA and DTPA.

Values of k_{obs} were also measured for iron removal by varying concentrations of NTA both in the absence and in the presence of a constant concentration of 75 mM MDS. The results are shown in Figure 4.6. At concentrations of NTA below 75 mM, the iron removal reaction does not go to completion, and the value of k_{obs} was calculated as explained in methods in Chapter 2 using equation (2.3) to fit the intensity vs time data. The data in the absence of MDS confirm previous reports (*11*) that iron release by this ligand is a simple first-order process, with an observed rate constant of 0.32 ± 0.01 min^{-1}. This rate constant is essentially identical to the value of $k' = 0.33 \pm 0.01$ min^{-1} published previously (*11*). The results in Figure 4.6 also confirm the previous report that the plot of k_{obs} vs [NTA] has a zero y-intercept and thus shows no indication of a saturation component for iron release by this ligand.

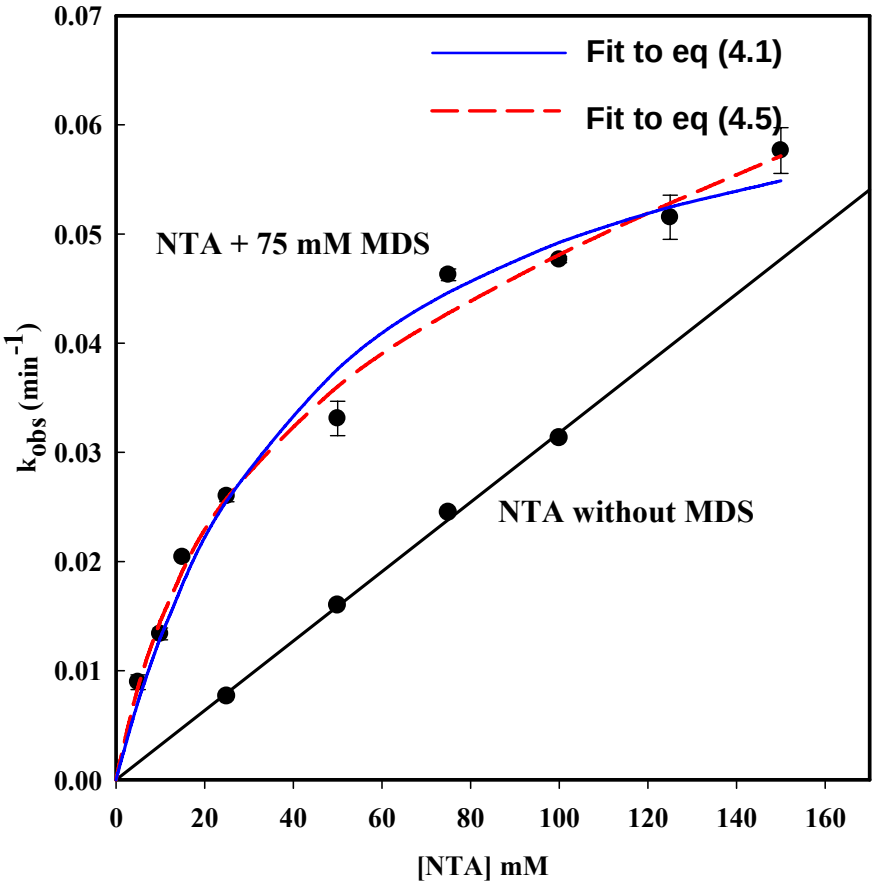

Figure 4.6. Plots of k_{obs} for the removal of iron from the C-terminal monoferric transferrin by varying concentrations of NTA in the presence of a constant 75 mM MDS at 25 ^{o}C, 0.1 M Hepes, pH 7.4.

It is obvious from the plot in Figure 4.6 that the addition of MDS has dramatically changed the ligand dependence of iron removal by NTA. The reaction is clearly no longer a simple first-order process. The data on iron removal in the presence of the MDS have been fit to both equation (4.1) and equation (4.5), and the resulting parameters are

shown in Table 4.3. Visually the quality of the fits looks similar, but the use of equation (4.5) reduces the sum of squares of the residuals by 40% compared to that obtained by use of equation (4.1). The improvement in the fit to equation (4.5) is statistically significant for $\alpha = 0.05$. Thus we conclude that iron release by NTA in the presence of MDS is best described as a combination of saturation and first-order pathways. It is presumed that this change from strictly first order kinetics to a combination of saturation and first order kinetics is related to the binding to the MDS to the KISAB site of the protein and increasing the rate of the closed-to-open conformational change in the protein.

Table 4.3

Rate Parameters for Iron Release from C-Terminal Monoferric Transferrin in the Presence and in the Absence of MDS

	k_{max} (min^{-1}) x 10^3	k_d x 10^3 (M)	k` x 10^3 ($M^{-1}min^{-1}$)	. σ_y
NTA	-	-	0.32 ± 0.01	0.0006
NTA+75mM[a] MDS	71 ± 4	45 ± 7	-	0.0025
NTA+75mM[b] MDS	42 ± 10	22 ± 8	0.14 ± 0.05[b]	0.0021

[a]Parameters from fit to equation (4.1)

[b]Parameters from fit to equation (4.5)

4.3

Discussion

It has been well established iron removal by many ligands shows simple saturation behavior with respect to the ligand concentration (*1;2;19-21*). This behavior is described by equation 4.1. Bates and co-workers (*1*) were the first to report this behavior and proposed the mechanism shown in equations (4.2) – (4.4), in which saturation kinetics result from a rate-limiting conformational change in the protein. In the Bates mechanism, each lobe of ferric transferrin exists in a mixture of open and closed forms, with iron release occurring only from the open form. If one assumes steady state concentrations of the intermediate species Fe-CO_3-Tf^* (equation 4.2) and AHA-Fe-CO_3-Tf^* (equation 4.3), then the k_{max} parameter in equation 4.1 is equal to k_1, the rate constant for the conversion of the protein from the closed to the open form in equation 4.2.

The Bates proposal of a gating conformational change has been reinforced by subsequent reports of the crystal structures of apo- and holotransferrin, which show that the removal of iron results in a very large conformational change. Upon the removal of iron, there is a hinge movement that opens the cleft between the two domains in each lobe of the protein by approximately 63 degrees (*22*). One can view the crystal structure of ferric transferrin as a reasonable representation of the closed form. The "open" form proposed by Bates would presumably correspond to some intermediate conformation along the reaction pathway between ferric transferrin and the fully open conformation of apotransferrin. The precise degree to which the protein conformation must change in order to enable attack of the chelating agent and the effective removal of iron has not been established.

It has been known for some time that a variety of simple inorganic anions can alter the rates of iron release by various chelating agents. It is important to note that these kinetic effects do not correlate well with simple changes in ionic strength of the solution. Nor do they correlate well with the general lyotropic effects of the anions. The Hoffmeister series describing general anion affects on protein structure is (*23;24*)

$$CO_3^{2-} < SO_4^{2-} < H_2PO_4^- < F^- < Cl^- < Br^- \sim NO_3^- < I^- < ClO_4^- < SCN^-$$

Less denaturation more denaturation

The precise effect of anions on the rates of iron release depends to some degree on the choice of the chelating agent used to remove the iron. As an example, the effect of anions on the first order component for iron release by PP_i is (*3*)

$$SCN^- < F^- \sim NO_3^- < Cl^- \sim HCO_3^- < SO_4^{2-} < ClO_4^-$$

Slower iron release faster iron release

One would expect that those anions that promote denaturation would have the greatest impact on terms of enhancing the rate of iron release to a LWM chelating agent. However, there is a very poor correlation between the Hoffmeister series and the ability of anions to accelerate the rate of iron release. Thus it is widely accepted that the transferrin molecule has one (or more) specific binding site(s) for the allosteric anions, which is typically referred to as the *k*inetically *s*ignificant *a*nion *b*inding site, or the KISAB site.

The new data reported here in Figure 4.3 confirms that the allosteric anion can exert its impact not by drastically changing the mechanism of iron release, but by changing the k_{max} and k_d parameters associated with the Bates conformational change mechanism. Thus one can regard iron release as proceeding from two transferrin populations that are linked by an anion binding equilibrium. Such a model was proposed much earlier by Bertini et al. (*4*). Their original kinetic model can be simplified and expressed as an expansion of equation (4.1) as

$$k_{obs} = \frac{k_{\max}[L]}{k_d + [L]}\left(\frac{1}{1 + K_A[A]}\right) + \frac{k'_{\max}[L]}{k'_d + [L]}\left(\frac{K_A[A]}{1 + K_A[A]}\right) \qquad (4.7)$$

where the parameters k_{max} and k_d refer to the "native" protein structure and the parameters k_{max}' and k_d' refer to an alternative conformation as modified by binding of the anion (A) to the KISAB site, and K_A is the anion-protein binding constant. The terms in parenthesis simply partition the overall protein population into the fraction existing in the native structure and the fraction in the modified structure.

The results reported here on the effects of sulfonate anions on iron release by AHA and deferiprone consistently show a simple linear dependence of k_{obs} on the anion concentration. Equation (4.7) can explain this linear dependence, but only under rather restricted conditions. One must assume that anion-binding is weak, so that $K_A[A] << 1$ for all anion concentrations studied. Under these conditions, and at a fixed concentration of ligand, the dependence of k_{obs} on the anion concentration reduces to

$$k_{obs} = k_{native} + k_{\mathrm{mod}} K_A [A] \qquad (4.8)$$

where k_{native} is the observed rate constant at the specified ligand concentration for the native form of the protein, and k_{mod} is the corresponding rate constant at the same ligand concentration for the allosterically modified form of the protein. From linear plots, it is impossible to deconvolute individual values for k_{mod} and K_A. Our experiments involved anion concentrations of up to 100 mM. If we assume that this produces only 10% saturation of the anion binding sites, so that the plots remain linear, this would put an upper limit on K_A of ~1. One could speculate that this very low binding affinity reflects a process in which a more favorable ΔG for anion binding is largely offset by an unfavorable ΔG for a concomitant protein conformational change. One should also note that since the slopes of the plots in Figures 4.1 and 4.2 are related to the product of $k_{mod}K_A$, it is impossible to tell whether the greater efficacy of the disulfonates in promoting iron release is a result of a larger k_{mod} for iron release or a larger K_A for anion binding.

In principle one could continue to measure k_{obs} at higher anion concentrations until one observes sufficient curvature in the plot to determine individual values of k_{mod} and K_A. However, we felt that to do so would require anion concentrations so large that non-specific salt effects were highly likely to confuse and/or mask the specific allosteric effects associated with anion binding at the KISAB site.

Others have proposed that the KISAB site must be occupied by some anion in order for any iron release to occur (*25*). In this model, the anion-binding reaction

referred to above would actually represent the partial displacement of an original anion from the buffer by the added sulfonate. Other than treating K_A as an anion exchange equilibrium rather than a simple anion binding equilibrium, the form of equation (4.7) would remain the same.

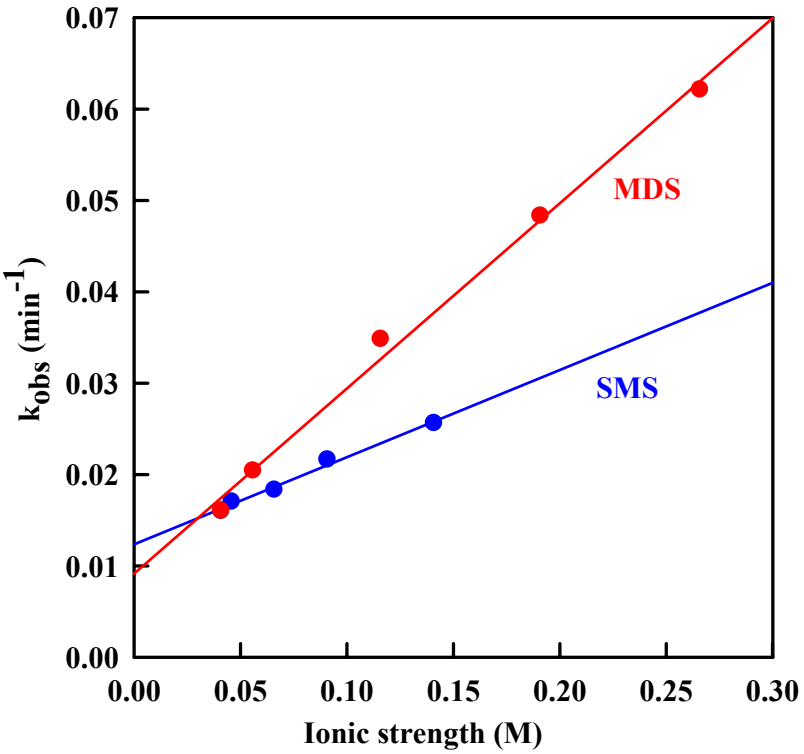

Figure 4.7 Variation in k_{obs} for iron removal from C-terminal monoferric transferrin by 200 mM AHA as a function of the ionic strength of the solution. The ionic strength of the 100 mM Hepes buffer is 0.041. Ionic strength was increased by adding either SMS or MDS.

Evaluating the rates of iron removal as a function of ionic strength was not an original objective of this study. Nevertheless, one can use the data shown in Figure 4.1 to prepare a plot of the rate constant for iron release by 200 mM AHA as a function of the ionic strength, as shown in Figure 4.7. The plots for MDS and SMS both extrapolate back to a rate constant of about 0.01 min^{-1} at zero ionic strength. These data would argue that there is small, but non-zero rate of iron release even when the KISAB site is not occupied.

The Bates mechanism is sufficient to describe iron removal by ligands such as deferiprone, AHA, and LICAMS that follow simple saturation kinetics (*1;2;19;20*). However, there are a number of ligands for which the rates of iron release are described by equation (4.5), with a combination of saturation and first-order components. These include PP_i (*3-5;26*), a series of aminophosphonic acids (e.g. nitrilotris(methylenephosphonic acid) (*3;5;11*), and a series of phosphonocarboxylic acids (e.g. phophonoacetic acid) (*27;28*). Although conformational gating is widely accepted as the basis for the saturation component of iron release, there is no consensus on the origin of the first order component.

Previous studies on iron removal by NTA and DTPA have shown that k_{obs} has a simple first-order dependence on the ligand concentration. The absence of any element of saturation kinetics for NTA and DTPA is puzzling. There is no obvious reason why these ligands should not be able to rapidly remove iron from the proposed open conformation of ferric transferrin. One possible explanation for a negligible k_{max} value for NTA is that the anionic carboxylate functional groups of NTA bind at the KISAB site and reduce the value of k_{max}. We evaluated the effect of acetate on the rates of iron

release by AHA. As shown in Table 4.1, the presence of acetate causes only a small acceleration in the rate of iron release. In addition, EDTA and citrate both have easily detectable k_{max} values. Thus it seems unlikely that the acetate groups of NTA could be responsible for the dramatically lower k_{max} value for NTA.

The previous explanation for first-order kinetics was that iron release by NTA was described by equation (4.2), but the k_{max} value for the saturation component was so low that it could not be detected against the background of faster iron release via the first-order pathway (*11*). This interpretation for iron release by NTA is supported by the present results. The addition of 50 mM MDS increases the value of k_{max} for iron removal by AHA by a factor of 4, from 0.016 min^{-1} to 0.072 min^{-1}. This rate parameter is presumed to represent the forward rate constant for the transition from the closed to the open protein conformation. As one would then expect, the addition of MDS increases the k_{max} for iron release by NTA from its previous negligible value to 0.042 min^{-1}.

The addition of MDS reveals the saturation component for iron release by NTA, but it does not eliminate the first-order component for iron release. The results for iron release in the presence of 75 mM MDS show that the sulfonate anion decreases the k' value for iron release by NTA by about 50%, from 0.32 M^{-1} min^{-1} to 0.14 $M^{-1}min^{-1}$. Thus the general observation is that anion binding at the KISAB site substantially enhances iron release via the saturation pathway, but modestly reduces iron release via the first order pathway.

It would be possible to observe an apparent first-order process for iron release due to the binding of anions to the KISAB site. We previously reported such an example involving a comparison of iron release rates for two solutions of deferiprone, one

prepared from the free base and one prepared from the deferiprone hydrochloride salt (*2*). In the latter case, the increase in the Cl^- concentration that accompanied each increase in the deferiprone concentration led to a linear increase in the rate constant, whereas experiments using the free base showed simple saturation kinetics. This result would be consistent with equation (4.8), with Cl^- occupying the anion binding site.

It is possible that the anionic carboxylate groups of NTA could bind to the KISAB site and increase the k_{max} for iron release by allosteric effects as the NTA concentration is increasing, and that this could account for the apparent first-order dependence on the NTA concentration. However, the data reported here do not support such a model. We have examined the effect of acetate groups as KISAB allosteric anions. The addition of 100 mM acetate accelerates iron release by AHA by only about 25%, from 0.016 to 0.020 min^{-1}. To account for the linear component of iron release by NTA, the acetate groups would have to enhance k_{max} from essentially zero (upper limit of ~0.002) by a factor of at least 20 to about 0.03 min^{-1} at 100 mM NTA. It seems unlikely that the weakly allosteric acetate group could account for a 20-fold increase.

Others (*25*) have proposed that the first-order component is basically an artifact that is produced as the changes in the ionic strength of the solution and this causes a gradual change in the k_{max} value of the conformational change. However, it is quite clear that the kinetic effect of anions is not related to changes in ionic strength. Marques et al. have shown that selective anion effects on the rates persist, even when ionic strength is held constant (*13*). In addition, Brook et al. (*28*) have shown that the first-order term for iron removal by PP_i disappears for tripolyphosphate, which removes iron by a simple

saturation process, even though it would have a larger impact on any changes in ionic strength.

Another proposal is that the first-order component for iron release represents a different reaction pathway that is independent of the gating conformational change, and that this pathway involves the replacement of the synergistic carbonate anion to form a Fe-ligand-Tf ternary intermediate (*29*). The data presented here on the effects of MDS are consistent with two distinct pathways for iron release. The dianion increases the k_{max} value for both AHA and NTA, while resulting in a slight reduction in the k' value for NTA.

Despite considerable work on the effects of anions on iron removal, the location of the KISAB site has not been established. Previous computational studies identified several possible sites, but did not establish a clear choice among the possible locations (*16*). The data reported here that disulfonates are more effective KISAB anions than monosulfonate and methanedisulfonate should provide additional information to help identify the site.

Sulfonic acids accelerate the rate of iron release from C-terminal monoferric transferrin. This presumably reflects their ability to bind to the KISAB site on transferrin. The consistent difference between the mono- and disulfonates suggests that the KISAB site is sufficiently complex and structured to allow it to interact with both functional groups of the disulfonates. Binding of the disulfonates increases the k_{max} value for the saturation pathway. For NTA, this increase reveals a saturation pathway that was not observable for iron release in the absence of the anions. In contrast to the large

increase in k_{max} for the saturation pathway, there is a slight decrease in the k' value for iron release by NTA via the first-order pathway.

References

1. Cowart, R. E., Kojima, N., and Bates, G. W. (1982) *J. Biol. Chem. 257*, 7560-7565.

2. Li, Y. and Harris, W. R. (1998) *Biochim. Biophys. Acta 1387*, 89-102.

3. Harris, W. R. and Bali, P. K. (1988) *Inorg. Chem. 27*, 2687-2691.

4. Bertini, I., Hirose, J., Luchinat, C., Messori, L., Piccioli, M., and Scozzafava, A. (1988) *Inorg. Chem. 27*, 2405-2409.

5. Harris, W. R., Rezvani, A. B., and Bali, P. K. (1987) *Inorg. Chem. 26*, 2711-2716.

6. Bali, P. K. and Harris, W. R. (1990) *Arch. Biochem. Biophys. 281*, 251-256.

7. Marques, H. M., Egan, T. J., and Pattrick, G. (1990) *South African Journal of Science 86*, 21-24.

8. Harris, W. R., Bali, P. K., and Crowley, M. M. (1992) *Inorg. Chem. 31*, 2700-2705.

9. Egan, T. J., Ross, D. C., Purves, L. R., and Adams, P. A. (1992) *Inorg. Chem. 31*, 1994-1998.

10. Marques, H. M., Walton, T., and Egan, T. J. (1995) *J. Inorg. Biochem. 57*, 11-21.

11. Bali, P. K., Harris, W. R., and Nesset-Tollefson, D. (1991) *Inorg. Chem. 30*, 502-508.

12. Baldwin, D. A. and De Sousa, D. M. R. (1981) *Biochem. Biophys. Res. Commun. 99*, 1101-1107.

13. Marques, H. M., Watson, D. L., and Egan, T. J. (1991) *Inorg. Chem. 30*, 3758-3762.

14. Nurizzo, D., Baker, H. M., He, Q. Y., MacGillivray, R. T. A., Mason, A. B., Woodworth, R. C., and Baker, E. N. (2001) *Biochemistry 40*, 1616-1623.

15. He, Q. Y., Mason, A. B., Tam, B. M., MacGillivray, R. T. A., and Woodworth, R. C. (1999) *Biochemistry 38*, 9704-9711.

16. Amin, E. A., Harris, W. R., and Welsh, W. J. (2004) *Biopolymers 73*, 205-215.

17. Baldwin, D. A. (1980) *Biochim. Biophys. Acta 623*, 183-198.

18. He, Q. Y., Mason, A. B., Nguyen, V., MacGillivray, R. T., and Woodworth, R. C. (2000) *Biochem. J. 350*, 909-915.

19. Carrano, C. J. and Raymond, K. N. (1979) *J. Am. Chem. Soc. 101*, 5401-5404.

20. Kretchmar Nguyen, S. A., Craig, A., and Raymond, K. N. (1993) *J. Am. Chem. Soc. 115*, 6758-6764.

21. Turcot, I., Stintzi, A., Xu, J., and Raymond, K. N. (2000) *J. Biol. Inorg. Chem. 5*, 634-641.

22. Jeffrey, P. D., Bewley, M. C., MacGillivray, R. T. A., Mason, A. B., Woodworth, R. C., and Baker, E. N. (1998) *Biochemistry 37*, 13978-13986.

23. Zhang, Y., Furyk, S., Bergbreiter, D. E., and Cremer, P. S. (2005) *J. Am. Chem. Soc. 127*, 14505-14510.

24. Zhang, Y. and Cremer, P. S. (2006) *Curr. Opin. Chem. Biol. 10*, 658-663.

25. Kretchmar, S. A. and Raymond, K. N. (1988) *Inorg. Chem. 27*, 1436-1441.

26. Bali, P. K. and Harris, W. R. (1989) *J. Am. Chem. Soc. 111*, 4457-4461.

27. Harris, W. R., Brook, C. E., Spilling, C. D., Elleppan, S., Peng, W., Xin, M., and Wyk, J. V. (2004) *J. Inorg. Biochem. 98*, 1824-1836.

28. Brook, C. E., Harris, W. R., Spilling, C. D., Peng, W., Harburn, J. J., and Srisung, S. (2005) *Inorg. Chem. 44*, 5183-5191.

29. Harris, W. R. (1984) *J. Inorg. Biochem. 21*, 263-276.

Chapter 5

Effect of Phosphonate and Phosphonocarboxylate Anions on Saturation and First order Kinetic Pathways of Iron Release from Transferrin

5.1

Introduction

This chapter is in continuation with our attempt to have a better understanding of the effects of allosteric anions on the saturation and first order pathways of iron release. In Chapter 4, a series of sulfonates with one or two anionic functional groups were studied for their effect on the first order and saturation pathways of iron release. The interesting results obtained inspired us to extend our study to a different series of anions, the phosphonates and phosphonocarboxylates.

5.1.1

Kinetic pathways for iron removal

Kinetic studies on iron removal from transferrin by a variety of chelating agents have been performed. Different mechanisms have been proposed on the basis of the order of the reaction with respect to the ligand concentrations. The rate of iron release from transferrin by a number of ligands shows saturation with respect to the ligand concentration. Bates explained this kinetic behavior on the basis of a rate limiting conformational change in the protein (*1*). Acetohydroxamic acid (AHA) and deferiprone

are two such ligands that follow saturation kinetics (*1;2*). The ligand dependence on the rate is described by equation (5.1).

$$k_{obs} = \frac{k_{max}[L]}{k_d + [L]} \qquad (5.1)$$

Saturation is usually attributed to a rate limiting conformational change in the protein according to the mechanism proposed by Bates and co-workers (*1*). In this mechanism, $k_{max,}$ the rate constant under saturating concentrations of the ligand, represents the rate of a conformational change from a closed form of ferric transferrin to a more reactive open form of the protein.

Not all ligands studied so far follow the Bates mechanism. Many ligands, such as pyrophosphate (PPi) (*3-5*) and phosphonic acids (*6-10*), show a more complex ligand dependence. They appear to follow saturation kinetics at low ligand concentrations, but the rate continues to increase linearly with increasing concentrations of the ligand. This kind of kinetic behavior is described by equation (5.2), where the first term represents a saturation component and the second term represents a first-order component.

$$k_{obs} = \frac{k_{max}[L]}{k_d + [L]} + k'[L] \qquad (5.2)$$

A third type of kinetic behavior is observed for iron removal by the simple aminocarboxylic acids nitrilotriacetic acid (NTA) and diethylenetriaminepentaacetic acid (DTPA). Iron removal by these ligands shows a simple first order dependence on the

ligand concentration (*6;11*). It has been proposed that for iron removal by these ligands, the k_{max} values are so small that equation (5.2) reduces to a simple first-order dependence on the ligand concentration.

Nonsynergistic anions affect the rate of iron release, but the effect varies for the two lobes of the protein and for different chelating agents. For example, chloride at pH 7.4 increases the rate of iron release from C-terminal monoferric transferrin by ethylenediaminetetraacetic acid (EDTA), but slows the rate of iron release from N-terminal monoferric transferrin (*12;13*). For iron release by citrate, chloride increases the rate for both C- and N- monoferric transferrins (*14*). Lastly, for iron release by pyrophosphate, chloride increases the rate for C-terminal monoferric transferrin and has no effect on the rate of iron from N-terminal monoferric transferrin (*10;15*). It has been proposed that these variable anion effects on the rates of iron release reflect the binding of the anions to an allosteric binding site known as the **Ki**netically **S**ignificant **A**nion **B**inding (KISAB) site (*14*). However, the exact location or the structure of this proposed anion binding site has not been established (*16-18*).

We have proposed that for complex kinetic systems described by equation (5.2), the first term reflects iron release via the Bates conformational change mechanism, while the second term reflects iron release via an alternative reaction pathway that is not restricted by a rate limiting conformational change (*8;9;19*). However, others have proposed that the appearance of the first-order term arises when the ligand binds to the KISAB site and changes the value of k_{max} (*4;14;15*). To help distinguish between these two possibilities, we are now attempting to evaluate how anionic ligands such as phosphonoacetic acid might act as an allosteric anion as well as an iron chelating agent

and to assess the degree to which it might alter its own rate of iron release by binding to the KISAB site. To differentiate allosteric effects on the saturation and first order components of iron release, these studies use the chelating agents acetohydroxamate and deferiprone, which remove iron exclusively via a saturation process (*1;2*), and NTA, (*6*) which removes iron exclusively via a first order process.

In Chapter 4 we have reported the effect of a series of sulfonates on the rates of iron release by these ligands. The sulfonates accelerate iron release via the saturation component and decrease the rate of iron release via the first order component. This Chapter reports a continuation of these studies using two different classes of anions, diphosphonates and phosphonocarboxylates. The primary difference from the sulfonate study in Chapter 4 is that some of these new anions are themselves good iron chelating agents. This dual role of the chelating anions complicates the analysis of the kinetic data for iron release by mixtures of the anions and the reference chelating agents. However, it allows us to address the issue of how an anionic chelating agent may also act as an allosteric anion to modulate the rate of its own iron removal.

5.2.

Results

The anions used in this study contain various combinations of carboxylate and phosphonate functional groups. The focus is on bifunctional compounds, e.g. phosphonoacetic acid or methylenediphosphonic acid. To provide a basis for assessing the degree to which the two functional groups in these compounds work cooperatively, the rates of iron release from C-terminal monoferric transferrin by 200 mM AHA have

been measured in the presence of the monofunctional anions methylphosphonate (MPA) and acetate. The rate constants for iron release by AHA in the presence of 100 mM concentrations of these anions are shown in Table 5.1.

Table 5.1

Effect of methylphosphonate and acetate anions on the rate of iron removal by 200 mM AHA[a]

	k_{obs} (min^{-1}) x 10^3
200 mM [AHA]	16.2 $\pm$ 0.4
[AHA] + 100 mM MPA	25.4 $\pm$ 0.2
[AHA] + 100 mM Acetate	20.4 $\pm$ 0.3

[a]0.1 M HEPES, pH 7.4, 25 ºC

5.2.1

Effects of phosphonocarboxylates on iron release by AHA

The rates of iron release by AHA in the presence of MPA, phosphonoacetic acid (PAA), and 3-phosphonopropionic acid (PPA) have been evaluated. As reported previously, PAA is a good iron chelating agent that removes iron from transferrin with a combination of saturation and first order components (*20;21*). Although PPA contains the same two metal-binding functional groups, the simultaneous coordination of both groups forms a thermodynamically unstable 7-membered chelate ring. Control experiments confirmed that over the concentrations used in these studies, neither PPA nor

MPA removes any significant amount of iron. Thus PPA and MPA are treated as non-complexing allosteric anions.

Rates of iron release by 200 mM AHA were measured in the presence of increasing concentrations of PPA and MPA. To minimize the effects of day-to-day variations in the data, reactions with and without the added anion were always run simultaneously. Both of these anions increase the rates of iron release by AHA. This increase is represented as shown in equation (5.3),

$$\%\Delta k = \frac{k'_{obs} - k_{obs}}{k_{obs}} \; x100 \qquad (5.3)$$

where k_{obs} is the rate for AHA alone, and k'_{obs} is the rate for AHA in the presence of the anion. Plots of %Δk vs [anion] are shown in Figure 5.1.

The values of %Δk increase linearly with the anion concentration for both MPA and PPA. The slope of the plot for PPA is greater than that for MPA. The effect of 100 mM PPA is greater than the sum of the effects of equimolar concentrations MPA alone and acetate alone. Thus, the two functional groups of PPA appear to act cooperatively, presumably by binding more strongly to the transferrin.

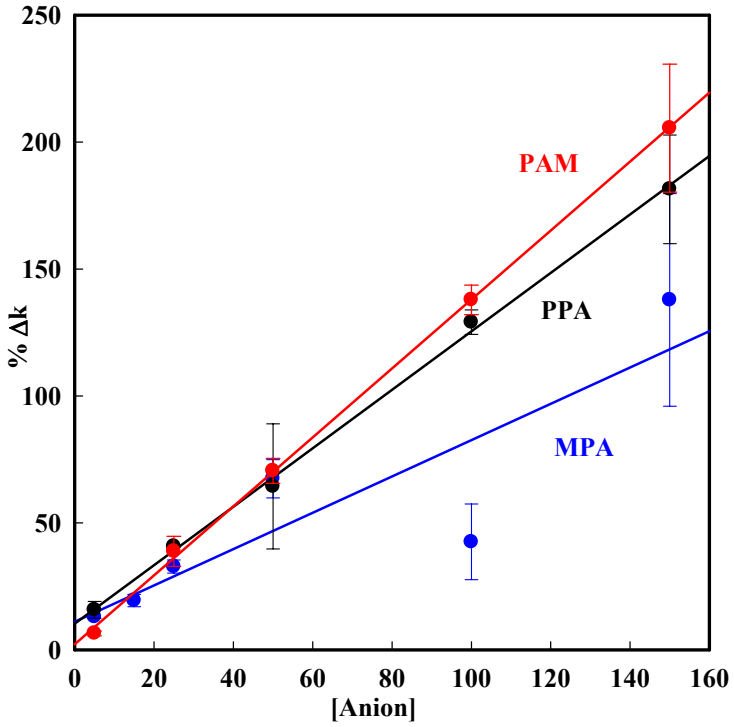

Figure 5.1. Plots of %Δk for the removal of iron from C-terminal monoferric transferrin by 200 mM AHA in the presence of methanephosphonate (MPA) and 3-phosphonopropionic acid (PPA) and phosphonoacetamide (PAM) at 25 ºC in 0.1 M Hepes, pH 7.4.

The "anion" PAA is also a good iron chelating agent (*20;21*). The rates of iron release by PAA alone and its methyl and ethyl derivatives have been evaluated in Chapter 3, and they show a combination of saturation and linear kinetics. We evaluated the effect of the anion PAA on iron release by AHA by measuring the rate constants for iron release

by AHA alone, by PAA alone, and by a mixture of AHA and PAA. To minimize day-to-day variations in the data, these experiments were run by taking the same stock solution of C-terminal monoferric transferrin, preparing the three kinetic samples, and running the reactions simultaneously using a rotating 4-position cuvette holder in the fluorimeter. The apparent rate constant for iron release by AHA in the presence of PAA was calculated as shown in equation (5.4)

$$k_{app}(AHA) = k_{obs}(AHA + \mathrm{PA}A) - k_{obs}(\mathrm{PA}A) \qquad (5.4)$$

In these experiments, the concentration of AHA was held constant at 200 mM. Figure 5.2 shows the values of k_{obs} for the samples with PAA alone and the mixture of PAA and AHA. The k_{obs} value for AHA alone was consistently 0.016, so these data are not shown in Figure 5.2.

The apparent rate constant (k_{app}) for the removal of iron by AHA in the presence of PAA was obtained by subtracting the rate constant for the AHA/PAA mixture from the matched sample of PAA alone. As shown in Figure 5.2, the value of k_{app} is constant for all PAA concentrations, with an average value of 0.008 ± 0.002 min^{-1}. This is 50% of the k_{obs} for AHA in the absence of PAA. In contrast to the allosteric effects of MPA and PPA, which significantly accelerate the rate of iron release by AHA, PAA appears to slow the release of iron by AHA.

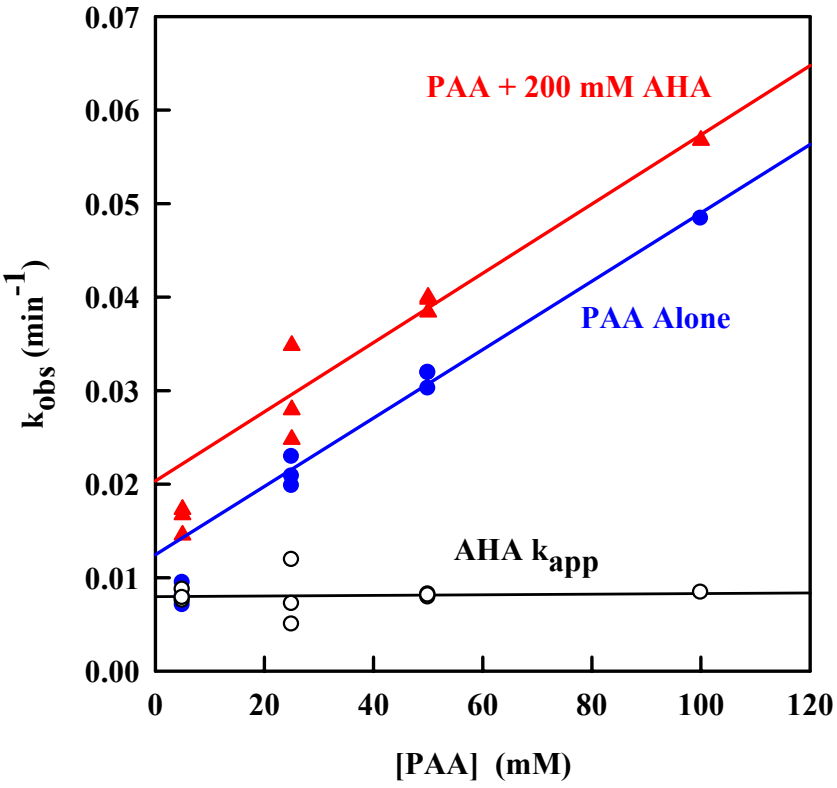

Figure 5.2. Plots of k_{obs} for the removal of iron from the C-terminal monoferric transferrin by varying concentrations of phosphonoacetic acid (PAA) and by mixtures of 200 mM AHA with variable concentrations of PAA at 25 °C in 0.1 M Hepes, pH 7.4. The k_{app} value for AHA is calculated as shown in equation (5.4).

The most obvious difference between PAA and PPA is the ability of PAA to form a more stable 6-membered chelate ring. This suggests that the variations in the kinetic effects of PAA and PPA are related to their different iron-binding affinities. To test this hypothesis, we conducted additional studies using phosphonoacetamide (PAM). The

conversion of the free acetate group of PAA to an amide essentially destroys the ability of PAM to chelate iron, so that PAM cannot remove iron from transferrin and can act only as an allosteric anion. Rates of iron release by AHA in the presence of increasing concentrations of PAM were measured. The data were used to calculate values for %Δk as per equation (5.3), and the results are shown in Figure 5.1. The conversion of the acetate to an amide fully restores the positive allosteric effect seen for PPA.

The effect of phosphonocarboxylates on iron removal by deferiprone has also been measured. The effects of the allosteric anions MPA, PAA, PPA, and PAM on iron release by deferiprone have been determined as described above for the studies which used AHA as the reference ligand. The variations in the rate constants for deferiprone have been converted to values of %Δk and plotted in Figure 5.3. The results are essentially the same as those observed for iron removal by AHA. The non-chelating anions MPA, PPA, and PAM all accelerate iron removal, while the chelating anion PAA retards the rate of iron removal by deferiprone.

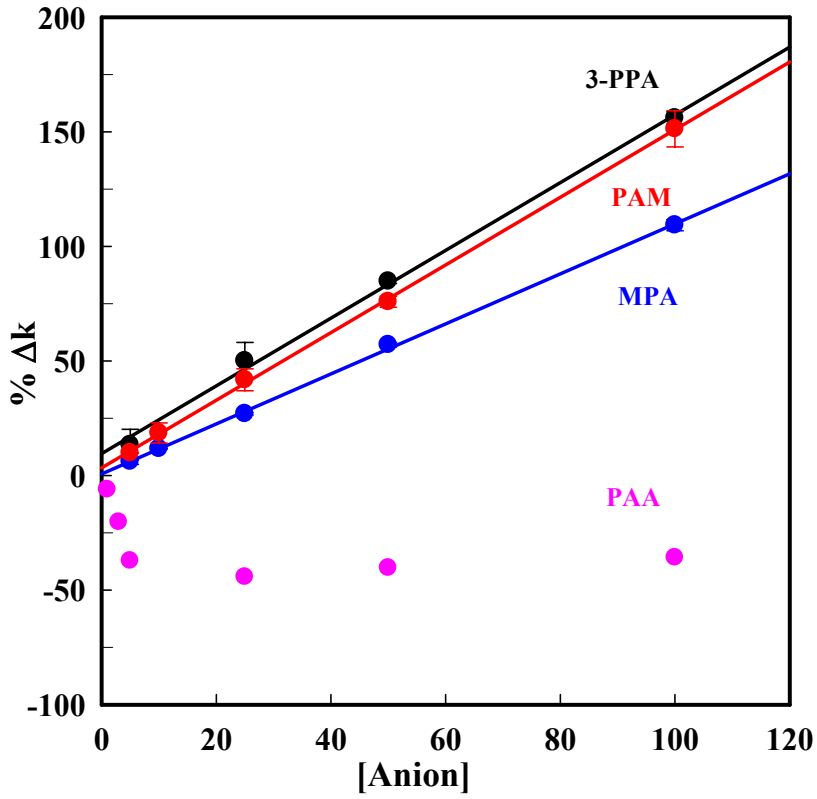

Figure 5.3. Plots of %Δk for the removal of iron from the C-terminal monoferric transferrin by 20 mM deferiprone (L1) in the presence of methane phosphonate (MPA), phosphonoacetic acid (PAA), 3-phosphonopropionic acid (PPA) phosphonoacetamide (PAM) at 25 °C in 0.1 M Hepes, pH 7.4.

5.2.2

Effect of excess bicarbonate on inhibition by PAA.

Since the inhibition of iron release by PAA appears to be linked to its ability to bind Fe^{3+}, we considered the possibility that the PAA might replace the synergistic carbonate anion to form an Fe-PAA-Tf ternary complex that reacts more slowly than the

original Fe-CO_3-Tf complex with AHA. If this were true, the addition of excess carbonate to the solution should reduce the degree of formation of the Fe-PAA-Tf complex and thus should reduce the inhibitory effect of the PAA.

In addition to its well-known role as the synergistic anion for the formation of the normal Fe-CO_3-Tf ternary complex (*22*), bicarbonate might also act as an allosteric anion and bind to the KISAB site. Therefore, an additional set of experiments were conducted to measure the rates of iron release by both PAA and AHA in solutions with bicarbonate concentrations of 0, 1, 5, 15, and 20 mM to measure the degree to which bicarbonate acts as a KISAB anion to alter the rates of iron release. A linear extrapolation was used to calculate the rate constant for iron removal by PAA and AHA at 25 mM bicarbonate. The rate constant for iron release by PAA was essentially unaffected by excess bicarbonate, with a rate constant of 0.0212 min^{-1} at both 0 and 25 mM bicarbonate. The rate of iron release by AHA changed from 0.0107 min^{-1} with no bicarbonate to 0.0168 min^{-1} at 25 mM bicarbonate.

The rate constant for iron release for a solution containing a mixture of AHA/PAA/carbonate was determined to be 0.0287 min^{-1}, which is presumed to be the sum of the rate constant for PAA and the apparent rate constant for AHA. If one subtracts the value of 0.0212 min^{-1} for iron removal by PAA, the apparent rate constant for AHA is 0.0075 min^{-1}, or 45% of the value for AHA in the presence of 25 mM bicarbonate. This is essentially identical to the degree of inhibition by PAA on iron release by AHA at ambient carbonate. Thus it appears that the inhibition by PAA on the rate of iron removal by AHA does not involve the displacement of the synergistic carbonate anion.

5.2.3.

Effect of phosphonocarboxylates on k_{max} and k_d for iron removal by AHA.

The ligand dependence of iron removal by AHA has been described by equation (5.1). The change in k_{obs} for iron removal by AHA produced by PAA and PPA (Figure 5.1) could be due either to changes in k_{max}, changes in k_d, or to some combination of both. To distinguish among these possibilities, k_{obs} values were measured for iron removal by varying concentrations of AHA, both in the absence and in the presence of a constant concentration of either 50 mM PPA or 5 mM PAA. Since the inhibition by PAA is essentially constant for concentrations of PAA $\geq$ 5 mM, a lower concentration of PAA was chosen so that the overall rate of iron release for the mixture would be due mainly to iron release by AHA.

Plots of k_{obs} vs [AHA] for AHA alone, AHA + 5 mM PAA, and AHA + 50 mM PPA are show in Figure 5.4. Each set of data has been fit both to equation (5.1), which describes simple saturation kinetics, and to equation (5.2), which described a combination of saturation and linear kinetics. It is clear from inspection that equation (5.2) gives a better fit to the data when either PPA or PAA is present. For the data on iron release by AHA alone, the fits of equation (5.1) and equation (5.2) are very similar. An R-factor ratio test (*23*) indicates that the improvement in the fit for equation (5.2) is statistically significant at $\alpha = 0.05$. The rate parameters obtained from the fit of the data in Figure 5.2 to equation (5.2) are shown in Table 5.2

Table 5.2

Rate parameters for the release of iron from C-terminal monoferric transferrin by AHA alone and in combination with either 5 mM PAA or 50 mM PPA

	$10^3 k_{max}$ (min^{-1})	k_d (mM)	$10^3 k'$ ($M^{-1}min^{-1}$)	σ_y[a]
AHA alone	13.6 ± 1.3	59 ± 10	0.0102 ± 0.026	0.0004
AHA + PPA	16.8 ± 0.7	8.0 ± 1.1	0.0307 ± 0.026	0.0007
AHA + PAA	4.3 ± 0.6	10 ± 5	0.0213 ± 0.022	0.0005

[a]Standard deviation in the fit of of k_{obs}vs [AHA] to equation (5.2)

Both PPA and PAA cause a significant decrease in k_d for iron removal by AHA, such that the reaction approaches saturation at lower AHA concentrations. Since PPA also increases the k_{max} value, the net result is a significant increase in the rate or iron release at low AHA concentrations. In contrast, PAA reduces k_{max}, so that even though this system reaches saturation quickly, the rate of iron release is lower than that for AHA alone.

Previous studies have reported that iron release by AHA follows simple saturation kinetics (*2*). Thus the most unexpected result from Figure 5.4 is that AHA may have a small, but statistically significant, first-order component for iron release. Both PAA and PPA result in a significant increase in the first order process, so that iron release in the presence of these anions must be described as complex kinetics with both saturation and first-order components.

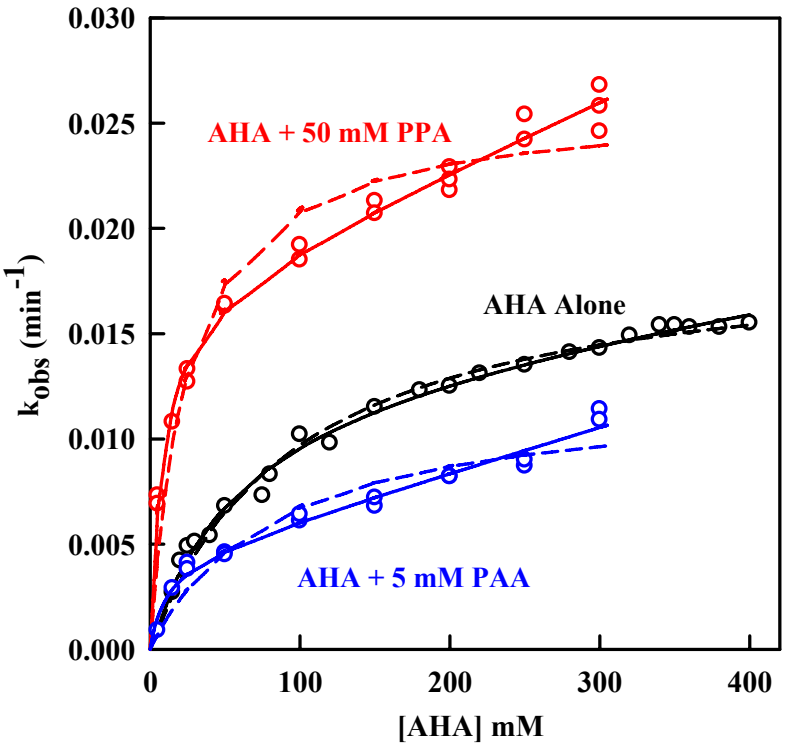

Figure 5.4. Plots of k_{obs} for the removal of iron from C-terminal monoferric transferrin by acetohydroxamic acid (AHA), AHA in the presence of 50 mM 3-phosphonopropinonic acid (PPA) and AHA in the presence of 5 mM phosphonoacetic acid (PAA) at 25 °C in 0.1 M Hepes pH 7.4.

5.2.4

Effects of phosphonocarboxylates on iron release by NTA

The rate of iron release from transferrin is first order with respect to the concentration of NTA (*6*). To study the effect of phosphonocarboxylates, on the first order component for iron release the rate of iron release from C-terminal monoferric transferrin by NTA was measured in the presence of increasing concentrations of MPA,

PAA and PPA. Both MPA and PPA behaved as a simple anion without removing any iron on their own, and their effect on the rate of iron release by NTA was calculated as %Δk as shown in equation (5.3). Since PAA is a good chelating agent and does remove iron, the apparent rate constant for iron release by NTA was calculated as shown in equation (5.4). This apparent rate constant was then used to calculate %Δk for PAA. Plots of %Δk vs [anion] are shown in Figure 5.5.

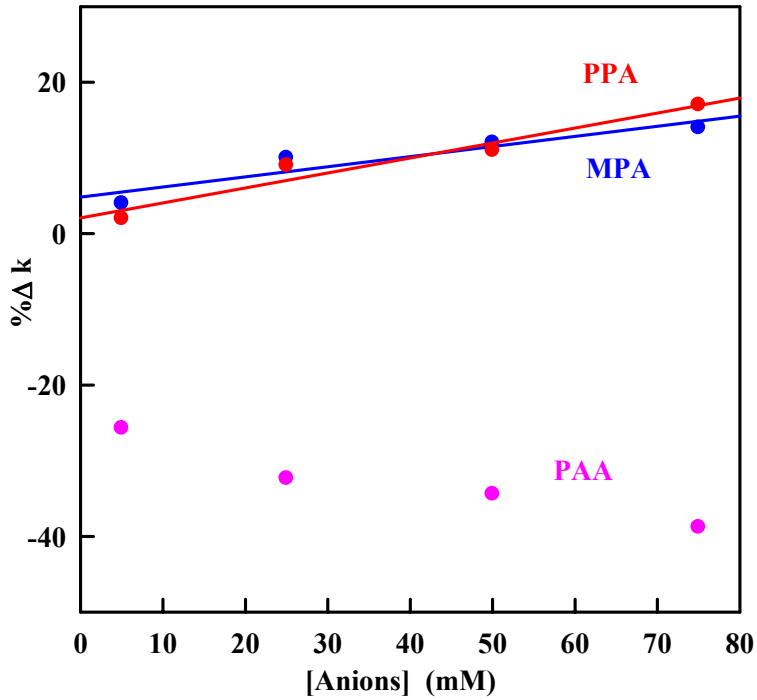

Figure 5.5. Plots of %Δk for the removal of iron from C-terminal monoferric transferrin by 100 mM nitrilotriacetic acid (NTA) in the presence of methanephosphonate (MPA), phosphonoacetic acid (PAA), 3-phosphonopropionic acid (PPA) at 25 ºC in 0.1 M Hepes, pH 7.4.

The effects of MPA, PAA, and PPA on the rates of iron removal by NTA are qualitatively similar to their effects on iron removal by AHA. Both MPA and PPA increase the rates of iron removal, but the increases for NTA are much smaller, ~20%, compared to 200% acceleration for iron release by AHA and deferiprone. The presence of PAA decreases the rate or iron removal for NTA by about 40%, which is comparable to its effect on iron release by AHA. However, the inhibition of NTA requires slightly high concentrations of PAA.

5.2.5

Effect of phosphonocarboxylates on k_{max}, k_d, and k' for NTA

Rates of iron release by various concentrations of NTA were measured using samples of C-terminal monoferric transferrin that all contained 50 mM PPA. The plot of k_{obs} vs [NTA] is shown in Figure 5.6 for samples with and without the PPA. At concentrations of NTA $\leq$ 50 mM, the iron removal reaction does not go to completion, and the values of k_{obs} were calculated using equation (2.3) from Chapter 2 to fit the intensity vs time data. The data in the absence of PPA confirm that iron release by NTA is a simple pseudo first-order process, with an observed rate constant of 0.33 ± 0.01 M^{-1} min^{-1}. This is essentially identical to the value of k' = 0.32 ± 0.03 $M^{-1}min^{-1}$ published previously (*6*).

The addition of PPA dramatically changes the ligand dependence of iron removal by NTA. The reaction is clearly no longer a simple first-order process. The data on iron removal in the presence of the PPA have been fit to both equation (5.1) and equation (5.2), and the resulting parameters are shows in Table 5.3. As one would expect from

inspecting Figure 5.6, there is a highly significant improvement in the fit for equation (5.2), as shown by the decrease in σ_y from 0.0029 to 0.0008. Thus we can conclude that iron release by NTA in the presence of 50 mM PPA is best described as complex kinetics, representing a combination of saturation and first-order pathways.

The rate constants for iron release from C-terminal monoferric transferrin were also measured by varying concentrations of NTA in the presence 25 mM PAA. For each experiment, the measured k_{obs} value would reflect the total rate of iron release by both NTA and PAA. The apparent rate constant for iron removal by NTA was calculated by subtracting the measured rate constant for 25 mM PAA (0.0223 min^{-1}) from the total k_{obs} value for each mixture to give the k_{app} for iron release by NTA in the presence of 25 mM PAA. These k_{app} values are plotted in Figure 5.6.

The plot of the k_{app} values for NTA is essentially linear with a small y-intercept. It appears that there might be a slight curvature at low concentrations of NTA, and we attempted to fit the data to equation (5.2) for saturation-linear kinetics. However, the correlations among the 3 adjustable parameters are extremely high, and the errors in the calculated parameters are all well over 100%. Therefore, the data were fit to a simple linear function, with the assumption that the slope was equal to k', and the y-intercept was equal to k_{max}. The results are shown in Table 5.3.

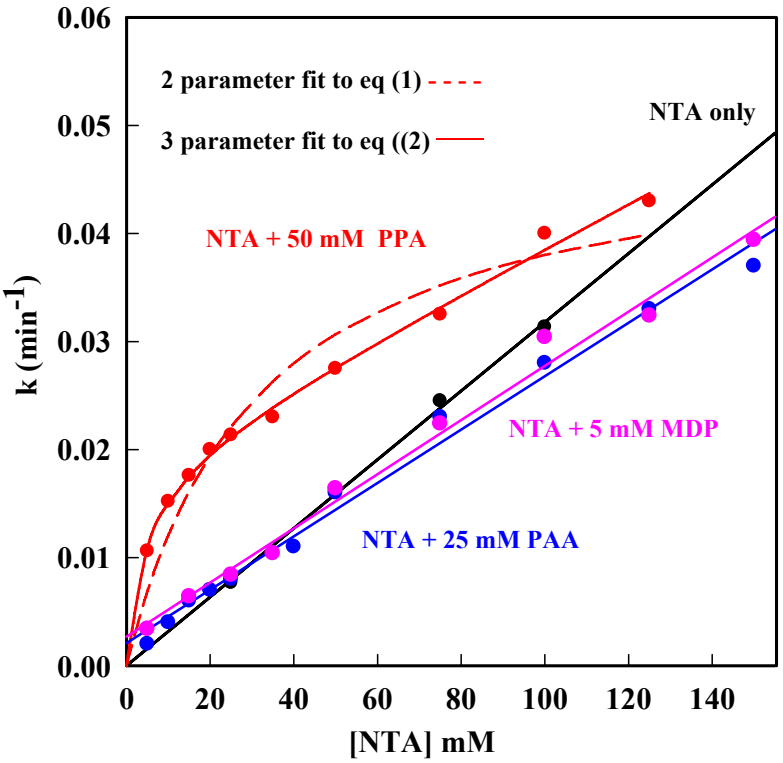

Figure 5.6. Plot of rate constant for the removal of iron from C-terminal monoferric transferrin at 25 ˚C in 0.1 M Hepes, pH 7.4 by varying concentrations of nitrilotriacetic acid (NTA), NTA in the presence of 50 mM 3-phosphonopropionic acid (PPA), NTA in the presence of 25 mM phosphonoacetic acid (PAA) and NTA in the presence of 5 mM MDP.

Table 5.3

Rate parameters for iron release from C-terminal monoferric transferrin by NTA in the presence of selected anions.

Anion	10^3 k_{max} (min^{-1})	k_d (mM)	10^3 k` ($M^{-1}min^{-1}$)	σ_y
None	-	-	0.325 ± 0.012	
50 mM PPA[a]	50 ± 4	32 ± 7	-	0.0029
50 mM PPA[b]	19 ± 1	5 ± 1	0.200 ± 0.012	0.0008
25 mM PAA	2.1 ± 0.6	-	0.247 ± 0.009	0.0014
5 mM MDP	2.7 ± 0.8	-	0.251 ± 0.010	0.0014

[a]Data fit to equation (5.1) with two adjustable parameters

[b]Data fit to equation (5.2) with three adjustable parameters

Both PPA and PAA appear to give a similar reduction of ~30% in k'. However, they have very distinct effects on k_{max}. The addition of 50 mM PPA increases k_{max} for NTA from essentially zero to 0.050 min^{-1}. A very similar increase in k_{max} for NTA has been observed in the presence of methylenedisulfonic acid (MDS) in Chapter 4. In contrast, the presence of PAA has little, if any, impact on k_{max} for iron removal by NTA. The linear fit gives a small non-zero intercept of 0.0021 ± 0.006. This value of k_{max} is more than three times its standard deviation, which suggests that the difference from a value of zero is statistically significant. However, the k_{app} values are obtained by subtracting the rate constant for PAA from each value of k_{obs} for the mixture of NTA and PAA. The value of the intercept would correspond to an error of only 10% in the value used for the rate constant for PAA. Thus the significance of the small k_{max} value for

NTA in the presence of PAA is not clear. Whether or not k_{max} is slightly greater than zero, the major impact of PAA on the overall rate of iron release by NTA is the decrease in the k` value.

5.2.6

Effect of diphosphonates on iron removal by AHA

The effects methanediphosphonate (MDP) and ethanediphosphonate (EDP) on iron release by AHA have been evaluated. The rates of iron release by MDP alone and mixtures of MDP with 200 mM AHA were measured and are plotted in Figure 5.7. The mixtures show a consistent increase in k_{obs} relative to the same concentration of MDP without AHA. The k_{obs} values for each mixture is assumed to be the sum of the rate constants for MDP and AHA. At each concentration of MDP, the rate constant for MDP alone is subtracted from the rate constant for the mixture to obtain a value of k_{app} for AHA. This value of k_{app} is used with the rate constant for AHA alone to calculate value of $\%\Delta k$ by use of equation 5.3.

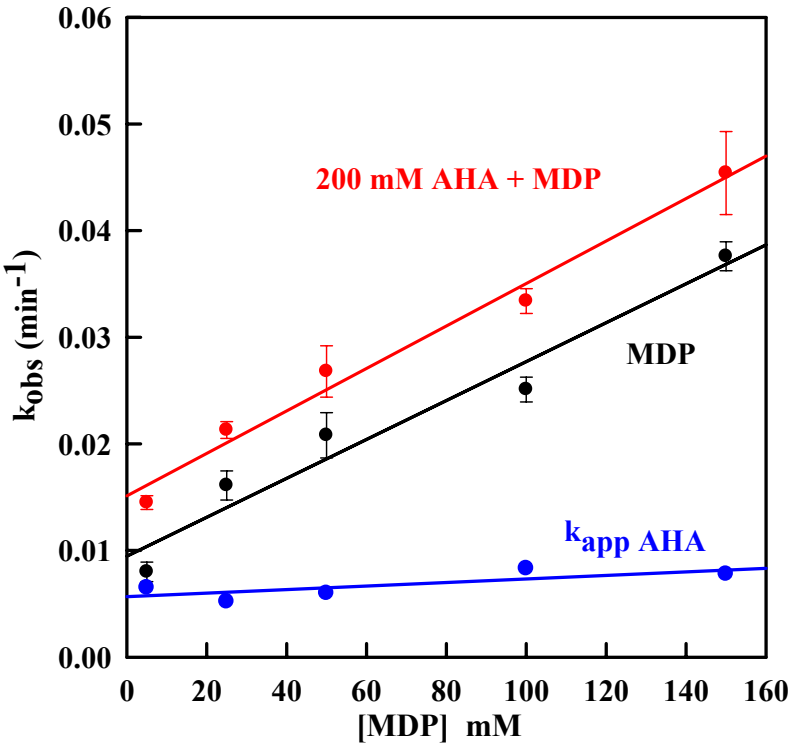

Figure 5.7. Plots of k_{obs} for the removal of iron from the C-terminal monoferric transferrin by methanediphosphonate (MDP) and by the mixture of 200 mM AHA and MDP at 25 ºC, 0.1 M Hepes, pH 7.4. The values of k_{app} represent the rate constant of the mixture minus the rate constant for MDP alone.

Values of %Δk vs [anion] for 200 mM AHA are plotted in Figure 5.8. The data on the monophosphonate MPA shows the linear increase due to this non-chelating anion. The chelating MDP anion has a very different impact on iron release from AHA. All concentrations of MDP that were test reduced the rate of iron release by AHA by approximately 50%. This result is very similar to the rate reduction caused by PAA.

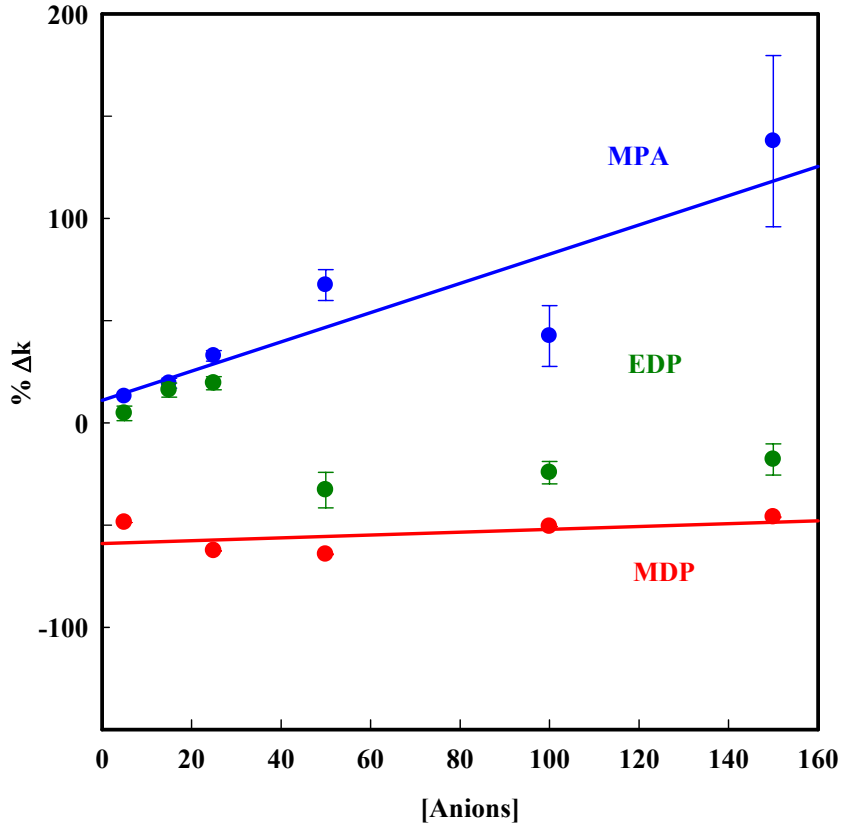

Figure 5.8. Plots of %Δk for the removal of iron from C-terminal monoferric transferrin by 200 mM AHA in the presence of methanephosphonate (MPA), methanediphosphonate (MDP), ethanediphosphonate (EDP), at 25 ºC in 0.1 M Hepes, pH 7.4.

We also studied the effect of the longer diphosphonate, EDP, on the rate of iron removal by AHA. Rates of iron release were measured for paired samples that contained increasing concentrations of EDP, with and without 200 mM AHA. At low concentrations, EDP fails to remove any appreciable amount of iron, so the observed rate

constants were due entirely to iron removal by AHA. However, EDP concentrations greater than 25 mM remove appreciable amounts of iron in the absence of AHA. Thus for higher concentrations of EDP, the apparent rate constant for AHA was obtained by subtracting the rate constant for iron removal by EDP from the observed rate constant of the AHA/EDP mixture.

Values of %Δk for EDP are also plotted in Figure 5.8. The results for EDP are more complex than those observed for any other anion. At low concentrations, EDP behaves as a typical non-chelating anion and increases the rate constant for AHA just as MPA does. However, as soon as the concentration of EDP reaches a level sufficient to remove iron from transferrin, its behavior changes to the same inhibitory effect as that observed for MDP. Thus high concentrations of EDP inhibit iron release by AHA by about 50%.

5.2.7

Effects of diphosphonates on iron release by NTA

The effects of MPA, MDP, and EDP on iron release by NTA were also evaluated, and the resulting %Δk values are plotted in Figure 5.9. The results can be compared with the data on phosphonocarboxylates that are shown in Figure 5.5. The MDP mimics the behavior of PAA and inhibits iron release by NTA by about 40%. Low concentrations of EDP behave similarly to MPA and also accelerate iron release, but high concentrations of EDP mimic MDP and inhibit iron release by NTA.

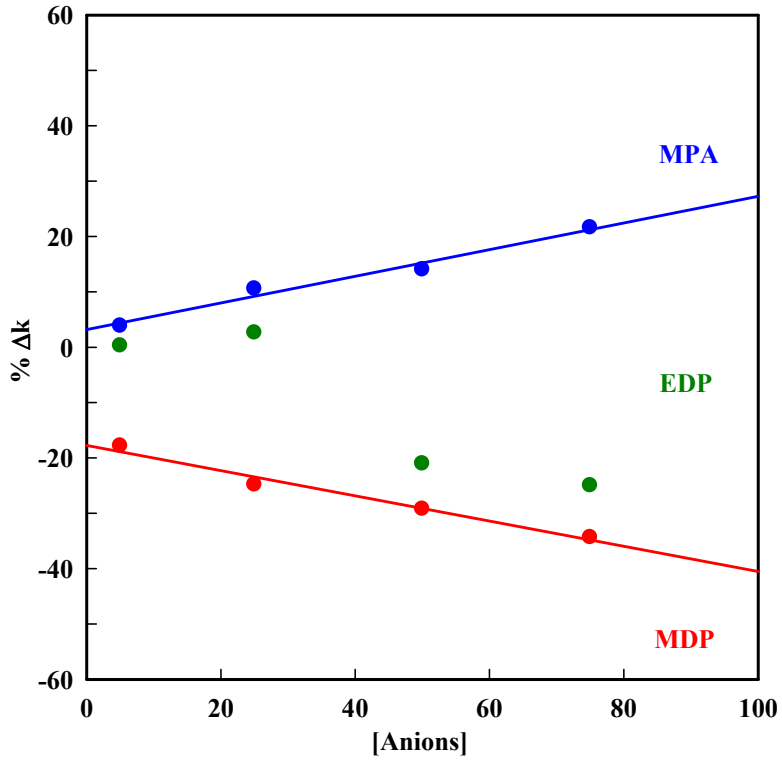

Figure 5.9. Plots of %Δk for the removal of iron from C-terminal monoferric transferrin by 100 mM nitrilotriacetic acid (NTA) in the presence of methanephosphonate (MPA), methanediphosphonate (MDP) and ethanediphosphonate (EDP) at 25 ºC in 0.1 M Hepes, pH 7.4.

5.2.8

Effect of MDP on k_{max}, k_d, and k' for NTA

To determine the effect of MDP on the k_{max}, k_d, and k' rate parameters for iron release by NTA, rate constants were measured using a constant MDP concentration of 5 mM in combination with a series of NTA concentrations. The apparent rate constants for

NTA were determined by subtracting the rate for MDP alone from the rate of the mixture. A low concentration of MDP was selected for these studies so that the k_{obs} for the mixture would be largely due to iron release by NTA. The data in Figure 5.9 indicated that even 5 mM MDP would still have a significant allosteric effect on iron release by NTA.

The observed/apparent rate constants for iron release by NTA with and without the 5 mM MDP are shown in Figure 5.6. It is obvious that 5 mM MDP and 25 mM PAA have essentially the same effect on iron release by NTA. The data for the MDP/NTA mixture is highly linear, so no effort was made to fit them to either equation 5.1 or 5.2. Instead, simple linear fit was used, and the slope and intercept, are listed in Table 5.2. As seen in Figure 5.6, 5 mM MDP appears to accelerate iron removal by low concentrations of NTA. But above 40 mM NTA, the net effect of MDP becomes inhibitory. The rate parameters for iron release by NTA in the presence of MDP are listed in Table 5.3.

5.3

Discussion

An early kinetic study on the removal of iron from transferrin by the tricatechol ligand 3,4-LICAMS showed that the rate of iron release followed saturation kinetics with respect to the ligand concentration (*24*). The logical inference from that observation, in line with the Michaelis-Menton model for enzyme kinetics, was that the ligand was forming a stable mixed-ligand intermediate complex with ferric transferrin, and that the rate at saturation represented the dissociation of this intermediate. Shortly thereafter, similar studies using AHA as the chelator also showed saturation kinetics removal (*1*). But this study also included kinetics experiments on the donation of iron to apotransferrin

from $Fe(AHA)_3$, and these data showed conclusively that the AHA-Fe-CO_3-Tf mixed-ligand intermediate did not accumulate to detectable levels during iron release. Something besides the dissociation of the mixed-ligand intermediate had to be rate-limiting for iron release, and the authors proposed that it was a slow conformational change from the native form of ferric transferrin to a more labile "open" conformation.

The Bates mechanism was proposed based purely on kinetic data (*1*). However, it was subsequently supported by crystal structures, which consistently showed that there was a major conformational change between the ferric and apo forms of the protein (*25-27*). This mechanism has been enormously influential on the discussions of iron release kinetics. However, as more studies on iron release have been conducted using a wider variety of ligands, it has become clear that there are many ligands that do not show simple saturation kinetics for iron removal. Most of them show "complex" kinetics, consisting of a saturation component at low ligand concentrations and a first-order component at high ligand concentrations.

The Bates mechanism can account for the saturation component. The bigger question has been, what is responsible for the first-order component? The first order component is missing or minimal for AHA (*2*), catechols (*28*), and hydroxypyridinones (*2*), which have high pK_as and thus carry little net charge at neutral pH. Conversely, the first order term is routinely observed for ligands that contain functional groups such as acetate and phosphonate that are more acid and are largely ionized at neutral pH.

There are two basic models that attempt to link the ionic nature of the ligand with the prominence of a first order component of the iron release. One model includes two separate pathways for iron release. One pathway consists of the Bates mechanism and

accounts for the saturation component of iron release. The second component is a separate pathway that is independent of the conformational change and involves the replacement of the synergistic carbonate anion by the incoming anionic ligand (*2;20;21;29*). According to this model, the k' term in equation (5.2) is the second order rate constant for this second pathway.

An alternative explanation for the first order component for iron release is that it is essentially an artifact produced by allosteric effects from anions binding to the KISAB site on the protein (*4*). In this "allosteric" model, the system consists of two forms of ferric transferrin that are linked by an anion binding equilibrium. If one assumes that each form of ferric transferrin releases iron via a Bates mechanism, then the effect of anion-binding on the observed rate of iron release could be described by equation (5.5).

$$k_{obs} = \frac{k_{\max}[L]}{k_d + [L]}\left(\frac{1}{1 + K_A[A]}\right) + \frac{k'_{\max}[L]}{k'_d + [L]}\left(\frac{K_A[A]}{1 + K_A[A]}\right) \qquad (5.5)$$

In this equation, K_A is the equilibrium constant for anion binding to the KISAB site. The rate parameters are k_{max} and k_d for the "native" form of the protein, and k_{max}' and k_d' for the "modified" form that is produced by anion binding. In the special case where the anion in equation (5.5) is also the ligand being used to remove the iron, then this model attributes the apparent first-order component to a gradual transition from the native protein to a modified protein with a larger k_{max}' value.

At ligand concentrations high enough to saturate the anion binding site, equation (5.5) reduces to $k_{obs} = k_{max} + k_{max}'$, i.e. one would still observe saturation kinetics. However, one could account for the observed complex kinetics rather easily simply by

assuming that the anion binding site is far from saturation and that $k_{max}' >> k_{max}$. This is illustrated by the family of simulated plots in Figure 5.10.

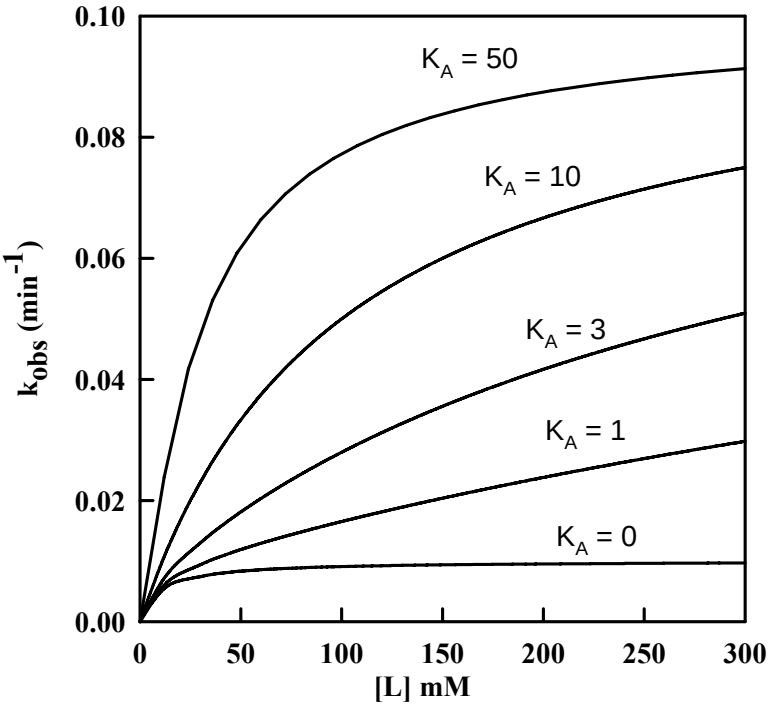

Figure 5.10. Plots of equation (5.5) simulating the value of k_{obs} for selected rate parameters and KISAB anion binding constants. For all plots, k_{max} = 0.01 min^{-1}, k_{max}' = 0.1 min^{-1}, and $k_d = k_d'$ = 10 mM. The KISAB anion binding constants are listed next to each plot.

Figure 5.10 shows plots of equation (5.5) for fixed values of k_{max}, k_{max}', k_d and k_d' with various values of the anion binding constant K_A. Obviously when K_A = 0, one obtains simple saturation kinetics with a plateau at the value of k_{max}. For a large anion binding constant, the data also appear as simple saturation kinetics, with a plateau at $k_{max} + k_{max}'$. For small values of K_A, such that the KISAB site remains far from saturation,

the plots indicate complex kinetics, with a saturation component and what appears to be a clear first order component. Thus the allosteric model can account for complex kinetics so long as K_A is very small and $k_{max}' >> k_{max}$.

In this Chapter we report that MPA and PPA accelerate the rate of iron release by both AHA and NTA. More detailed data on PPA show that this anion does increase the value of k_{max} for both reference ligands. These observations would be consistent with the allosteric model. However, the unexpected result reported here is that both PAA and MDP significantly inhibit iron release by AHA. Furthermore, the decrease in the rate of iron release by AHA can be attributed specifically to a smaller value for k_{max}. These new results on the effect of PAA and MDP on AHA are not consistent with the allosteric model for complex kinetics.

The difference between PAA and PPA structurally is one additional methylene group between the phosphonate and carboxylate functional groups in PPA. In Chapter 4, our studies on the anion effects of disulfonates, methylenedisulfonic acid (MDS) and ethylenedisulfonic acid (EDS) had very similar accelerating effects on iron release by AHA. Thus it is unlikely that the additional group in PPA would lead to a large difference in the binding of PAA and PPA as allosteric anions. Furthermore, the amide PAM has virtually the same allosteric effect on iron release as PPA. Thus the anion-binding reaction appears to be quite robust to changes in the anion.

The most obvious consequence of the elongation of PAA to PPA is the loss of iron-binding affinity for the longer anion. The PPA ligand would form an unstable 7-membered chelate ring, and thus does not remove any iron from transferrin, whereas PAA is a much strong chelator.

The comparison between MDP and EDP is a more complicated. EDP must also form a larger and thus less stable chelate ring. At lower concentrations, EDP like PPA, acts as an allosteric anion but does not remove any iron from the protein. However, higher concentrations of EDP do remove iron, presumably because phosphonate groups have a higher affinity for Fe^{3+} than does the acetate group of PPA. As soon as the EDP concentration is high enough to remove iron from the protein, the effect of this anion on iron removal by AHA switches from stimulatory to inhibitory. In fact, high concentrations of EDP have the same inhibitory effect as PAA and MDP on the rate of iron release. Thus there is a clear correlation between inhibition of iron release by AHA and the ability of the allosteric anion to bind iron.

In the Bates mechanism for the saturation component of iron release by low-molecular-weight ligands, the protein conformational change occurs prior to any interactions with the ligand, and thus the value for k_{max} should be independent of the ligand. Table 5.3 lists the k_{max} values for iron removal from both C-terminal and N-terminal monoferric transferrins by a series of ligands. There is clearly a variation in k_{max} among ligands, particularly for the N-terminal site. The new data on how ligands such as PAA can also bind to the KISAB site provides a possible reason for this variation in k_{max}. If this hypothesis is correct, then NTA and DTPA represent the extreme in self-inhibition by chelating agents, since they have k_{max} values of zero.

McGillivray et al. (*27*) have reported crystal structures for the ferric complex of the recombinant N-lobe that shows disorder of the synergistic carbonate anion. They have proposed that this results from a mixture of two conformations. In one conformation, the carbonate is bound as expected as a bidentate ligand. In the second

conformation, the carbonate has rotated and is coordinated as a monodentate ligand. This obviously frees one coordination site for an incoming ligand.

The inhibition of iron release by AHA is associated specifically with chelating anions, but not monodentate anions. The implication is that the inhibiting anions are binding as bidentate ligands to the iron. This change in the conformation of the carbonate could provide one coordination site. The second coordination site could be generated by going from 6-coordinate to 7-coordinate iron, or by the displacement of one of the protein ligands. It has been proposed that when iron binds to apoTf, coordinate bonds to the two tyrosine residues form first, and the bonds to histidine and aspartic acid form later as the protein structure moves toward a closed conformation (*30*). Thus one would expect that either the histidine or the aspartic acid would be more likely to dissociate early in the iron release process. The aspartic acid is the only protein ligating group from domain I in each lobe. He and Mason (*31*) have suggested that the weakening of the coordinate bond to the aspartate, in conjunction with the binding of a chelating agent or KISAB anion, is an early step in iron release.

Harris et al. (*29*) used citrate to study the rate of metal release from the C-terminal site for Fe^{3+}, Ga^{3+}, In^{3+}, Al^{3+}, and Tb^{3+}. They showed that the value of k_{max} was very strongly dependent on the identity of the metal ion, with values ranging from 0.004 min^{-1} for Fe^{3+} to ~0.7 min^{-1} for In^{3+} and Al^{3+} to ~ 2.0 min^{-1} for Ga^{3+} and Tb^{3+}. This is another indication that the magnitude of k_{max} is sensitive to the making and/or breaking of metal ligand bonds.

Table 5.4

k_{max} and k' parameters for iron release from C-terminal monoferric transferrin

Ligand	10^3 k_{max} (min^{-1}) C-terminal monoferric Tf	10^3 k_{max} (min^{-1}) N-terminal monoferric Tf	Reference
PPi	7.7	51	(*3*)
DHBA	9.18	50.4	(*32*)
AHA	13.6[a]	46.6	(*2*)
L1	7.4	44.7	(*2*)
3,4-LICAMS	13.5	39	(*28*)
1H2P	12.9	36.2	(*2*)
Citrate	4.0	37.1	(*33*)
MDP	10.0[a]	30.8	(*20*)
PAA	17[a]	27.9	(*20*)
Methyl-PAA	26[a]	26.1	(*20*)
L-Mimosine	23	25.9	(*32*)
EDTA	6.4	24.9	(*8*)
EDTP	8.3	20.4	(*8*)
Ethyl-PAA	40[a]	20.0	(*20*)
NTP	9.8	15.8	(*6*)
DTTP	7.9	4.7	(*11*)
NTA	0[a]	0	(*6*)
DTPA	0	0	(*11*)

The two-pathway model

Based on the new results reported here, it does not appear that the first-order component for iron release is associated with an allosteric effect from the chelating agent. The alternative explanation is that there is a separate first-order pathway for iron release. There is considerable evidence that the first-order component is directly associated with the displacement of the synergistic carbonate anion. Schlabach and Bates established structural criteria for anions which are capable of replacing the synergistic carbonate (*22*). These were later refined based on epr studies by Dubach et al (*34*) on a more extensive set of anions. In general, synergistic anions form 5- or 6-membered chelate rings. One coordination site is occupied by a carboxylate group. The second coordinating group may be another carboxylate group, but can also be an alcohol, a ketone, or an amine. If there is a methylene group within the chelate ring, there is a steric restriction that the methylene can have one substituent, but not two. For example, lactate can serve as a synergistic anion, but 2-methyllactate cannot (*22*). The ligands which typically follow simple saturation kinetics (hydroxamates, catechols, and hydroxypyridones) have structures that do not conform to this standard structural model for a synergistic anion. Thus the hypothesis was that the first order pathway requires the incoming ligand to replace the synergistic carbonate (*6;11;35*).

Brook et al. (*21*) have provided additional data to support this hypothesis. The kinetics of iron release were evaluated for PAA, benzyl-PAA, and dibenzyl-PAA. The monosubstituted benzyl-PAA showed complex kinetics with only slight changes in the rate parameters from those for PAA. However, disubstitution in dibenzyl-PAA reduced k' by an order of magnitude (*21*).

The ligand that removes iron most quickly via a first-order process is pyrophosphate (*7*). Bailey et al. (*36*) reacted a lysine near the metal-binding site of ovotransferrin with hydroxypyruvate and created an endogenous, covalently bound synergistic anion. This modified protein binds iron in the absence of carbonate. Bailey et al. (*36*) conducted kinetic studies using pyrophosphate to release the iron both from the native Fe-CO_3-ovoTf complex and the carbonate-free Fe-OvoTf' complex of the chemically modified protein. Pyrophosphate removed iron from the native complex via complex kinetics, with a value of k' very similar to that reported for serum transferrin. However, iron release from the modified protein changed to simple saturation kinetics, with k' = 0, providing strong evidence that replacement of the carbonate is a key requirement for the first-order process.

Kinetic studies have also been conducted on iron release from the R124A mutant of the transferrin N-lobe (*37*). Arginine 124 is a key residue that hydrogen bonds to the synergistic carbonate to strengthen the Fe-CO_3-Tf ternary complex. The R124A mutant still binds iron using carbonate as the synergistic anion, but the complex is much weaker. Rates of iron release from the R124A mutant were studied using both AHA and deferiprone. In both cases, iron release followed a simple first order process, with k' parameters of 57 $M^{-1}min^{-1}$ for AHA and 980 $M^{-1}min^{-1}$ for deferiprone. The largest k' value reported for wild type N-lobe transferrin is 0.4 $M^{-1}min^{-1}$ for iron removal by pyrophosphate. Thus the disruption in R124A of the hydrogen-bonding network that holds the carbonate in place changes the kinetics from essentially pure saturation kinetics to simple first-order kinetics with a rate constant 3 to 4 orders of magnitude larger than any k' value reported for the wild-type protein.

These previous studies are all consistent with a reaction pathway that involves the replacement of the synergistic carbonate anion. The present work on allosteric anion binding shows that anions have quite distinct effects on the saturation and first-order components for iron release and provides evidence that the binding of the ligand as an allosteric anion is very unlikely to generate an apparent first-order process for iron release.

References

1. Cowart, R. E., Kojima, N., and Bates, G. W. (1982) *J. Biol. Chem. 257*, 7560-7565.
2. Li, Y. and Harris, W. R. (1998) *Biochim. Biophys. Acta 1387*, 89-102.
3. Bali, P. K. and Harris, W. R. (1989) *J. Am. Chem. Soc. 111*, 4457-4461.
4. Bertini, I., Hirose, J., Luchinat, C., Messori, L., Piccioli, M., and Scozzafava, A. (1988) *Inorg. Chem. 27*, 2405-2409.
5. Marques, H. M., Egan, T. J., and Pattrick, G. (1990) *South African Journal of Science 86*, 21-24.
6. Bali, P. K., Harris, W. R., and Nesset-Tollefson, D. (1991) *Inorg. Chem. 30*, 502-508.
7. Harris, W. R. and Nesset-Tollefson, D. (1991) *Biochemistry 30*, 6930-6936.
8. Harris, W. R. and Bao, G. (1997) *Polyhedron 16*, 1069-1079.
9. Harris, W. R., Rezvani, A. B., and Bali, P. K. (1987) *Inorg. Chem. 26*, 2711-2716.
10. Harris, W. R. and Bali, P. K. (1988) *Inorg. Chem. 27*, 2687-2691.
11. Harris, W. R., Bali, P. K., and Crowley, M. M. (1992) *Inorg. Chem. 31*, 2700-2705.
12. Baldwin, D. A. and De Sousa, D. M. R. (1981) *Biochem. Biophys. Res. Commun. 99*, 1101-1107.
13. Williams, J., Chasteen, N. D., and Moreton, K. (1982) *Biochem. J. 201*, 527-532.
14. Marques, H. M., Watson, D. L., and Egan, T. J. (1991) *Inorg. Chem. 30*, 3758-3762.
15. Egan, T. J., Ross, D. C., Purves, L. R., and Adams, P. A. (1992) *Inorg. Chem. 31*, 1994-1998.
16. Nurizzo, D., Baker, H. M., He, Q. Y., MacGillivray, R. T. A., Mason, A. B., Woodworth, R. C., and Baker, E. N. (2001) *Biochemistry 40*, 1616-1623.
17. He, Q. Y., Mason, A. B., Tam, B. M., MacGillivray, R. T. A., and Woodworth, R. C. (1999) *Biochemistry 38*, 9704-9711.

18. Amin, E. A., Harris, W. R., and Welsh, W. J. (2004) *Biopolymers 73*, 205-215.

19. Harris, W. R. (1984) *J. Inorg. Biochem. 21*, 263-276.

20. Harris, W. R., Brook, C. E., Spilling, C. D., Elleppan, S., Peng, W., Xin, M., and Wyk, J. V. (2004) *J. Inorg. Biochem. 98*, 1824-1836.

21. Brook, C. E., Harris, W. R., Spilling, C. D., Peng, W., Harburn, J. J., and Srisung, S. (2005) *Inorg. Chem. 44*, 5183-5191.

22. Schlabach, M. R. and Bates, G. W. (1975) *J. Biol. Chem. 250*, 2182-2188.

23. Hamilton, W. C. (2010) *Statistics in Physical Science* Ronald Press, New York.

24. Carrano, C. J. and Raymond, K. N. (1979) *J. Am. Chem. Soc. 101*, 5401-5404.

25. Zuccola, H. J. (1992) *The crystal structure of monoferric human serum transferrin (Ph.D. thesis)* Georgia Institute of Technology, Atlanta, GA.

26. Jeffrey, P. D., Bewley, M. C., MacGillivray, R. T. A., Mason, A. B., Woodworth, R. C., and Baker, E. N. (1998) *Biochemistry 37*, 13978-13986.

27. MacGillivray, R. T. A., Moore, S. A., Chen, J., Anderson, B. F., Baker, H., Luo, Y., Bewley, M., Smith, C. A., Murphy, M. E. P., Wang, Y., Mason, A. B., Woodworth, R. C., Brayer, G. D., and Baker, E. N. (1998) *Biochemistry 37*, 7919-7928.

28. Kretchmar, S. A. and Raymond, K. N. (1986) *J. Am. Chem. Soc. 108*, 6212-6218.

29. Harris, W. R., Wang, Z., Brook, C., Yang, B., and Islam, A. (2003) *Inorg. Chem. 42*, 5880-5889.

30. Baker, E. N. (1994) *Adv. Inorg. Chem. 41*, 389-463.

31. He, Q. Y., Mason, A. B., and Woodworth, R. C. (1997) *Biochem. J. 328*, 439-445.

32. Hamilton, D. H., Turcot, I., Stintzi, A., and Raymond, K. N. (2004) *J. Biol. Inorg. Chem. 9*, 936-944.

33. Harris, W. R., Wang, Z., and Hamada, Y. Z. (2003) *Inorg. Chem. 42*, 3262-3273.

34. Dubach, J., Gaffeny, B. J., More, G. R., and Eaton, S. S. (1991) *Biophys J. 59*, 1091-1100.

35. Bali, P. K. and Harris, W. R. (1990) *Arch. Biochem. Biophys. 281*, 251-256.

36. Bailey, C. T., Byrne, C., Chrispell, K., Molkenbur, C., Sackett, M., Reid, K., McCollum, K., Vibbard, D., and Catelli, R. (1997) *Biochemistry 36*, 10105-10108.

37. Li, Y., Harris, W. R., Maxwell, A., MacGillivray, R. T., and Brown, T. (1998) *Biochemistry 37*, 14157-14166.

Chapter 6

A Comparative Study of Iron Removal from C-terminal Monoferric Human Serum Transferrin by NTA and its Phosphonate Analogue PIDA

6.1

Introduction

This chapter describes the kinetics of iron release from C-terminal monoferric transferrin by N-(phosphonomethyl)iminodiacetic acid (PIDA). The results are compared with data on iron release by nitrilotriacetic acid (NTA) alone and by a mixture of NTA and methylphosphonic acid (MPA). These data are used to compare the role of the phosphonate group when incorporated into the ligand PIDA versus the role of the free phosphonate group in a mixture with NTA.

The tripodal phosphonate analogues of NTA such as PIDA, N,N-bis(phosphonomethyl)glycine (DPG) and nitrilotris(methylenephosphonic acid) (NTP) have been studied by our group (*1*). The rates of iron removal from diferric human serum transferrin by these phosphonate analogues of NTA were studied, and the data were fit to equations 6.1 and 6.2, the empirical equations used to describe simple saturation kinetics,

$$k_{obs} = \frac{k_{\max}[L]}{k_d + [L]} \qquad (6.1)$$

and complex kinetics,

$$k_{obs} = \frac{k_{\max}[L]}{k_d + [L]} + k'[L] \qquad (6.2)$$

The ligands PIDA, DPG and NTP followed complex kinetics for iron release from diferric transferrin, whereas the tricarboxylate analogue NTA showed simple first order kinetics with respect to the NTA concentration (*1*). It has been proposed that equation 6.2 reduces to a simple first order dependence for NTA due to a very small k_{max}. Previous studies have also indicated that the phosphonate group has a higher affinity for Fe(III) than the carboxylate moiety in these ligands (*1;2*). This chapter compares the effect of the one phosphonate group along with two carboxyl moieties in PIDA with that of the three carboxyl moieties in NTA on iron release from transferrin.

6.2

Results

6.2.1

Iron release from C-terminal monoferric transferrin by PIDA

Iron release from C-terminal monoferric transferrin was followed over the concentration range of 1 to 125 mM PIDA. The data for PIDA is shown in Figure 6.1. There is an increase in k_{obs} between 0 and 15 mM concentrations, after which the plot starts to curve but does not reach a plateau. On the contrary, the values for k_{obs} continue to increase linearly with increasing ligand concentration. In other words, the rate follows a combination of saturation and first-order kinetics that can be described by equation 6.2. The data in Figure 6.1 have been fit to both equations 6.1 and 6.2, and the rate parameters are listed in Table 6.1. The data for iron release from C-terminal monoferric transferrin fits well with the 3 parameter fit to equation 6.2.

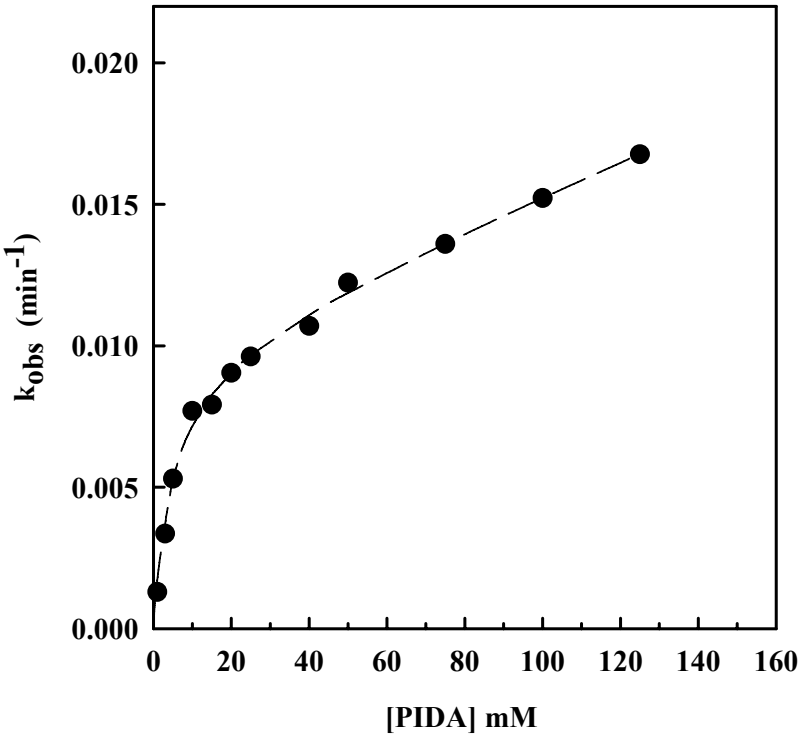

Figure 6.1. Rate constants for iron release from C-terminal monoferric transferrin by PIDA in 0.1 M hepes buffer at pH 7.4 and 25 °C.

Table 6.1.

Rate parameters for iron removal from C-terminal monoferric transferrin by PIDA[a]

	k_{max} (min^{-1}) x 10^3	k_d x 10^3 (M)	k' (M^{-1} min^{-1})
PIDA[c]	10.1 ± 0.5	5.5 ± 0.8	0.060 ± 0.005
PIDA[b]	17.12 ± 0.93	16.30 ± 2.9	-

[a] 25 °C, 0.1 M Hepes, pH 7.4

[b]Data fit using two adjustable parameters to eq (6.1)

[c]Data fit using three adjustable parameters to eq (6.2)

In earlier studies (*1*), the PIDA ligand sample contained 10% of an impurity identified as (hydroxymethyl)phosphonic acid (HMP), so it was possible that the first order parameter for iron release was due to anion effects of HMP. The PIDA ligand used in this study was commercially available and did not contain any HMP impurity, so the appearance of the first order parameter is solely due to PIDA and is not a mere anion effect.

6.2.2

Effect of phosphonate on iron release by NTA

The effect of phosphonate anions on the rate of iron release by 100 mM NTA has been studied as described in Chapter 5. We measured the rates of iron release from C-terminal monoferric transferrin by 100 mM NTA and by a mixture of 100 mM NTA and increasing concentrations of MPA. The results are shown in Figure 6.2. The mixtures of NTA and MPA had higher rates than NTA by itself. MPA behaves as a simple allosteric anion and accelerates the rate of iron release by 100 mM NTA by binding at the KISAB site on the protein.

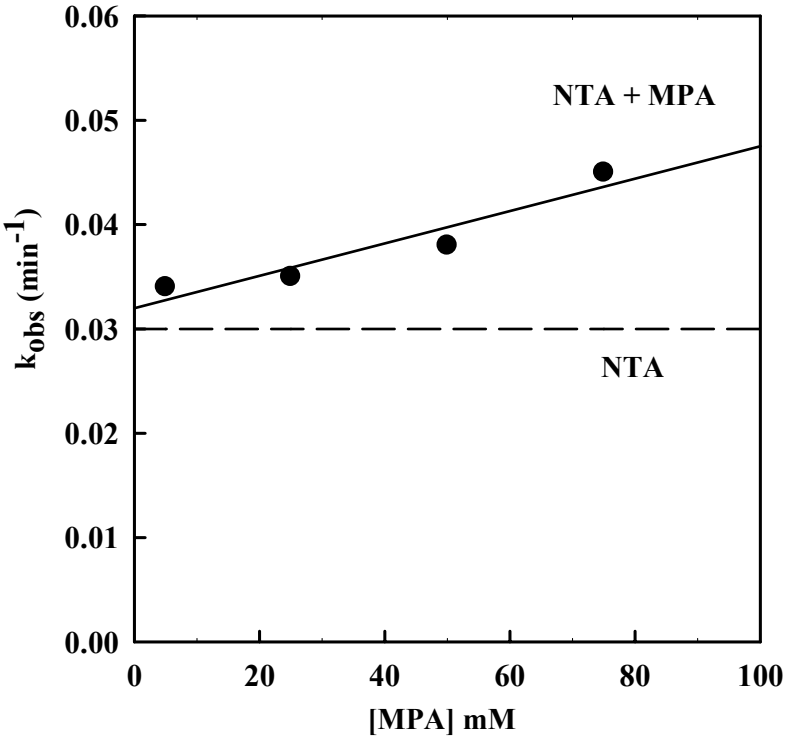

Figure 6.2. Plots of k_{obs} for the removal of iron from C-terminal monoferric transferrin by 100 mM nitrilotriacetic acid (NTA) in the presence of methanephosphonate (MPA,●) at 25 ºC in 0.1 M Hepes, pH 7.4.

6.2.3

Effect of different modes of phosphonate group on iron release pathways

One of the goals of this study was to evaluate the effect of the phosphonate group when incorporated into the ligands versus the effect of a free phosphonate group in a mixture with the ligand. To observe the effect of a phosphonate incorporated as a moiety into the ligand, we have evaluated iron release by PIDA, which contains two carboxylate

groups and a phosphonic acid group. When compared with the structure of NTA, it can be seen as one carboxyl group of NTA that has been replaced with a phosphonic acid group. To compare the effect of the free phosphonate group, we performed experiments with mixtures of equimolar concentrations of NTA and MPA. The pseudo first-order rate constants for iron removal by NTA from C-terminal monoferric transferrin were determined as reported previously (*1;2*). Iron removal by NTA shows a first order dependence on the concentration of NTA, with a zero intercept, as can be seen in Figure 6.3, indicating the absence of any other pathway at low concentrations of NTA. Figure 6.3 also shows the rate constants for iron removal by equimolar mixtures of NTA and MPA. For both NTA alone and the NTA/MPA mixtures, we limited the studies to NTA concentrations > 25 mM. At lower concentrations of NTA, very little iron was removed and the rate constants were difficult to determine.

As shown in Figure 6.3, iron release from C-terminal monoferric transferrin by the mixture of NTA and MPA shows a linear dependence of the rate constant k_{obs} on the ligand concentration over the concentration range of 25-100 mM of the mixture. The linearity of the plot and the nonzero intercept are consistent with the equation for complex kinetics assuming that [L] >> k_d over the available range of ligand concentration. Under these conditions, equation (6.2) for complex kinetics, reduces to equation (6.3), a simple linear equation with a slope of k' and a y-intercept of k_{max}.

$$k_{obs} = k_{\max} + k'[L] \qquad (6.3)$$

Under these conditions $k_{d,}$ which is the concentration of ligand required to reach half saturation, could not be determined. This type of observation has been made by iron release from C- and N-terminal transferrin by PAA (*3;4*). In these previous studies it was assumed that the plots of k_{obs} versus PAA concentration would curve towards zero at lower ligand concentrations. This curvature has now been demonstrated by the results in Chapter 3 for iron release from C-terminal monoferric transferrin by low ligand concentrations of PAA and its alkyl derivatives.

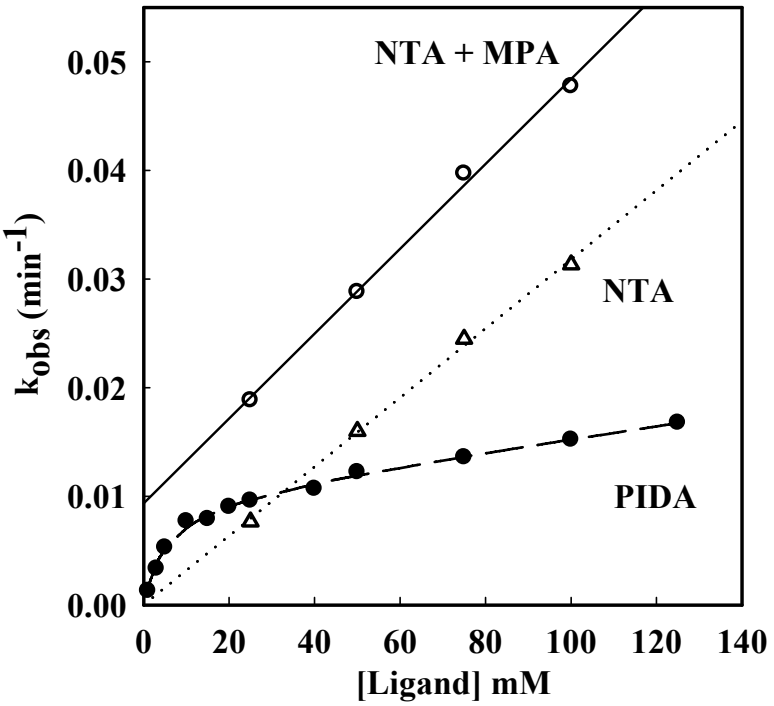

Figure 6.3. Rate constants for iron removal from C-terminal monoferric transferrin by PIDA, by NTA and by equimolar mixtures of NTA and MPA at 25 ºC in 0.1 M Hepes, pH 7.4.

The NTA/MPA mixtures have higher rate constants than NTA alone, which demonstrates yet again the accelerating effect of the simple anion MPA on the rate of iron release by NTA. Also, the presence of MPA introduces a non-zero k_{max} value for iron release by NTA in the mixture. It appears that MPA in the mixture with NTA acts as a simple allosteric anion, and by binding to the KISAB site, it accelerates the rate of iron release by increasing the saturation rate parameter k_{max}, which is otherwise not seen for NTA. The allosteric binding of MPA also produces a small increase in the k' parameter for the first-order pathway.

The studies on iron release by PIDA included data at lower ligand concentrations, such that the initial curvature in the plot in Figure 6.3 is clearly visible. The appearance of the curvature at low ligand concentrations clearly displays the presence of a saturation pathway. The rate parameters derived from the data in Figure 6.3 are listed in Table 6.2. The value of k_{max} obtained from the three-parameter fit of the PIDA data to eq (6.2) is essentially the same as the k_{max} for NTA in the presence of equimolar MPA. However, incorporating the phosphonate group into the ligand structure results in a dramatic decrease in the k' parameter for PIDA, even though the NTA/MPA mixture showed a slight increase in k'.

Table 6.2.

Rate parameters for iron release from C-terminal monoferric transferrin

	k_{max} (min^{-1}) x 10^3	k_d x 10^3 (M)	k' ($min^{-1}M^{-1}$)
NTA	-	-	0.325 ± 0.012
NTA+MPA	9.4 ± 1.1	-	0.390 ± 0.016
PIDA	10.1 ± 0.5	5.5 ± 0.8	0.060 ± 0.005
NTP[a]	9.8 ± 2.0	7.6 ± 1.1	0.053 ± 0.006

[a] Results from ref (*2*)

6.3

Discussion

In Chapters 4 and 5, we studied extensively the effect of sulfonates, diphosphonates and phosphonocarboxylates on the kinetic pathways of iron removal from transferrin. In all these studies, the effect of anions was studied using mixtures of the anion and a reference ligand. This chapter focused on the effect of the phosphonate group in two different modes on iron release.

In the NTA/MPA mixtures, the phosphonate group can only act as an allosteric anion. Anions have been reported previously to alter the rates of iron release, and this effect has been attributed to their selective binding to an allosteric binding site usually referred to as KISAB site (*5*). MPA increases the rate of iron release by NTA in the mixture, presumably by binding to the proposed allosteric site of the protein. This anion binding introduces a significant value for k_{max} for iron release by NTA, and thus appears

to accelerate the conformational change in the protein. The results for the MPA in the mixture are consistent with the allosteric anion effects reported in Chapters 4 and 5 for other non-coordinating anions.

The free MPA group does not seem to have much effect on the k' value for NTA. There is a modest increase in k' for the MPA/NTA mixtures. This minor change in k' is nonetheless in contrast with the effect of the non-chelating bifunctional anions MDS and PPA, both of which cause a reduction in k' for iron release by NTA, as described in chapters 4 and 5, respectively.

Incorporation of the phosphonate group into the ligand PIDA improves its iron binding affinity and makes it easier to study iron release at lower ligand concentrations. Thus the curvature at low ligand concentrations, consistent with a saturation component for iron release, can be easily observed for PIDA. The k_{max} value for PIDA of 0.010 min^{-1} is essentially the same as that of the triphosphonate ligand NTP (*2*), as shown in Table 6.2. The surprising result is that the mixture of NTA/MPA has the same k_{max} value. This indicates that the increase in k_{max} observed upon going from NTA to PIDA and NTP can be attributed to the binding of the phosphonate groups of these ligands to the KISAB site.

The incorporation of the phosphonate group into PIDA also results in a distinct decrease in the first order component, k' from 0.325 M^{-1} min^{-1} for NTA to only 0.060 M^{-1} min^{-1} in PIDA. This decrease in k' is quite different from the NTA/MPA mixtures, which show a slight increase in k'. Thus it is difficult to attribute the decrease in k' to allosteric binding of a phosphonate group of PIDA.

A k' value of ~0.05 M^{-1} min^{-1} seems to be characteristic of aminophosphonic acids. The k' value for EDTA of 0.114 M^{-1} min^{-1} decreases to 0.036 for

ethylenediaminetetra(methylenephosphonic acid), EDTP (*6*), and the k' value for diethylenetriaminepenta(methylenephosphonic acid), DTPP is 0.070 M^{-1} min^{-1} (*7*). The results reported here for PIDA suggest that only a single phosphonic acid group is necessary for this reduction in k'.

In chapter 5 we discussed the observation that chelating anions had very different effects than non-chelating anions on iron release by the reference ligands. Thus one possibility is that the decrease in k' is related to the ability of the aminomethylphosphonate functional group to form a stable chelate ring. However, other phosphonate chelating agents, such as PAA and MDP, retain high k' values of 0.38 and 0.18 M^{-1} min^{-1}, respectively, and pyrophosphate has a very large k' value of 0.84 M^{-1} min^{-1} (*2*). Thus it is difficult to attribute the drop in k' directly to some sort of chelate effect.

The non-chelating, bifunctional anions PPA and MDS also caused a reduction in the k' value for iron removal by NTA. Thus one could speculate that the decrease in k' does reflect the binding of PIDA to the KISAB site, but as a bifunctional anion, similar to PPA and MDS, as opposed to the monofunctional MPA. Since the amide PAM has essentially the same allosteric effect as PPA, it is possible that the PIDA could bind to the allosteric site using a combination of the phosphonate and amine group of PIDA. Alternatively, the PIDA could bind using a combination of the phosphonate group and one of the carboxylate groups.

The absence of a saturation component for iron release by NTA has been linked to the weaker binding of the carboxylate group to the protein as an anion as compared to the phosphonate group (*2*). The appearance of a consistent k_{max} value for iron removal by the NTA/MPA mixture, PIDA, and NTP appears to be due to the binding of the phosphonate

group to the KISAB site on the protein. This binding of the phosphonate anion to ferric transferrin as an anion to the cationic side chains of the protein appears to be different from the allosteric KISAB site. Thus we speculate the presence of more than one anion binding site in the transferrin and further studies are needed to confirm these speculations.

The first order pathway has been proposed to be associated with the replacement of synergistic anion by the incoming ligand, followed by the fast dissociation of the iron ligand complex (*1*). The incorporation of the phosphonate group into the ligand in PIDA and NTP reduces the k' parameter for the first order pathway. In contrast, the binding of the free phosphonate group of MPA increases k_{max}. Thus the reduction in k' for PIDA and NTP cannot be attributed to the binding of a phosphonate arm of the ligand to the KISAB site. This suggests that the reduction in k' may be related to a direct binding of the incoming ligand to the ferric ion in the iron-protein complex during the iron removal reaction. However, the structure of this possible ligand-iron-carbonate-protein quaternary complex is not known.

The bifunctional, non-chelating anion MDS and PPA also reduce the value of k' for the first order pathway. It is possible that the different allosteric effects of the monofunctional anion MPA and these bifunctional anions reflect the existence of more than one KISAB site. The possibility of multiple KISAB sites has been suggested by Halbrooks et al based on kinetic studies of mutant transferrins produced by site-directed mutagenesis (*8*). The ability of the aminophosphonate ligands to increase k_{max} while decreasing k' could reflect their ability to bind to two different KISAB sites.

References

1. Harris, W. R., Rezvani, A. B., and Bali, P. K. (1987) *Inorg. Chem. 26*, 2711-2716.

2. Bali, P. K., Harris, W. R., and Nesset-Tollefson, D. (1991) *Inorg. Chem. 30*, 502-508.

3. Harris, W. R., Brook, C. E., Spilling, C. D., Elleppan, S., Peng, W., Xin, M., and Wyk, J. V. (2004) *J. Inorg. Biochem. 98*, 1824-1836.

4. Brook, C. E., Harris, W. R., Spilling, C. D., Peng, W., Harburn, J. J., and Srisung, S. (2005) *Inorg. Chem. 44*, 5183-5191.

5. Marques, H. M., Watson, D. L., and Egan, T. J. (1991) *Inorg. Chem. 30*, 3758-3762.

6. Harris, W. R. and Bao, G. (1997) *Polyhedron 16*, 1069-1079.

7. Harris, W. R., Bali, P. K., and Crowley, M. M. (1992) *Inorg. Chem. 31*, 2700-2705.

8. Halbrooks, P. J., Giannetti, A. M., Klein, J. S., Bjorkman, P. J., Larouche, J. R., Smith, V. C., MacGillivray, R. T. A., Everse, S. J., and Mason, A. B. (2005) *Biochemistry 44*, 15451-15460.

Chapter 7

Conclusions

The ligand-dependence of the rate of iron release from transferrin by various low molecular weight ligands has shown three different patterns, described as saturation kinetics, first-order kinetics, and complex kinetics. In most cases, saturation kinetics are attributed to the Bates mechanism (*1*) for iron release, in which the rate-limiting step for iron removal is a conformational change in the protein.

It is well known that various non synergistic anions affect the rate of iron release (*2;3*). It has been proposed that these anion effects reflect the binding of the anions to an allosteric binding site known as the kinetically significant allosteric anion binding (KISAB) site (*4-6*). Despite several attempts to locate this site, the exact location of the KISAB site is still unknown (*7;8*).

There has not been a consensus on the mechanism for the first-order component for iron release. Our group has proposed that the first-order component represents a reaction pathway that is independent of the protein conformation change, one in which the rate limiting step is the replacement of the synergistic carbonate anion by the incoming ligand, which destabilizes the Fe-L-Tf complex and triggers iron release (*9-12*). Others have proposed that the first-order component arises because anionic ligands can bind to the KISAB site, and that this allosteric effect increases the k_{max} values for the protein conformational change as the ligand concentration increases (*4;6;13*).

This dissertation focuses on the effect of three main classes of anions: sulfonates, phosphonates and phosphonocarboxylates. These anions can be further divided into two

types: (a) simple, non-chelating anions and (b) anions which are also competent chelating agents that can remove iron from transferrin. In our studies, the impact of these anions on the iron release from C-terminal monoferric transferrin has been evaluated using two types of reference ligands. Acetohydroxamic acid (AHA) and deferiprone (L1) remove iron exclusively via a saturation pathway (*1;14*), while NTA and DTPA remove iron exclusively by a first order pathway (*9;10*). The objective was to evaluate the effect of the anions on the individual iron release pathways.

The non-chelating anions consistently increase the rates of iron release by all ligands. The anions appear to act primarily by increasing the k_{max} value associated with the saturation pathway (eq 1.1 in chapter 1). This increase was apparent even for NTA, which in the absence of the anions has a k_{max} value of zero. This increase in k_{max} presumably reflects the binding of the anions to the KISAB site on transferrin.

The anion effects are consistently higher for bifunctional anions (e.g. phosphonoacetic acid) compared to the individual anionic functional groups (e.g. acetate and methylphosphonate). However, there were not large variations in the anion effects among the bifunctional non-chelating anions.

The effect of non-chelating anions on the first-order pathway are somewhat variable. The rate of iron release via this pathway is represented by the k' parameter in eq (1.2) in chapter 1. Non-chelating anions reduce the k' for NTA by a modest amount. Conversely, they increase the k' value iron release by AHA. In general, these changes in k' have less effect on the overall rate of iron release than the consistent increases in k_{max}.

At the beginning of this study, we anticipated that the analysis of the kinetic data would be more complicated for experiments that involve chelating anions because it

would be necessary to account for the simultaneous release of iron by the reference ligand and the chelating anion. We developed methods to partition the overall rate constant for iron release into individual components attributed to the reference ligand and the chelating anion. We expected that once the overall rate was properly partitioned between the two components, that the allosteric effect due to the binding of the chelating anions would closely resemble the effect of the non-chelating anions. Unexpectedly, the chelating anions PAA and MDP significantly reduced the k_{max} value for the reference ligand. This reduction in k_{max} appears to be specifically associated with the ability of the anion to form a stable chelate ring with the Fe^{3+}. This obviously requires some conformational change in the protein to expose vacant coordination sites. We speculate that this could involve a change in the coordination mode of the synergistic carbonate from bidentate to monodentate, possibly combined with the dissociation of the carboxylate group from the aspartic acid.

Although the mode of binding of the chelating anions is still uncertain, the observed reduction in k_{max} values associated with the chelating anions does help differentiate between alternative mechanisms for iron release. The Bertini mechanism (*4*) proposes that the first-order term is an artifact that appears because the anionic chelating agent is binding to the KISAB site to gradually increase the k_{max} value. We have now shown that the binding of these chelating anions to the protein decreases, rather than increases, the rate of iron release. This is strong evidence against the Bertini mechanism.

The anion effects for both non-chelating and chelating anions were studied using mixtures of the anions and the reference ligands. We also evaluated the effect of the phosphonate anion when it is incorporated into the chelating agent PIDA versus the effect

of MPA in an equimolar mixture with NTA. In both PIDA and the MPA/NTA mixture, the phosphonate binds to the KISAB site and causes the expected increase in k_{max} for iron release via a saturation pathway.

The free MPA anion causes a small increase in the k' parameter for iron release by NTA. However, incorporating the phosphonate group into PIDA drastically reduces the k' value for iron release via the first-order process. A similar reduction in k' has been reported for the ligand NTP (*9;15*), in which all three of the carboxylate groups of NTA are replaced by phosphonic acid group.

We have proposed that the first-order pathway is associated with ligands that can replace the synergistic carbonate anion. Work by Schlabach and Bates (*16*) and by Dubach et al. (*17*) have established structural criteria for ligands that can serve as a synergistic anion. According to the Bates-Dubach model, NTA, PIDA and NTP should all be able to replace the carbonate. Thus there is no obvious reason why k' is so much smaller for NTP and PIDA compared to NTA. Similar unexpected decreases in k' have been observed for other phosphonates that meet the Bates-Dubach model for a viable synergistic anion (*18*). Thus it appears that (a) the Bates-Dubach model is incomplete, and some structural feature of the phosphonates is unexpectedly destroying their ability to replace the synergistic bicarbonate, or (b) our original hypothesis that k' is intimately linked to the replacement of the carbonate is incorrect. Further work is needed to resolve this issue.

References

1. Cowart, R. E., Kojima, N., and Bates, G. W. (1982) *J. Biol. Chem. 257*, 7560-7565.

2. Baldwin, D. A. and De Sousa, D. M. R. (1981) *Biochem. Biophys. Res. Commun. 99*, 1101-1107.

3. Baldwin, D. A. (1980) *Biochim. Biophys. Acta 623*, 183-198.

4. Bertini, I., Hirose, J., Luchinat, C., Messori, L., Piccioli, M., and Scozzafava, A. (1988) *Inorg. Chem. 27*, 2405-2409.

5. Egan, T. J., Ross, D. C., Purves, L. R., and Adams, P. A. (1992) *Inorg. Chem. 31*, 1994-1998.

6. Marques, H. M., Watson, D. L., and Egan, T. J. (1991) *Inorg. Chem. 30*, 3758-3762.

7. He, Q. Y., Mason, A. B., Tam, B. M., MacGillivray, R. T. A., and Woodworth, R. C. (1999) *Biochemistry 38*, 9704-9711.

8. Amin, E. A., Harris, W. R., and Welsh, W. J. (2004) *Biopolymers 73*, 205-215.

9. Bali, P. K., Harris, W. R., and Nesset-Tollefson, D. (1991) *Inorg. Chem. 30*, 502-508.

10. Harris, W. R., Bali, P. K., and Crowley, M. M. (1992) *Inorg. Chem. 31*, 2700-2705.

11. Harris, W. R. and Bao, G. (1997) *Polyhedron 16*, 1069-1079.

12. Bali, P. K. and Harris, W. R. (1990) *Arch. Biochem. Biophys. 281*, 251-256.

13. Marques, H. M., Egan, T. J., and Pattrick, G. (1990) *South African Journal of Science 86*, 21-24.

14. Li, Y. and Harris, W. R. (1998) *Biochim. Biophys. Acta 1387*, 89-102.

15. Harris, W. R., Rezvani, A. B., and Bali, P. K. (1987) *Inorg. Chem. 26*, 2711-2716.

16. Schlabach, M. R. and Bates, G. W. (1975) *J. Biol. Chem. 250*, 2182-2188.

17. Dubach, J., Gaffeny, B. J., More, G. R., and Eaton, S. S. (1991) *Biophys J. 59*, 1091-1100.

18. Brook, C. E., Harris, W. R., Spilling, C. D., Peng, W., Harburn, J. J., and Srisung, S. (2005) *Inorg. Chem. 44*, 5183-5191.